A STUDY OF BONE QUALITY IN FEMORAL NECK OF OSTEOARTHRITIS

by

HANADI ALOUSAIMI

B.Sc., The University of King Abdul-Aziz, 2009

A THESIS SUBMITTED IN PARTIAL FULFILLMENT OF

THE REQUIREMENTS FOR THE DEGREE OF

MASTER OF APPLIED SCIENCE

in

THE FACULTY OF GRADUATE AND POSTDOCTORAL STUDIES

(Biomedical Engineering)

THE UNIVERSITY OF BRITISH COLUMBIA

(Vancouver)

August 2018

The following individuals certify that they have read, and recommend to the Faculty of Graduate and Postdoctoral Studies for acceptance, a thesis/dissertation entitled:

A study of bone quality in femoral neck of osteoarthritis

submitted by Hanadi Alousaimi in partial fulfillment of the requirements for the degree of Master of Applied Science

in Biomedical Engineering

Examining Committee:

Rizhi Wang, Materials Engineering

Supervisor

Peter Cripton, Mechanical Engineering

Supervisory Committee Member

Frank Ko, Materials Engineering

Supervisory Committee Member

Additional Examiner

ABSTRACT

Osteoarthritis (OA) is the most common joint disease and skeletal disorder related to aging. Hip OA is a common chronic degenerative joint disorder that causes pain, stiffness and physical disability in the elderly population. The cause of this disease is still unclear. However, it is estimated that the risk of fracture would increase with the development of hip OA. There is a lack of understanding regarding the effect of hip OA on bone quality. The aim of this thesis was therefore to study bone quality of hip OA in terms of both microstructure and material properties.

To assess cortical and trabecular bone microstructure, High-Resolution Peripheral Quantitative Computed Tomography (HR- pQCT) was used to analyze aged human proximal femora with OA compared to non-OA (control). It was found that OA group had a lower number of trabeculae and higher trabecular spacing than the control group at the femoral head and head-neck junction regions. Within the femoral neck region, OA group showed thicker cortex but higher porosity.

Bone mineralization was qualitatively observed by using backscattered electron (BSE) and Optical microscopy (OM). Regions of hypermineralization were found in the cortical bone of the OA femoral neck. It had similar morphological features to the hypermineralization found in control samples. It can thus be concluded that hypermineralization was not a result of OA, but may be related to age.

This thesis provided better understudying of bone quality in OA patients, specifically the microstructural changes in both cortical and trabecular regions. The findings provided a new clue in terms of the similarity of hypermineralization between OA and control group.

Further research along this direction may lead to development of new diagnosis techniques and better ways of hip repairing and reconstruction.

Lay Summary

It is estimated that the number of people with Osteoarthritis will increase by 57% in the next two years. Around 40% to 45% of patients with hip OA had an incidence of at least one fall in 2017. This may result in a serious hip fracture which increases the risk of treatment failure during the hip implants. It is essential to understand the bone quality changes of the femoral hip in OA. By studying both microstructural and material analyses of OA femoral hip bone and non- OA group, this thesis aimed to provide a comprehensive study to understand bone quality in OA.

Preface

This thesis is original, unpublished, independent work by the author, H. Alousaimi. All procedures for the use of this study were approved by the Clinical Research Ethics Review Board at the University of British Colombia, Ethics Certificate #H09-02073.

Table of Contents

List of Tables

List of Figures

Lists of Abbreviations

µCT	Micro-CT
aBMD	Areal bone mineral density
BMD	Bone Mineral Density
BSE	Backscattered Electron
BV/TV	Bone volume fraction
Conn.D	Connectivity density
Ct.Po	Cortical porosity
Ct.Th	Cortical thickness
DXA	Dual-energy X-ray Absorptiometry
FE	Finite Element
FTIR	Raman and Fourier's transform infrared spectroscopy
HA	Hydroxyapatite
HOA	Hip OA
HR-MRI	high-resolution magnetic resonance imaging
HR-pQCT	High-Resolution peripheral Quantitative Computed Tomography
HRTEM	High-resolution transmission electron microscopy
OA	Osteoarthritis
OM	Optical Microscopy
OP	Osteoporosis
pQCT	Peripheral Quantitative Computed Tomography
qBSE	Quantitative Backscattered Electron
ROI	Region of Interest
SEM	Scanning Electron Microscopy
Tb.N	Trabecular number
Tb.Sp	Trabecular separation
Tb.Th	Trabecular thickness
TEM	Transmission Electron Microscopy
THA	Total Hip Arthroplasty
vBMD	Volumetric bone mineral density

Acknowledgments

My thanks go first and foremost to my supervisor, Dr. Rizhi Wang. His guidance and interest in my progress are mainly to be credited for all the work presented here. The door of his office was always open whenever I had a question about my research. I am very grateful to have such a special advisor who has spent so much time, effort and energy inspiring me to continuously improve my research skills. I give my greatest thanks to him for all his efforts in teaching me and guiding me during the completion of my master's thesis.

My thanks also go to my committee members: Dr. Frank Ko and Dr. Peter Cripton for their time regarding this thesis.

I would like to extend my gratitude and deepest thanks to all those individuals who have made the completion of my M.Sc. possible. First, I would like to thank Dr. Danmei Liu for being an insightful, supportive, positive and encouraging person. I greatly appreciate her patience, her sharing of resources, her expertise and her cooperation regarding my many questions and ideas in my project. I am also grateful for her encouragement, her promotion of my research, and her support and trust regarding the use of XtremeCT (HR-pQCT).

I would like to thank all the members of the Biomaterials group for their help and friendship throughout my studies. Special thanks to Dr. Felipe, who would, many times, wake up early in the morning to be in the operating room collecting those femoral hips. He always went out of his way to make time to advise me and to help me with my project. I am also deeply grateful for Qiong Wang for helping me use the BSE and answering questions.

Many thanks to the volunteers who consented to participate in this project. This accomplishment would've not been possible without them.

From outside the Biomaterials group, many thanks go to Dr. Yassir Alhazmi, who has been my source of stability. For bringing motivation where there was a discouragement, assurance where there was confusion, and encouragement where there was frustration. For that and much, much more, I am grateful. Thanks for his willingness to support me and his help with all the questions I had regarding writing and statistics.

Lastly, I thank those who have been my personal supports, Carol Wilkinson, Layla, Sandi and her beautiful parents, Rim and Zina. Thank you for your prayers. Thanks to Aliaa for helping me with the figures that I included in my thesis.

My parents, Abdullah and Monia, as well as my siblings, also deserve my deepest thanks for their unconditional love, support, and encouragement. It is their influence that has shaped me into the person that I am today. I am forever and continuously grateful.

I would also like to acknowledge my funding source, The King Abdullah Scholarship Program (KASP) for their generous financial support. Thanks to the Centre for Hip Health and Mobility (CHHM) the use of their facilities and their support.

Finally, and most importantly, I thank God (Allah) for always blessing me to pursue every goal I dream to achieve.

To my Amazing Father

Who always supports me, whatever path I choose to take.

To the soul of King Abdullah bin Abdul-Aziz

Who had given me the opportunity to study abroad.

CHAPTER 1: Introduction

Osteoarthritis (OA) is one of the major health problems in the elderly population. OA is a degenerative disease of the joints, characterized by cartilage loss and joint pain [1]. It affects bone quality and quantity. Globally, around 3.3% to 3.6% of the population is diagnosed with OA. In the United States, 80% of the population who are over 65 years old have diagnosed with OA [2]. By 2020, it is estimated that the number of people with OA will increase by 57% [3].

There are many risk factors for over several years associated with hip osteoarthritis [4]. Hip fracture is one of the major risks associated with the development of hip OA. The incidence of falls with the late stage of hip OA leads to hip fractures [5]. It was reported that 40% to 45% of patients with hip OA had an incidence of at least one fall in 2017 [3]. Women with the late stage of hip OA have an increased risk of hip fracture result from falls [6]. It was recently reported that the appearance of OA at the same time of hip fracture will increase the risk of treatment failure during the implants [7].

Knowledge of both bone microstructures and materials of OA is a clue for understanding bone's pathophysiology and will improve the disease's diagnosis and treatment. Recent advances in medical imaging techniques allow bone microstructure to be assessed at different skeletal sites within the body whether in vivo non-invasively or ex-vivo [8]. High-resolution peripheral quantitative computed tomography (HR-pQCT) is one of the tools for assessing bone microarchitecture. It has the capability to image three-dimensional (3D) bone microstructures and provide quantitative measurements of cortical and trabecular microstructure [9].

Most of the published studies that used HR-pQCT have focused on the technical aspects and validation but recently there has been a large increase in the number of studies demonstrating the clinical application of HR-pQCT. It is important to note that none of these studies compared bone microarchitecture in the proximal femur (head and neck) between OA and non- OA (control group) by using HR-pQCT.

The work in this thesis focuses on analyzing the bone quality within OA and control group of the femoral heads and necks using high-resolution quantitative computed tomography (HR-pQCT) as well as back-scattered electron imaging (BSE) in order to give a better understanding of hip OA. To do so, femoral hips were initially scanned by HR-pQCT to investigate the microarchitecture differences in both cortical and trabecular components. Consequently, cortical bone at the femoral neck in OA samples was observed under BSE for the degree of mineralization.

The following chapter aims to provide some literature reviews in order to provide an overview of the ability of HR-pQCT to assess bone microarchitecture in OA and highlight the result from recent studies. In addition, previous reviews related to mineralization in cortical bone at the femoral necks were provided. Thus, this will help to improve the understanding of bone quality related to the various bone disease.

CHAPTER 2: Literature Review

2.1 Bone structure and Hip Anatomy

Bone is a mechanical structure that provides a supportive structure for the rest of the body. Bone consists of organic and inorganic materials [10]. The organic materials are mainly composed of collagen Type I [11]. The inorganic materials are composed of hydroxyapatite (HA) mineral [12]. The inorganic minerals provide bone strength and stiffness while the organic component provides flexibility and allows it to absorb energy [10], [13]. In terms of the microscopic observation, bone contains two levels, cortical and trabecular bone [14].

2.1.1 Materials and Structure of Bone

Normal bone is composed of different components including minerals, organic matrix, water and lipids. Minerals are among the major components as they account for 50 to 70% of the bone. Bone mineralization relates to the process of adding minerals to the matrix of the bone [13]. The main minerals in the bone are calcium and phosphorous with a small amount of magnesium and carbonate. Generally, the mineral content of bone is considered to be similar to hydroxyapatite (HA), $Ca_{10}(PO_4)_6(OH)_2$, which is the most important material in the mineral content of bone [12]. In bone mineralization, which is a common process in organisms across the animal kingdom, crystallization of calcium phosphate is regulated by bone forming cells that are called osteoblasts and deposited in precise amounts within the fibrous matrix of the bone. The precise amount of the minerals deposited in different tissues in the body help to provide rigidity in areas that they are laid down in high content, or

flexibility in areas that they are deposited in low amounts [15]. For instance, they are deposited in high amounts in teeth to help in withstanding heavy loads in chewing [16].

The process of mineralization is noted to be lifelong. McElderry in 2012, believed that mineralization triggered during fetal development where a complete cartilaginous skeleton that has joints and digits is formed by the eighth week of gestation [17]. It is important to note that the process of mineralization also plays a major role in tissue repair during fracture healing [18].

There are three main types of bone cells that are involved in bone growth, modeling, remodeling and repair: osteoblasts, Osteoclasts and osteocytes [15], [19].

Osteoblasts

Bones in a human body are under constant change. Various types of cells in the body are responsible for the changes that take place in the bones in relation to the age of a person, eating habits, lifestyle and exercise. Osteoblasts are one of the types of bone cells that are involved in the changes during bone formation [19]. Boskey in 2007, believed that these cells are responsible for producing the matrix making up the bone. They produce and package matrix to be laid down into the extracellular environment [20]. Osteoblasts are strategically positioned at the top or next to an existing bone. In this position, the matrix that they produce is effectively laid down on the bone where it becomes a new layer of the bone [21].

Osteoclasts

Osteoclasts function in such a way that they counter the activities of osteoblasts. According to Boskey, osteoclasts can be identified as reabsorbing cells [20]. They are derived from blood cells. They are involved in making and secreting digestive enzymes that

dissolve or break up the bone tissues [22]. The cells further take up the debris that has been broken down and dissolves it down inside the cell. The end products after the bone tissues are broken down are recycled to be utilized in other parts of the body [23]. For instance, the collagen is broken down into amino acids and used for building other proteins. The calcium and phosphate are also reused elsewhere in the body [15]. Just like osteoblasts, osteoclasts are found next to or on top of existing bone tissues. In this situation, they are able to effectively collapse the bone tissues that have been built by osteoblasts [21].

Osteocytes

Osteocytes are another type of bone forming cells that have been entrapped within the matrix of the bone. Osteocytes are derived from osteoblasts, which in the process of depositing bone tissues, become entrapped in the mineral bone matrix [24]. Osteocytes are involved in bone remodeling and repair and tend to balance the activities of osteoblasts and osteoclasts [21]. Osteoblasts, osteoclasts and various organs and tissues can communicate with each other through canaliculi to effectively perform their activities [25]. For instance, they can stimulate osteoclasts and osteoblasts or even inhibit them to effectively influence the repair and remodeling of surrounding bones. In the case where there is no effective communication by the osteocytes, it can lead to microdamage and eventual fracture or collapse of the bone under the load [26].

The activity of these three bone cells occurs within both trabecular or cancellous bone and cortical bone or compact bone in order to provide and maintain the structural strength of bone [15]. This structure of bone is based on the contribution of both trabecular, which provides an internal scaffold structure, and cortical bone that provides resistance to bending

and buckling. The human body consists of only two types of bone tissues that can be identified as trabecular bones and cortical bones (Figure 2-1).

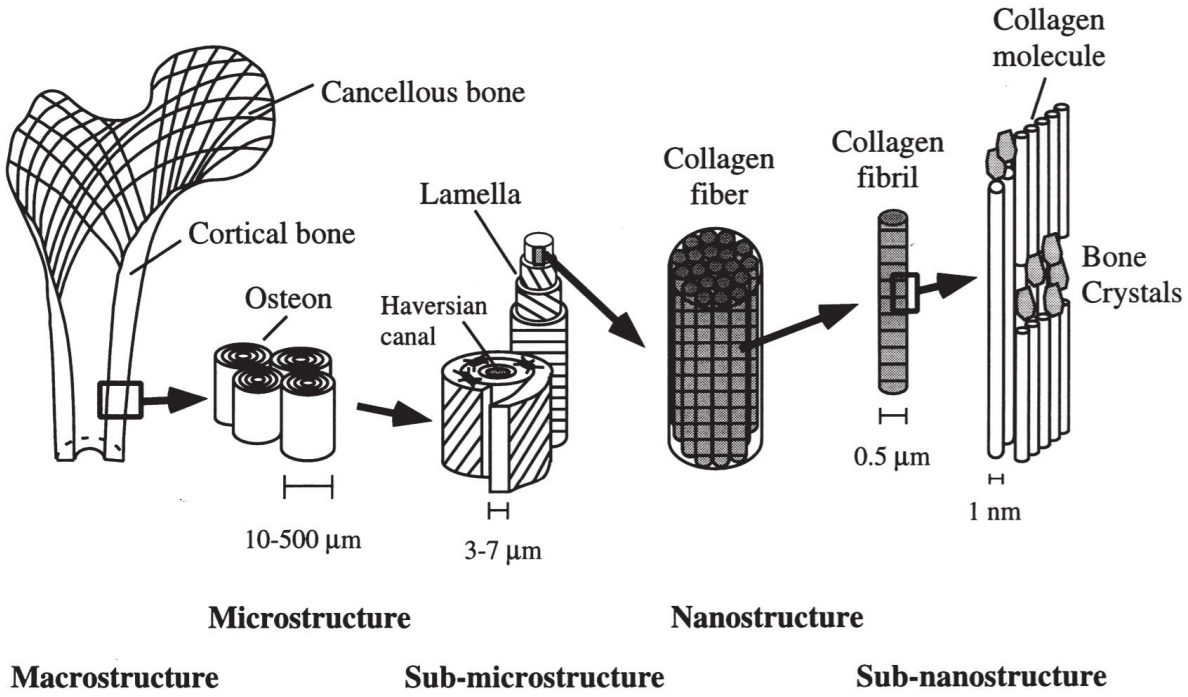

Figure 2- 1: The hierarchical levels of bone structure. Bone is divided into trabecular and cortical bone. Each component is made up of layers of bone tissue [27] with permission from Elsevier.

Trabecular and cortical bone

Cancellous bone also referred to as trabecular bone, is spongy in nature in relation to the fact that it has many open spaces connected by flat planes. They account for 20% of the weight of a human skeleton [28]. According to Keaveny, Morgan, Niebur and Yeh, in 2001, they exist at the ends of all long bones and those that are irregular and flat. They are found in features such as pelvis, spine, ribs, skull and sternum [29]. They are porous and contain red bone marrows that are responsible for the production of red blood cells. They also have stem

cells that are utilized in repairing and remodeling broken bones. Due to being porous and spongy, they are weak and hence easy to fracture. In addition to containing the red bone marrow and stem cells, just like the other types of bones, they are involved in providing structural support to the body [29], [30].

Cortical bones are known as lamellar or compact bones. They account for 40% to 60% of the human skeleton's weight [28]. They are the major part of long bones. Long bone's shaft such as the humerus and femur is one of the examples of this type of bone. They are strong, stiff, hard and dense and unlike the trabecular bones, they are difficult to fracture [31]. They are known to form the outer shell, also referred to as the cortex of most bones. Their major role is providing the body with structural support. They are also involved in protecting body organs, storing and releasing calcium and providing levers for movement. At their center, there is a canal consisting of blood vessels, bone marrow and nerves.

There are two major measurements of microstructures of cortical bone: cortical porosity and cortical thickness [32]. At the femoral neck, there is a significant regional difference in terms of cortical porosity and thickness. Superior cortex has a higher porosity [33] and thinner cortex [32] than inferior region. It was reported that femoral hips have higher porosity at superior region that inferior region [33]. Other study reported that with aging, cortical bone at superior region becomes thinner and leads to hip fracture, while the thickness of cortex at the inferior region does not change [32], [34], [35].

2.1.2 Hip Anatomy

The hip is one of the complex structures in the human body that is comprised of ball and joint structures. The design of the hip is very essential in terms of providing the stability of the human body [36]. Different muscles are connected across the hip, which allows human beings to perform a range of different activities such as walking, climbing stairs and squatting among others [37]. The hip is similar to other organs in our body, it has a unique anatomy that is responsible for its strength and flexibility as well as enabling it to bear weight and support movement [38]. In order to understand how the hip works, it is important to look at its structure by considering how the different layers are built and connected.

The acetabulum provides the stability in the hip [39]. Furthermore, stability comes from the joint capsule as well as surrounding muscles and ligaments [40]. The hip is formed at the point where the (femur) meets the pelvic bones (the ilium, ischium, and pubis) [39]. It is important to note that the legs are connected to the rest of the body at the hip joint. When the different bones meet in the body as joint, they are covered by articular cartilage [41]. The articular cartilage in the hips keeps movement easier by providing a smooth surface and absorbing shock [42]. The femoral head is connected to the acetabulum by the ligamentum teres ligament. It is a has a spherical shaped with a different diameter ranging from 40 mm to 60 mm [43].

Finally, the hip is comprised of muscles, blood vessels and nerves. These muscles are responsible for the movement of the hip as well as the position [37]. Nerves in the human body send messages from the brain to the hip muscles and signals back to the brain. Blood vessels also transport blood to the hip, helping with the flow of nutrients [44], [45].

2.1.3 Bone Quality

Bone quality determines whether bone will fail or not. Bones that are robust in nature will not fail easily while fragile bones are likely to fracture. Bone quality, therefore, can be compared to the quality of a bridge, its design, construction and its repair. Human bones just like the bridge require maintenance and repair so that they can handle the daily pressures from weights that are exerted on them without fracturing [46]. In general, bone quality is defined as ‘ the sum total of characteristics of the bone that influence the bone’s resistance to fracture”[47].

For bridge engineers, they use mechanical test to determine tensions and mechanical compressions by measuring the stiffness moduli at the early levels of bridge construction [48], [49]. The amount of mechanical stress and the mechanical strain that structural materials can handle as well as their stiffness is the key determent for best materials for bridges [50].

In terms of biological structures, bone quality is determined by structural and material properties that are influenced by bone turnover or remodeling. In the recent past, some group of biochemists have managed to develop biochemical markers of the bone turnover [51], [52]. Bone turnover or remodeling is a continuous process of bone formation in which old bones are reabsorbed and new bones are formed to replace them maintaining calcium homeostasis.

The bone mineral density (BMD), which counts to 70% for the variability in bone strength. BMD is measured by dual energy X-ray absorptiometry (DXA) to examine the distribution of areal bone mineral density (aBMD). T-score is used as the measurement to

represent the comparison of the mean of young adult with sex and race matched [53]. The lower BMD besides aging increases the risk of fracture [54].

Although BMD is considered as a good chance of bone quality, some bone quality components are independent of BMD. Age, past fracture history, bone disease like Osteogenesis Imperfecta, and low bone turnover contribute heavily to low bone quality and therefore the risk of fracture [49], [52].

Bone quality must be good to ensure that bones are strong and stiff to avoid failure [50]. Bone quality and quantity that is not normal can lead to increased bone fragility and high risk of fracture [55].

Bone structural properties include bone's geometry (size and shape) and microarchitecture; trabecular architecture and cortical thickness and porosity, while bone material properties include its mineral and collagen composition as well as microdamage [56]. The inclusion of these properties in addition to BMD will improve the properties of bone quality [57], [58].

2.2 Osteoarthritis (OA)

Osteoarthritis is the most common skeletal disorders related to aging [1]. OA is a joint disease that affects hips, hands and knees [59]. Hip OA is a common chronic degenerative joint disorder and cause of pain, stiffness and physical disability in the elderly population [1], [59]. It is characterized by cartilage degradation and subchondral bone. The formation of osteophytes that are associated with cartilage degradation leads to the osteophytic types of hip OA. Individuals with atrophic type of hip OA is characterized by the cartilage degeneration without the formation of osteophytes [60], [61].

The cause of this disease is still unclear. There are many risk factors have been identified for hip OA such as age, a history of hip injury, obesity, overuse, gender, heavy mechanical loads and joint trauma [62]–[64]. In addition to these risk factors, it is known that genes play a role in risk factors. Women have a high heritability estimate to suffer from OA, it is estimated that OA has 60 percent heritable [65]. Hip geometry also plays an important risk for hip OA, the differences in bone geometry of hip can influence the distribution of loading forces across the hip [66].

2.3 Hip Fracture

Hip fractures are a type of bone breaks that occur within the upper quarters of the femur. The anatomic location of this type of fracture is near the hip joint and classification of the specific type of hip fracture is based on the pattern of the fracture and whether the affected structure is the trochanter of the femur or the femoral neck [67]. Basically, the major types of hip fractures include the femoral neck fracture and the trochanteric fracture with the latter being classified as either subtrochanteric, greater trochanteric and intertrochanteric [68](Figure 2-2). The percentage of hip fractures is high among elderly people because of weakened bone structures and increased risk of falls [69]–[71]. It is estimated that the number of hip fractures worldwide will be doubled or tripled in the next 50 years [72], [73]. More specifically, women tend to have the highest percent risk of falling than men [73]. Other factors that increase the risk of hip fractures are low BMD, alcohol and tobacco consumption, smoking, and early menopause as these factors exposes individuals to osteoporosis which refers to the weakening of the bones [74]. Hip fracture that is caused from osteoporosis is the main concern for public health [74]. Bone geometry has been reported as a negative influence in risk fractures [75]. In addition, the decrease in bone mass

[76] in this region can be another factor to risk fractures. It is also estimated that the decrease of bone mass related to age is also a strong factor to hip fracture [77]. De Laet estimated that the risk of the fractures would be increased 13 times from 60-80 years, however, this number would be doubled with the contribution of decreased BMD [78]. Therefore, changes in bone microarchitecture are also important [79].

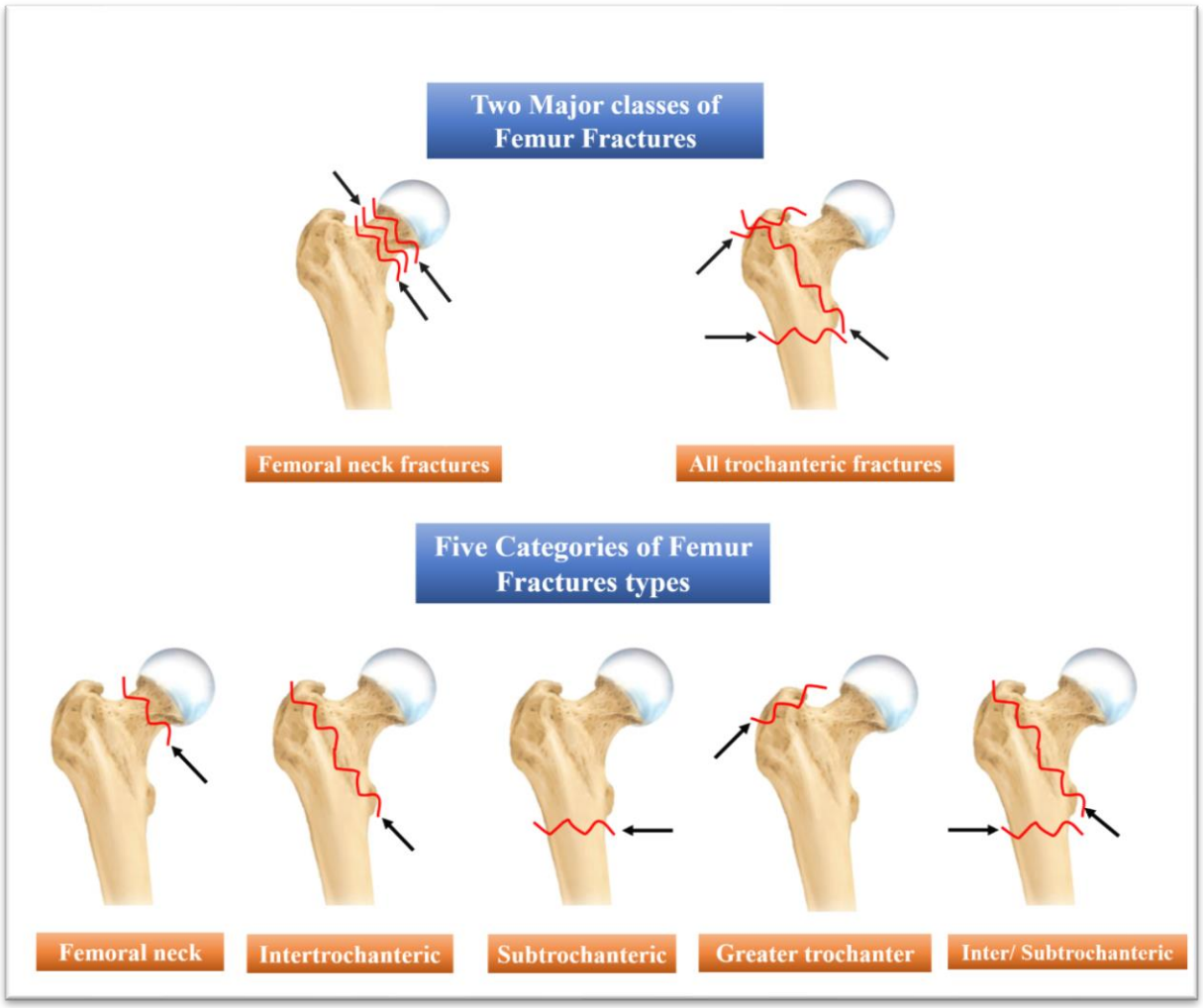

Figure 2- 2: Types of Hip Fracture. Modified from [67]. Open Access article with permits unrestricted use.

According to Carpintero in 2014, the medical complications that are likely to result from hip fractures include neurological and cognitive alterations. Complications arising from surgical treatment as well as the social implications are associated with hip fractures impact negatively on the lives of the affected individuals [80]. According to Carpintero in 2014, complications associated with this condition also arise due to surgical treatment and procedures [80]. For instance, dependency [81] and death [71] are associated with hip fracture. Therefore, hip fractures are important as far as affecting the elderly in the society are concerned [70]. It is also important to note that while this condition is highly common among the elderly, the rest of the population is also at risk because of the various risk factors.

2.4 Assessment Techniques of Bone Quality

Two properties that determine bone quality in addition to BMD: its structure including bone microarchitecture, and materials properties, including its mineral and collagen composition as well as microdamage [56]. New techniques to assess these properties of bone quality are being developed (Figure 2-3).

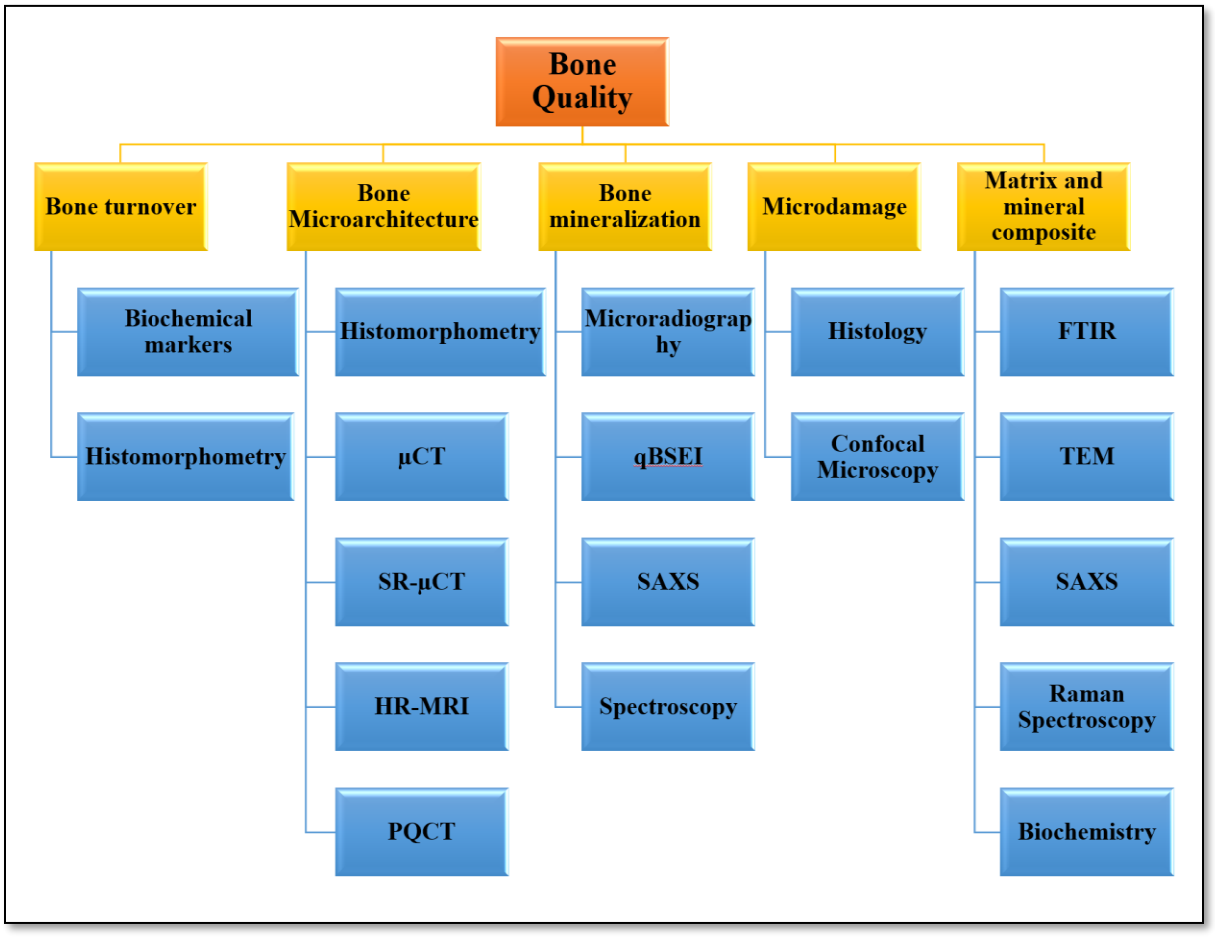

Figure 2- 3: Determinates and assessment of Bone Quality [82].

2.4.1 Assessment of microdamage

Microdamage is generally defined as cracks detected by light microscopy. It consists of microcracks and microfractures [82]. Although both of these two properties are a form of microdamage, their effects on bone quality are unclear. The relationship between these two properties is unknown and the accumulation of microdamage may result from increased secondary mineralization, making the bone more brittle [26]. Some techniques demonstrate the presence of microcracks that are produced in vivo in bone during life. In 1960, Frost was the first person who proposed a technique using bulk staining of bone to distinguish the source of microdamage before the preparation of a thin slice [83], [84]. Thirty years later, Burr and Stafford designed an experiment that clearly showed that Frost's staining technique is able to separate bone cracking that occurred by mechanical loading [85]. They tested microcracks of human rib that were bulk stained either before preparation of a thin slice or stained after grinding and both cases had the same number of total cracks [84].

Schaffler used a different experiment of this technique to provide visualization of bone microdamage at the ultrastructural level [86]. He observed a good correspondence at the light microscopic level with damage levels reported previously by Frost and Burr and Stafford [84] when he stained human ribs with lead-uranyl acetate.

Microdamage accumulation has been proposed to be a risk factor that might lead to increased bone fragility with age [83], [84]. Increased bone microdamage in the elderly has been reported in several locations. Frost was first claimed that microdamage appeared to accumulate in the human rib after the age of 40 [83], [84]. However, microcracks in the femoral head were double in women between the ages of 46 and 78 [84]. Femoral mid-diaphysis of both men and women reported rapidly increased damage, especially after the age

of 40 years [87]. Generally, the increase in damage with age in women is 50% faster than in men. To sum up, assessment of microdamage can currently be made only by histological techniques.

2.4.2 Assessment of bone mineralization, mineral composition and matrix

There is not enough evidence known about how bone matrix and mineral composition that contribute to bone quality. It is likely that when changes occur in collagen structure or mineralization, one or both are affected since they are associated [88]. Mineralization of bone matrix consists of two phases; primary and secondary mineralization. The primary mineralization occurs when the bone mineral is deposited during the bone remodeling cycle [83], [89]. To clarify, it happens when the new collagen matrix starts to mineralize fast and represents 50% to 60% of the mineralization. The secondary mineralization describes the process of mineralization after the remodeling process has been finished. When the amount of mineralization increases, bone tissue becomes more brittle and needs less energy to fracture [89]. Therefore, hypermineralized bone becomes more fragile than a bone with a lower degree of mineralization [90].

Assessment of the degree of bone mineralization and its distribution can currently be measured ex vivo by several techniques including quantitative back-scattered electron imaging (qBSE) and spectroscopic techniques. Raman and Fourier's transform infrared spectroscopy (FTIR) and transmission electron microscopy (TEM) are new techniques to study an ex vivo bone matrix and composition [56].

Hong and Kohn studied collagen fibrils and apatite crystals in fatigued and non-fatigued mouse femora. Samples were examined for the ultrastructural damage using high-

resolution transmission electron microscopy (HRTEM) [91]. In the fatigue femora, the arrangement of collagen fibrils appeared to be damaged and non-uniformly distributed and short. Based on their images, they suggested that some apatite crystals were broken into small pieces and a fraction of crystalline mineral apatite became amorphous during fatigue. According to Camacho in 1999, mineral crystallinity and orientation increase with age [92]. These age-related changes in mineral are also accompanied by an increase in collagen [91].

2.4.3 Assessment of bone microarchitecture

Changes in bone microarchitecture can be an important contribution to bone quality. Cortical and trabecular architecture are both important. The number and thickness of trabecular bone, their connectivity and orientation contribute to bone quality, while in cortical bone, its thickness and porosity are the main determinants [56].

Some of these architectural properties can be assessed in histological sections of bone using 2-dimensional approaches. However, more newer methods have now been developed to provide 3-dimensional visualization and quantification [93]. These include high-resolution magnetic resonance imaging (HR-MRI), high resolution peripheral quantitative computed tomography (HR-pQCT), micro-CT (μCT) and synchrotron radiation μCT [94].

Images of Bone- High-Resolution Peripheral Quantitative Computed Tomography (HR-pQCT)

High-Resolution Peripheral Quantitative Computed Tomography (HR- pQCT) is a CT scanner that uses computerized processing of X- ray for providing detailed images of cortical and trabecular bone. It is a non-invasive technique used 3D evaluation of bone microarchitecture in vivo [9], [95]. It is also using for microarchitecture analysis and changes of large bone specimens. It can assess microarchitecture of bone and measure trabecular and cortical compartments of bone [96]. Bone samples can be scanned at voxel sizes of 41 μm [97]. From 2D slices, we can produce a 3D image.

Image Acquisition and processing

The standard protocol is typically conducted with the following settings: X-ray tube current = 95mA, X-ray tube potential = 60 kVp, voxel size = 82m, and a 1536 × 1536 matrix [97], [98]. Prior to scan acquisition, the specimen initially is fixed in a carbon fiber shell that is fixed within the scan gantry to avoid artifacts resulting from motion, which could lead to the need for rescanning. An estimated image is obtained so that the operator can mark a reference line at the specimens. After the specimen is scanned, a scout view (2-dimensional X-ray scan) is acquired to establish a region of interest for the 3D evaluation [99] (Figure 2-4. B).

A scan takes 2.8 minutes to obtain an axial of 9.02 mm of one site, including 110 computerized tomography slices in the only currently available commercial system (XtremeCT; Scanco Medical, Brüttisellen, Switzerland) [100] (Figure 2-4. A).

After the acquisition of images is completed, the system automatically performs an initial evaluation consisting of two processes. First, processing of digital data in cross-sectional images (Figure 2-4. C). Second, construction of a 3D image [101] (Figure 2-4. D). Subsequently, it is important to determine cortical and trabecular compartments in order to evaluate them. The first contour is characterized by the outer contour of the specimen, which is then used to define the full compartment (Figure 2-4. C). Then, determine the inner contour defining cortical from trabecular bone, with the goal of obtaining isolated data relating to each of the compartments. This is a challenging process because the boundary is not always well defined.

The boundary between the cortical and trabecular compartments may be inaccurate when the cortex is thin or highly porous [101]. This procedure will automatically create the different compartments based on image processing [102]. The main parameters are defined in (Table 2-1).

Trabecular bone structure analysis

Bone grayscale images can be used to assess the microstructural properties of bone. Trabecular measurements are generally derived rather than directly measured from the images due to the resolution of HR-pQCT that is relatively similar to the size of individual trabecular [102]. Bone volume fraction (BV/TV, %) is determined from the trabecular volumetric bone mineral density assuming the density of fully mineralized bone is 1200 mg HA/cm3. The space between 3D ridges is calculated trough a distance transformation method [96]. The number of trabeculae (Tb.N, 1/mm) is defined as the inverse of the average spacing of the 3D ridges and it is directly measured [103]. Trabecular thickness (Tb.Th, mm) and separation (Tb.Sp, mm) are calculated by using semiderived methods (Tb.Th =

(BV/TV)/Tb.N and Tb.Sp = (1-BV/TV)/Tb.N) [102]. In addition to the standard manufacturer analysis, additional customized analyses can be performed on the trabecular region; such as individual trabeculae segmentation (ITS), connectivity, anisotropy, and structure model index [103].

Table 2- 1: The main parameters and their terminology, as used in the medical literature.

Parameter	Abbreviation	Description	unit
Bone volume fraction	BV/TV	Ratio of bone volume to total volume in region of sample	%
Trabecular thickness	Tb.Th	Mean thickness of trabeculae	mm
Trabecular separation	Tb.Sp	Mean space between trabeculae	mm
Trabecular number	Tb.N	Mean number of trabeculae	per mm
Connectivity density	Conn.D	Extent of trabecular connectivity normalized by TV	mm-3
Cortical thickness	Ct.Th	Average cortical thickness	mm
Cortical porosity	Ct.Po	Ratio between pore volume and total cortical volume	%

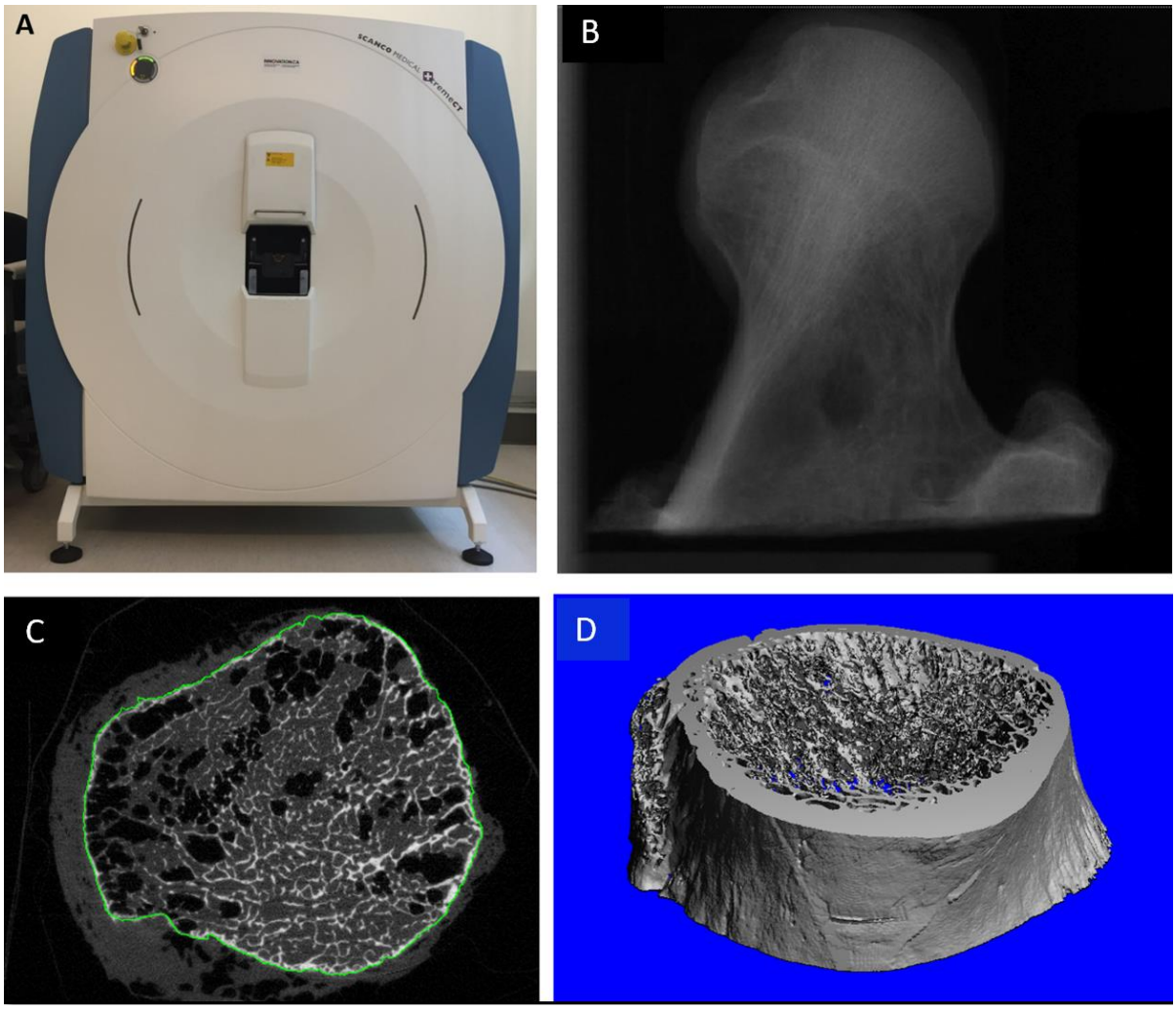

Figure 2- 4: High-Resolution Peripheral Quantitative Computed Tomography (HR-pQCT), XtremeCT, Scanco Medical. (A) Scanco XtremeCT HR-pQCT. (B) Scout view of proximal femur. (C) The sectional image of femoral neck, highlighting the trabecular in green. (D) a 3D model.

Cortical bone structure analysis

Cortical thickness (Ct.Th) can be measured directly as it can be well determined with HR-pQCT. However, depending on the compartment segmentation, derived Ct.Th measurements are also used. The direct measurement is based on a distance transform of the cortical region [103]. The derived measurement of Ct.Th is measured as cortical bone volume divided by outer bone surface [102]. Cortical porosity (Ct.Po) can also be measured from HR-pQCT images.

Clinical application related to age and sex and race

Many of the initial of HR-pQCT studies have focused on determining the age and sex related differences in bone microarchitecture.

Boutroy and colleagues have reported their first cross-sectional study on bone microarchitecture differences using HR-pQCT [104]. They found significant differences in bone microarchitecture when they compared premenopausal and postmenopausal women and those with osteoporosis. The first population HR-pQCT study to investigate the age related variation in both men and women (ages 21–97 years) concluded that the decline in BV/TV were similar between men and women but there were marked structural differences [105]. It was related to low thickness of the trabeculae in males, while in females there was a decrease in the number of trabeculae.

The differences in the structural basis of bone loss between men and women at both the radius and tibia was later confirmed by Dalzell and colleagues [106]. Canadian population-based samples between 20–99 years, reported as the most recent study that examined age and sex related variation with HR-pQCT in 2011. Boyd concluded that age related bone loss

varies not only between men and women but also between the cortical and trabecular compartments [107]. An increase in cortical porosity occurred with aging resulting in significant decreases in cortical bone density. HR-pQCT has also been used to provide bone growth analysis in children and adolescents [108]. Prospective study of over 100 boys found that those with fractures had lower Tb.BMD, Tb.N than boys without fractures of the same age. Ct.BMD and Ct.Th reported no difference between groups [109]. Furthermore, a large number of youth between 16 to 29 was examined at the radius and tibia by Lauren, David and Boyd in 2014 [110]. They reported that females had lower total area and BMD, trabecular BMD, T.N at the radius, Ct.Th and Ct.P. but higher cortical BMD. Three years later, they compared bone microarchitectural change between cross sectional and longitudinal changes in 466 subjects [111]. They reported in the longitudinal study that young people had higher total BMD, that started to decrease at the age of 40 years in females and 60 years in males. Subjects who are over 50 years old lost total BMD. This longitudinal data was similar to cross-sectional data for total density and cortical thickness at the radius and cortical density at the tibia [111].

Caucasian women have higher aBMD than Asian women and also have higher fracture rates that have been investigated with HR-pQCT. Studies have found that Caucasian women had less dense, and thinner cortex compared with Chinese women [112], [113].

Clinical application related to fracture

The main purpose of the clinical studies using HR-pQCT has been to examine associations with fracture, mostly in postmenopausal women with osteopenia and osteoporosis [114]–[116]. Two studies examined bone microarchitecture and fracture; they found that bone structure contributes to fracture risk independently of aBMD leading to the

importance of the structural information [117][118]. Comparing groups with hip fracture to controls, BV/TV, Tb.N, Ct.Th, and Ct.BMD were significantly decreased in fracture subjects than non fractures. When comparing wrist fracture with hip fracture, cortical parameters were significantly different [119].

Stein and colleagues compared postmenopausal women with and without previous fractures. They found that women with fracture had lower vBMD, more microarchitectural deterioration, and lower estimated bone strength by FE analysis [120]. Also, the severity of fractures has also been associated with bone microarchitecture. Cortical architecture was associated with the severity of vertebral fractures and was independent of aBMD in both women [114] and men [121]. In addition, postmenopausal women with vertebral fractures have found severe microarchitectural abnormalities compared with non fractures [116]. Nishiyama and colleagues studied bone microarchitecture of 44 postmenopausal women with previous low trauma fracture at distal radius and tibia [122].

Researches have studied the differences in bone microarchitecture between men with and without fracture [123], [124]. Vilayphiou compared men with and without fracture by matching age, height and weight. He demonstrated that microarchitecture and FE estimates of strength were associated with all different types of fractures [123].

Clinical application related to OA

Osteoarthritis has been an important area of HR-pQCT clinical applications, especially because this disease may affect bone quality differently. Boutroy and colleagues examined bone microarchitecture and OA in femoral neck [125]. They compared the distribution of cortical and trabecular bone between 2D histomorphometry and 3D imaging in the femoral

neck (~3mm thickness) of 21 hip osteoarthritis and 20 hip fractures. They found that there was significant correlation between 2D and 3D for trabecular bone volume, Tb.Th, Tb.Sp and Tb.N as well as Ct.Th. Cortical porosity did not report agreement between these techniques. Trabecular bone volume and trabecular connectivity were lower in hip fracture than in hip osteoarthritis [126]. Cortical thickness was reported to be lower in hip fracture than in hip OA at the inferior and posterior sectors [126]. They concluded that HR-pQCT results can confirm the results examined from histomorphometry.

2.5 CURRENT CHALLENGES

There is a lack of understanding on the effect of hip OA in bone quality in order to avoid the chance of risk fractures. The percentage of hip fractures is high among the elderly. However, it is estimated that the risk of the fractures would be increased with the contribution of hip OA. An increase of bone fragility and high risk of fracture can be caused due to the abnormalities of bone quality. Therefore, changes in bone microarchitecture the degree of mineralization are also considered to be important.

Together these results suggest that sex- and age-related differences as well as fractures, contribute to change bone microarchitecture and bone quality of the tibia and radius. However, few studies mentioned above have examined bone quality by HR pQCT in human femoral neck. Trabecular structure in femoral head with OA was studied but not in the femoral neck. The following chapter aims to provide our objective and hypothesis in this study.

CHAPTER 3: Hypotheses and Objective

As was mentioned previously, it is important to note that the comparison of bone structure between hip OA and non- hip OA samples using HR-pQCT has studied in either femoral neck or femoral head. The aim of this work is to provide a comprehensive study of bone microarchitecture and mineralization in the femoral head and neck together of OA and compare the result with control group in order to develop our understanding of bone quality in this disease.

Hypotheses

There are differences in bone microarchitecture at the proximal femurs of OA and control, and that trabecular and cortical bone microarchitecture are different in femoral head, junction and neck regions between OA and control and these differences are associated with hypermineralization of bone.

Objective

To assess bone quality by HR-pQCT and BSE among elderly with hip OA, and to investigate the difference of bone microarchitecture between subjects in the femoral head and neck. So far, no study has explained a detailed comparison of bone microarchitecture in femoral hips between OA and control. Secondly, to observe the distribution of hypermineralized tissue at the cortical bone in the femoral neck in OA using OM and BSE and compare the result to control group, which has previously reported by the author's lab.

CHAPTER 4: Materials and Methods

4.1 Specimens and sample preparation

Nine human proximal femurs (N=9, OA samples, three males and six females), with hip osteoarthritis were retrieved during total hip arthroplasty (THA) at the University of British Colombia Hospital; the mean age and standard deviation were (68 ± 9) years. Patients with OA were contacted two weeks before the total hip replacement to provide a written informed consent in this study. All procedures for the use of this tissue were approved by the Clinical Research Ethics Review Board at the University of British Colombia. During the surgery, OA hips were collected and doubled sealed in a box with ice to be shipped to the histology lab at the Center of Hip and Health Mobility. OA samples were fixed in 70% ethanol and dehydrated in ascending concentrations of ethanol (70, 80, and 90,100x2). OA samples were embedded in epoxy resin "EpoThin2, Buehler" for future histological analysis and HR-pQCT scanning (Figure 4-1).

Nine cadaveric femoral hips were collected from five female donors (aged 70 to 78 years) and four male donors (aged 64 to 73 years); the mean age and standard deviation were (71 ± 4) years. A summary of donor information is provided in (Table 4-1). T- scores was obtain by using dual energy X-ray absorptiometry (DXA) scans with a Hologic QDR 4500W bone densitometer (Hologic Inc., Waltham, MA) using the standard protocol for the proximal femur [127], [128].

Femoral head and neck segments were sectioned on a Buehler Isomet 4000 saw (blade speed: 2500 RPM, feed rate: 3 mm/min). The samples were then carefully sealed and

wrapped in a plastic bag to prevent tissue contamination in preparation for HR-pQCT scanning. The rest of bone tissues were kept frozen at -20 °C for future studies.

Table 4- 1: Summary of proximal femur samples donors. Mean ±SD (70 ± 7) years.

Age	Sex	Category	Weight (kg)	Height (cm)	Side
73	Female	OA	61	168	Left
74	Female	OA	-	-	Left
57	Female	OA	86	170	Right
59	Female	OA	59	165	Left
69	Female	OA	64	168	Left
89	Female	OA	64	157	Right
63	Male	OA	86	172	Left
67	Male	OA	104	178	Left
65	Male	OA	82	183	Left
73	Female	Control	56	168	Left
74	Female	Control	65	165	Left
78	Female	Control	54	154	Left
70	Female	Control	89	170	Left
74	Female	Control	57	167	Left
66	Male	Control	55	182	Left
64	Male	Control	43	193	Left
73	Male	Control	53	173	Left
71	Male	Control	77	193	Left

(Data not available represented by -), Osteoarthritis (OA) mean ± standard deviation (68 ± 9) years.

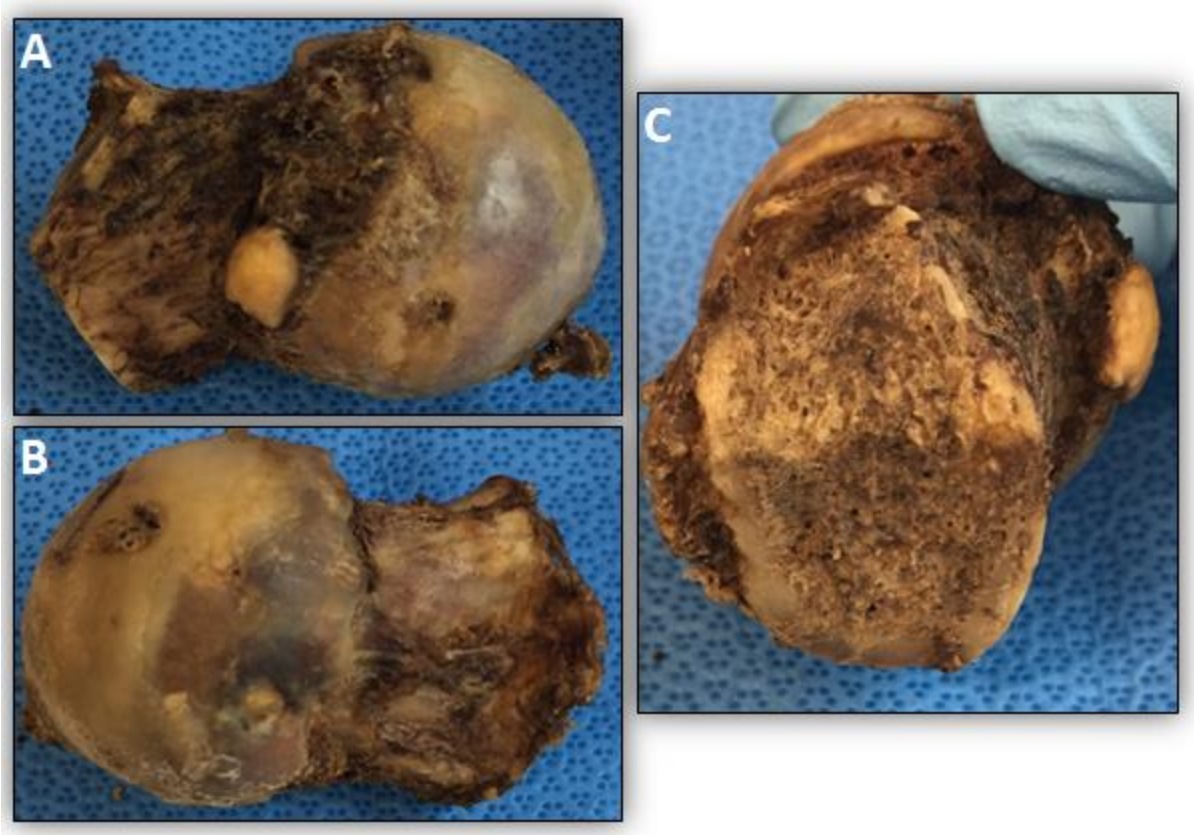

Figure 4- 1: Left side of fixed and dehydrated OA femoral hip and neck. (A) Posterior view. (B) Anterior view. (C) Cross-sectional view of femoral neck.

4.2 Imaging Technique and Processing

HR-pQCT imaging and scanning

Femoral bone samples were scanned using the first-generation HR-pQCT scanner (XtremeCT, Scanco Medical, Brüttisellen, Switzerland). The standard manufacturer protocol for ex-vivo scanning was used (60 kVp, 1000 µA, 300 ms integration time) at voxel size of 41 mm. The reference line was placed at the most proximal point of the femoral head in scout view (Figure 4-2). Scan length varied between samples due to their sizes, mean = 60 mm,

resulting in 1603 slices and the approximate scan time was one hour. The Femoral hip samples were aligned in their original transverse cross-sectional orientation as shown in the scout view.

After HR-pQCT scanning was completed, specimen's subsections were taken from anterior-posterior CT slice. According to the bone microarchitecture regional differences in proximal femur, samples analyses were divided into three regions (femoral head, head-neck junction, and mid neck), as described in (Figure 4-3). The regions of interest (ROI) representative of both trabecular bone and cortical bone for each sample was identified in 2-Dimensional CT images (grayscale image) by creating contour outlines of the both region by using software μCT Evaluation, version 6.6 (Scanco XtremeCT).

The following outcome parameters for trabecular bone microarchitecture were measured in each ROI. Bone volume fraction (BV/TV) was determined by bone connectivity density (Conn.D), which is the extent of trabecular connectivity. Trabecular numbers (Tb. N), trabecular thickness (Tb.Th) and trabecular separation (Tb.Sp).

For cortical bone microarchitecture parameters, cortical thickness (Ct.Th) and cortical porosity (Ct.Po) were measured only in the femoral neck region of both groups.

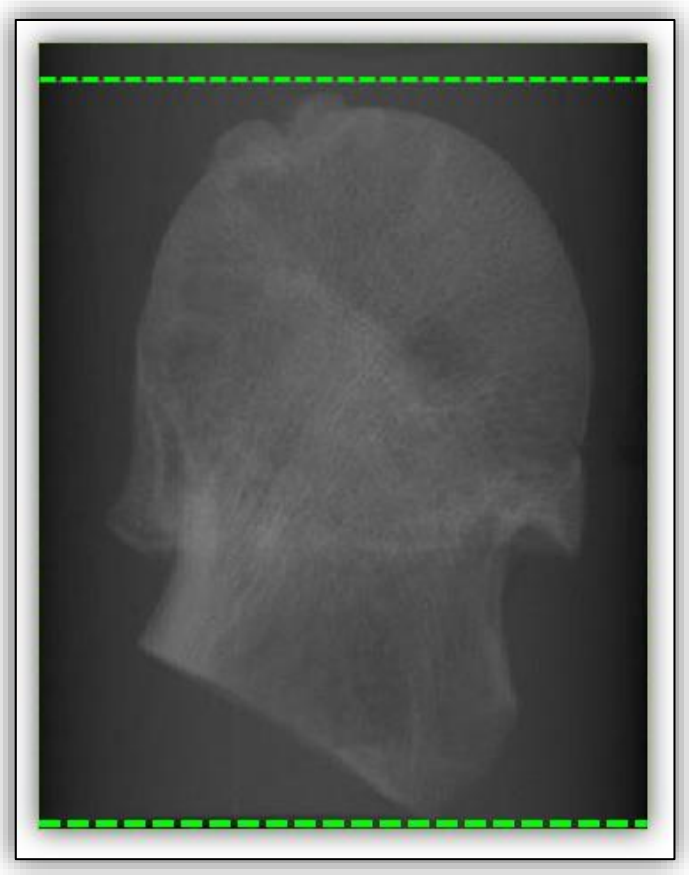

Figure 4- 2: A scout view of the femoral hip OA. The scan was occurred between the dashed green lines. The reference line was placed at the most proximal point of the femoral head and ended at the most distal point of OA specimens.

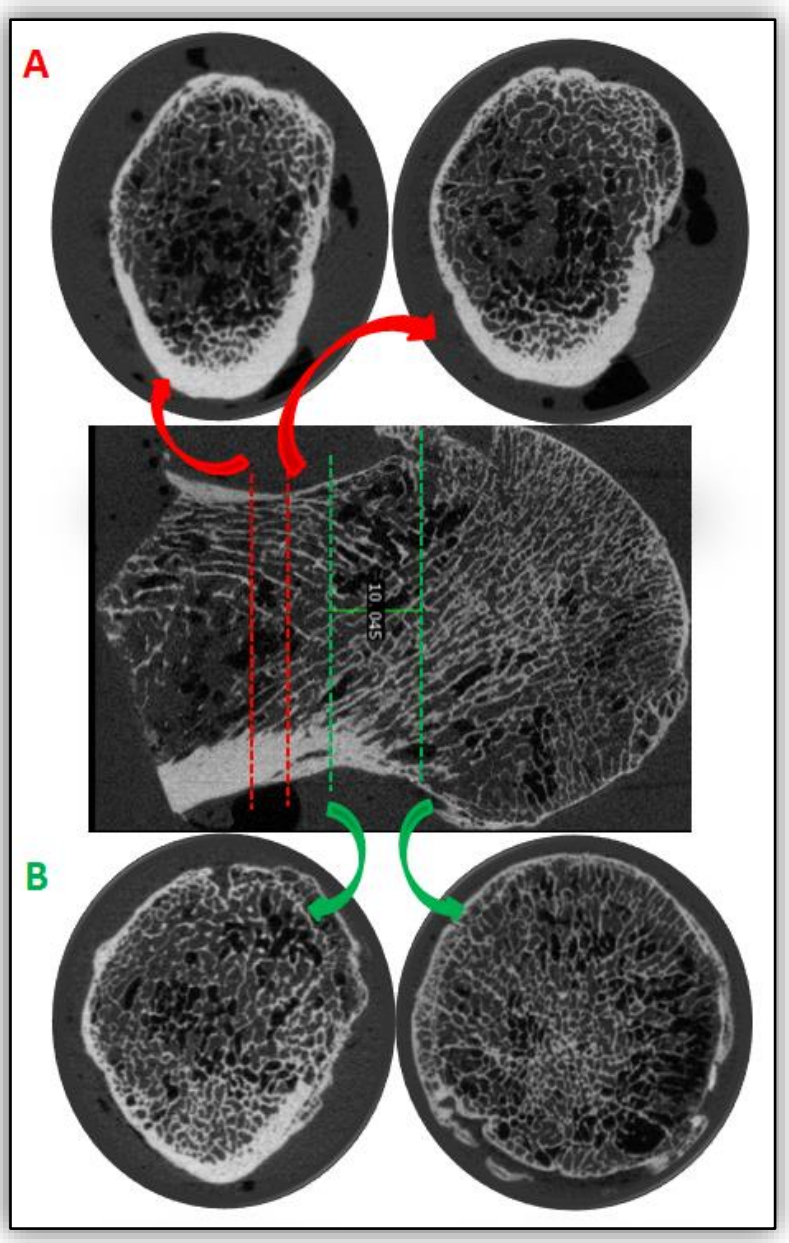

Figure 4- 3: HR-pQCT images of the femoral hip of a female patient with OA. The figure shows subsections of the evaluations regions. (A)- Femoral mid-neck (5 mm); with two-dimensional greyscale slices showing the starting and ending point. (B)- Femoral head-neck junction (10 mm); with two-dimensional greyscale slices showing the starting and ending point.

4.3 Imaging Analysis and Evaluation

To evaluate cortical and trabecular compartment separately, cortical bone must be segmented manually. CT slices were visually matched between each region to have consistent regions of interest, leading to the length of head-neck junction was 10mm, resulting in 244 slices, and mid-neck was approximate 1 mm, resulting in 66 slices. (Figures 4-4 and 4-5) contain a description of the creation of the contour outlines in OA and control group in the mid neck.

A fixed threshold was used for trabecular bone analysis of all the specimens (255mg HA/cm3). To avoid errors in trabecular spacing measurement, we filled bone marrow spaces by using script for the binarization.

For the femoral middle neck, the region was segmented to evaluate the cortical and trabecular separately. Cortical bone was segmented manually from trabecular bone on a slice by slice.

4.4 Optical Microscopy (OM) and Backscattered Electron BSE Imaging

OM and BSE images were performed to identify the potential regions of hypermineralized tissue; which does not have typical lamellar structure, in the femoral neck of OA samples where the same region of the microstructure measurements were done. The images were performed only in the periosteal cortical bone, since hypermineralization tissue appeared on the periosteal surface. Initially, a thin layer (2 mm thickness) in the femoral neck of the embedded samples was cut by diamond saw using Buehler Isomet 4000 saw (blade speed: 2500 RPM, feed rate: 3 mm/min). A surface of full neck was cut into four sectors:

superior to anterior (SA); anterior to inferior (AI); inferior to posterior (IP); posterior to superior (PS) (Figure 4-6). Following by re-embedding in epoxy resin “EpoThin2, Buehler” and kept them cured overnight at room temperature. Samples were ground with a series of carbide sandpapers, and polished with a diamond suspension at 6 μm, and 1 μm (Figure 4-6). Each polished bone sector was first observed by using reflective light under a light microscope (Nikon Eclipse E600 or Nikon Epiphot 300). Various objective lenses of 5×, 10×, and 20× were used to provide the overview images, and to identify the regions of hypermineralized tissue. Afterward, a quick survey to identify the hypermineralized tissue was done using backscattered electron (BSE) imaging (FEI Quanta 650, Oregon, USA) with the accelerating voltage was kept at 20 kV and various working distance. Then, for a close-up observation, the samples were coated with carbon for automated digital scanning electron microscopy (SEM) using backscattered electron (BSE) imaging with the accelerating voltage at 20 kV and working distance was 15 mm. In order to montage the entire region of each sector of the femoral neck in BSE, we used external control software (ESPRIT 2, Bruker) for taking images at a magnification of 50× (1536 pixels × 1326 pixels). The OM and BSE images were used for morphological observation of the distribution of hypermineralization around the femoral neck in OA.

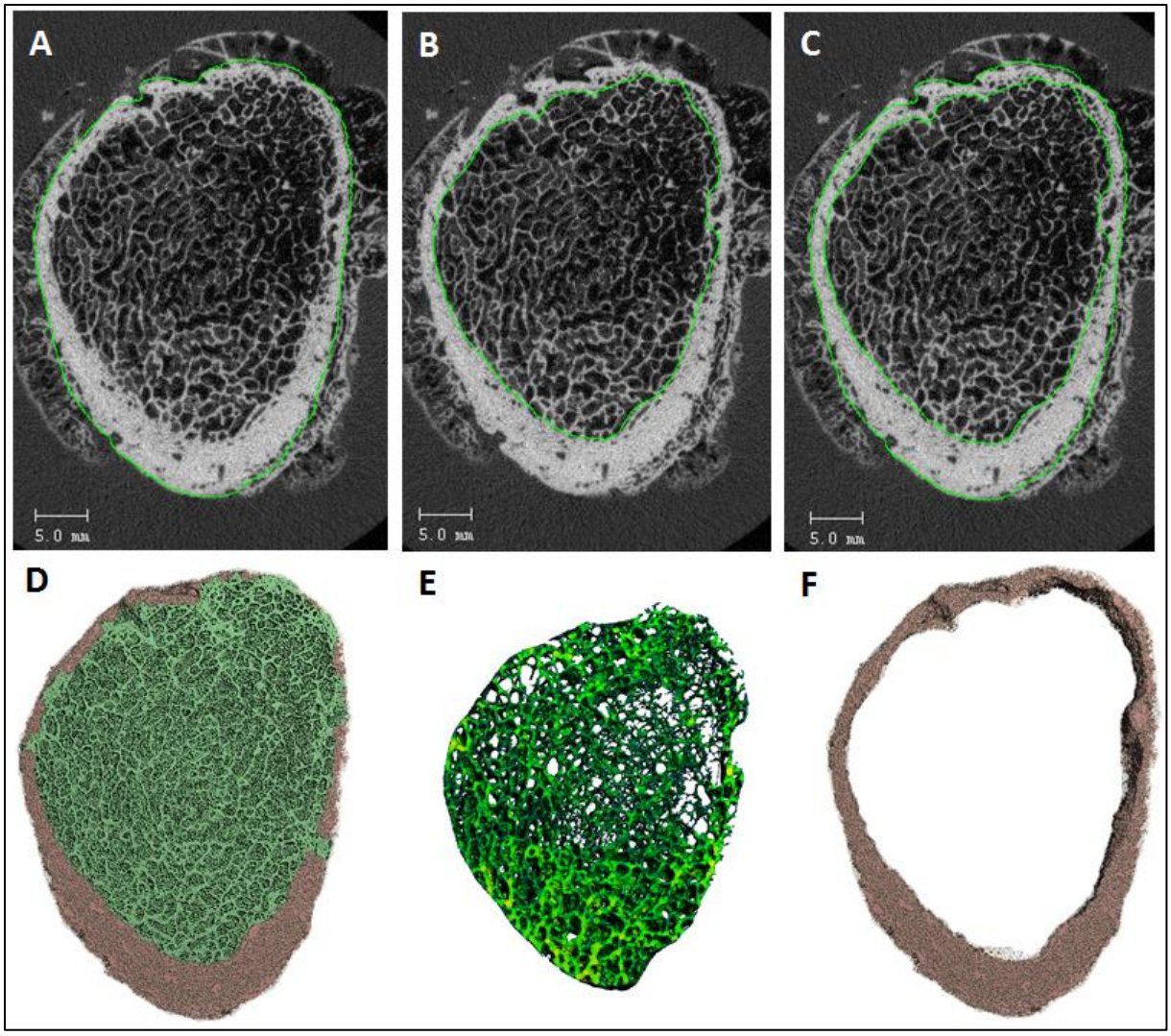

Figure 4- 4: An example of HR-pQCT analyses on the femoral neck with OA. (A)- Outer-contouring process with correction, (B)- Semi-contouring process with manual correction and (C)- cortical contouring. (D -E) 3-D trabecular and cortical segmentation.

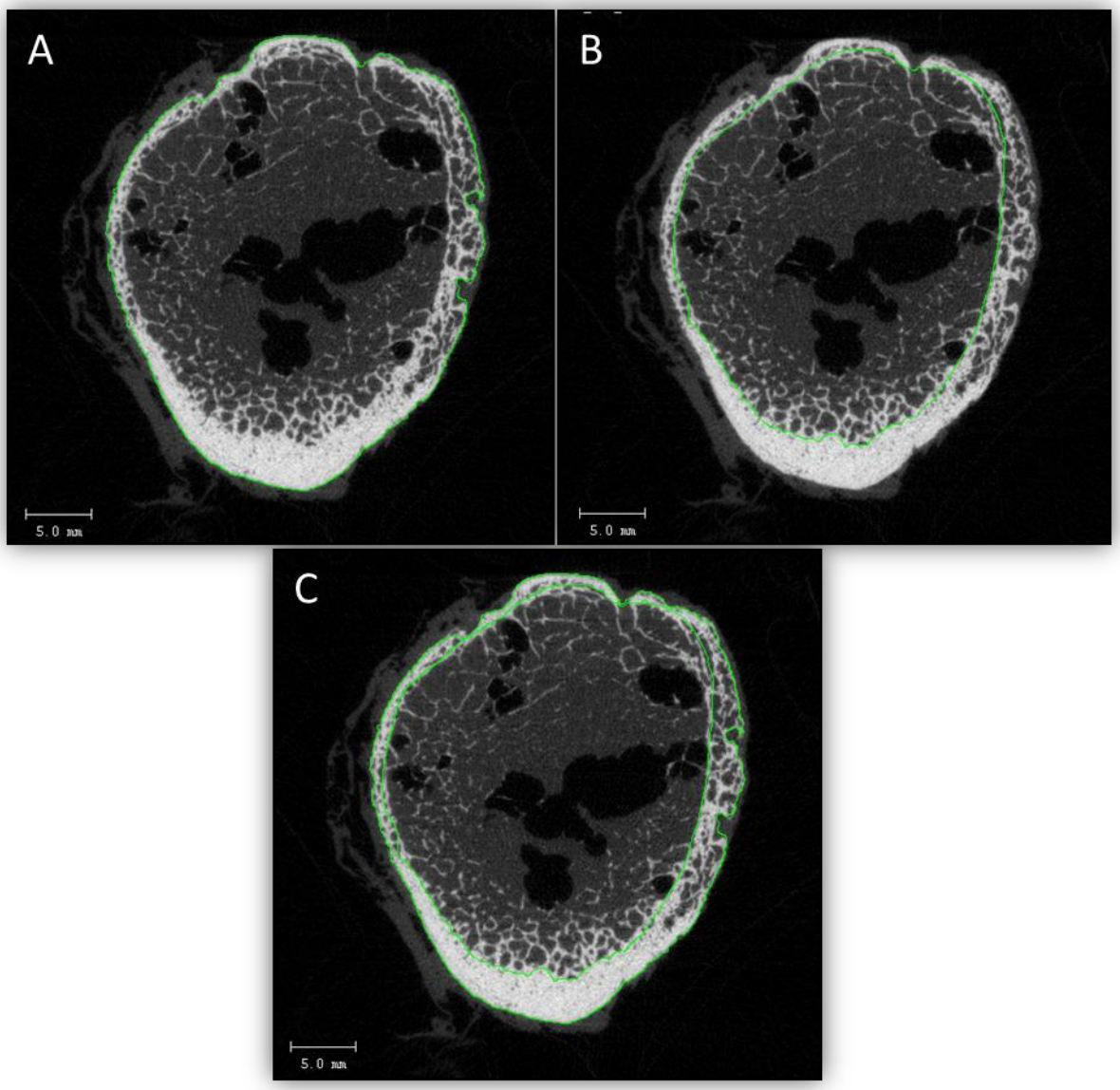

Figure 4- 5: Another example of HR-pQCT analyses on the control sample of femoral neck. A) outer- contouring process with correction, (B) Semi-contouring process with manual correction and (C) cortical contouring.

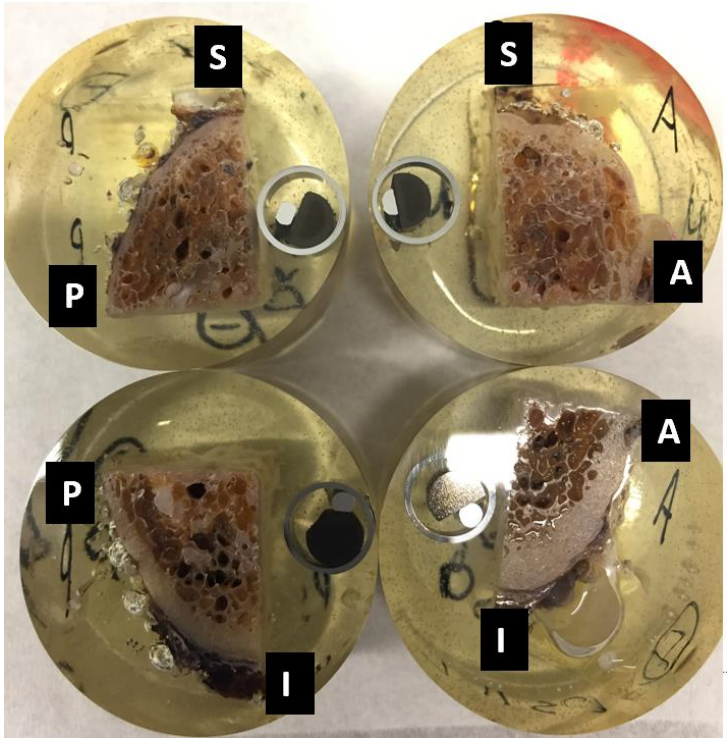

Figure 4- 6: A digital image of an embedded femoral neck sample in OA. Sample was divided into four sectors for OM and BSE analysis (superior to anterior (SA); anterior to inferior (AI); inferior to posterior (IP); posterior to superior (PS).

4.5 Statistical Analysis

Mean and standard deviation of the standard HR-pQCT parameters of the three segments were calculated. The Comparison between OA group and control group was performed by two-sample *t*-test with significance level at $\alpha = 0.05$. Microstructural differences between the three regions within the same group were tested by the analysis of variance (ANOVA). Linear regression was used to determine the (r) Pearson's correlation coefficient between BV/TV and other bone misconstruction parameters at $\alpha = 0.05$ to check if linear regression slopes were significantly different. Statistical analyses were performed using Microsoft Excel and SPSS software.

CHAPTER 5: Results

The following data represented the results of hip OA and control group. Firstly, qualitative comparisons were observed between OA and control group from scout views and 2D CT imaging. Secondly, the quantitative analysis was obtained from 3D parameters. Consequently, the correlation between BV/TV and bone microstructure parameters was calculated. Lastly, hypermineralized tissue was observed at the cortical bone around the entire femoral neck in OA.

5.1 Morphological Difference between OA and control groups

A qualitative comparison between hip OA and control is provided first based on visualization of representative scout views as well as grayscale cross- and longitudinal-section. From the scout view (AP view), the formation of osteophytes in OA patients started at the junction region while it was not observed in control specimens as it is shown in (Figure 5-1).

For the longitudinal- section view, OA samples had a short length of the neck due to a hip replacement surgery, which was challenging to adjust the same location (Figure 5-2). The longitudinal section produced distinct observations between cortical and trabecular regions. As a result of osteophytes, OA samples represented a less uniform head surface compared to control. In addition, the cortical region was unclear to visualize in the superior side of the mid neck of OA. Compared to OA, the cortical region in the mid neck in the inferior side of control sample is thinner than OA. Trabecular bone on the other hand had a clear observation in the longitudinal section of both cadaveric and OA hips. The distribution of trabecular region was clearly observed in hip OA than control indicating that the trabecular factors were

higher in OA group (Figure 5-2). Compared to control samples, the trabecular region was denser in the femoral head of OA. No visual differences could be detected in the trabeculae thickness between two groups. Therefore; each parameter of both trabecular and cortical bone was tested separately for agreement. From the grayscale cross-sectional of each segmented region in both cases, the presence of osteophytes started to form from the junction region and moving to the neck region, while no visual differences could be detected in the head region (Figure 5-3). Similar to the longitudinal section, there were no visual variations between groups for the trabeculae thickness in all three regions. However, the trabecular region in the femoral mid neck was less amount in control patients.

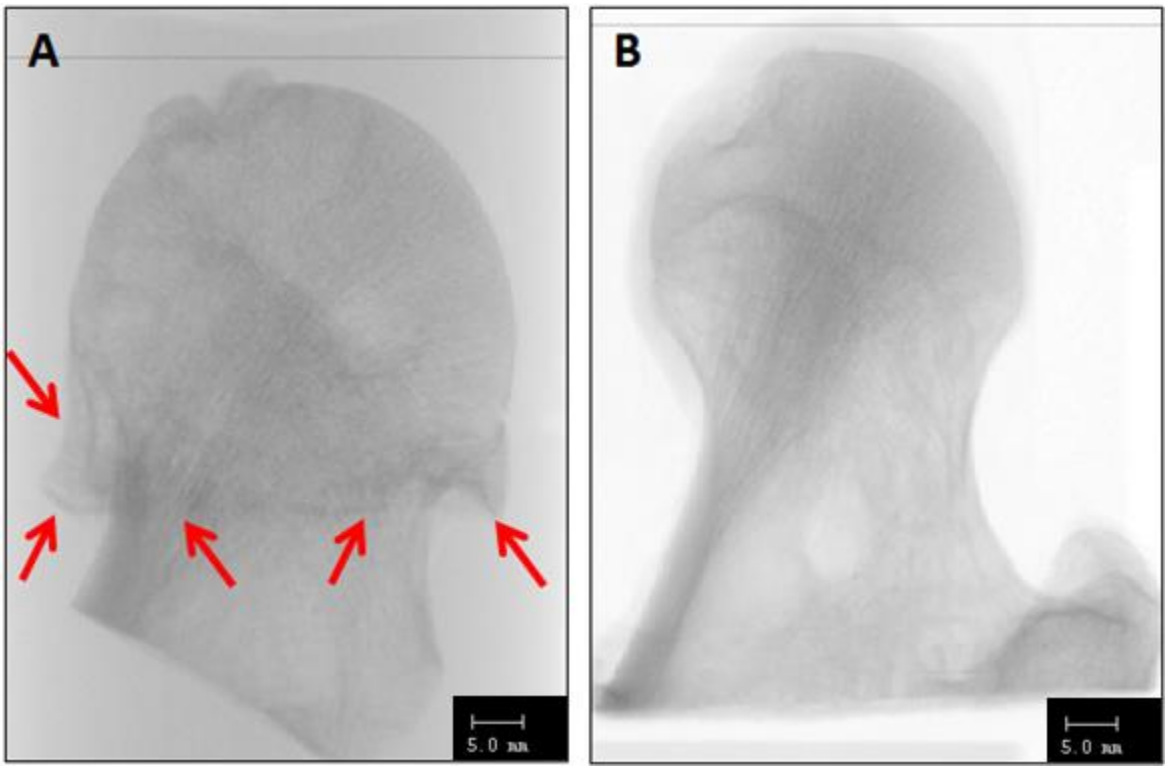

Figure 5- 1: Scout views of a human proximal femur. (A)- OA hip with a large number of osteophytes as indicated in red arrows. (B)- Cadaveric hip with complete femoral neck.

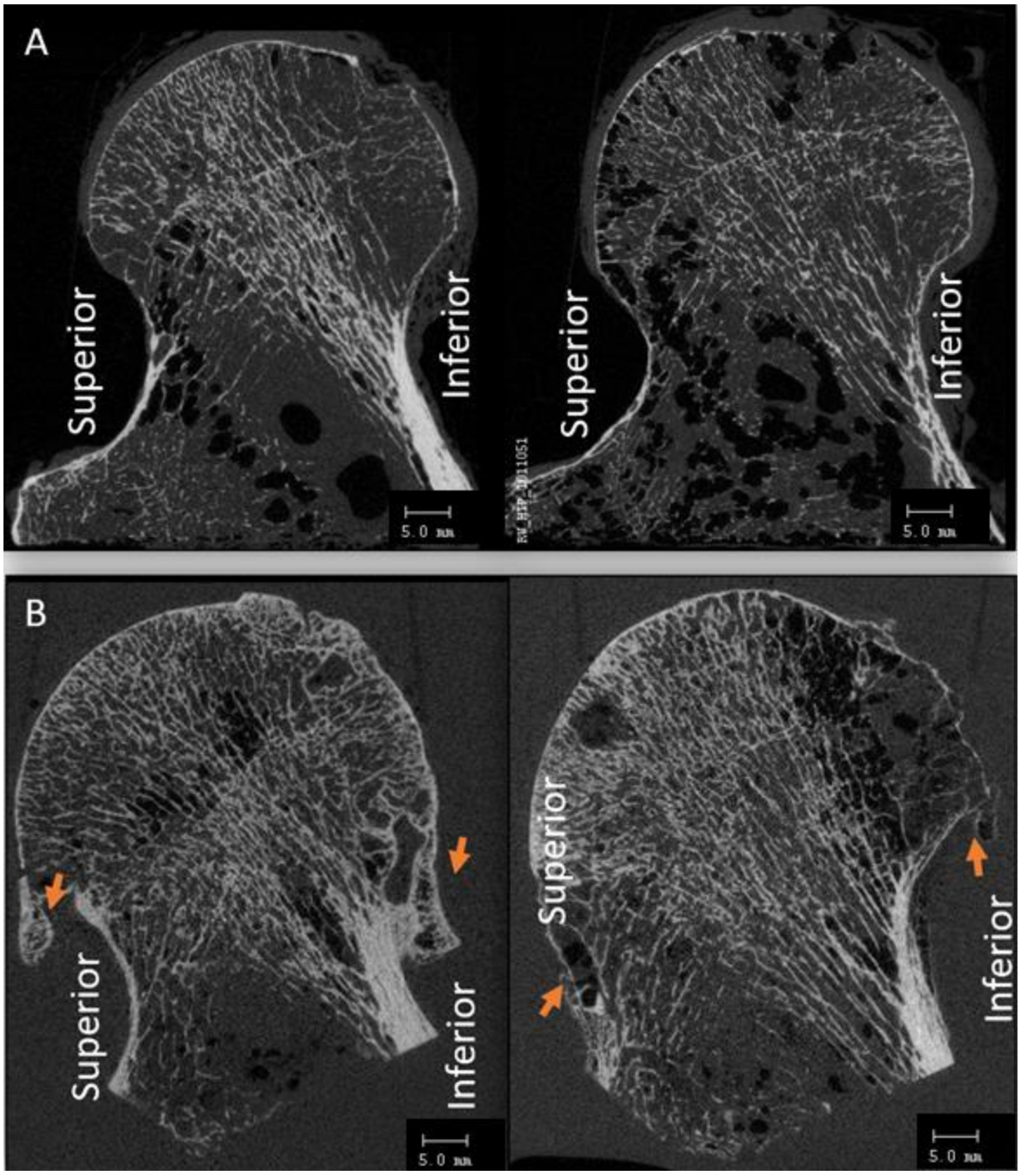

Figure 5- 2: longitudinal section of human femoral hips (AP views). (A)- Cadaveric hips of two different patients indicating the loss of trabecular bone and the cortical thickness. (B)- Hips with OA of two different patients representing severe deformities and a large number of osteophytes indicated in arrows.

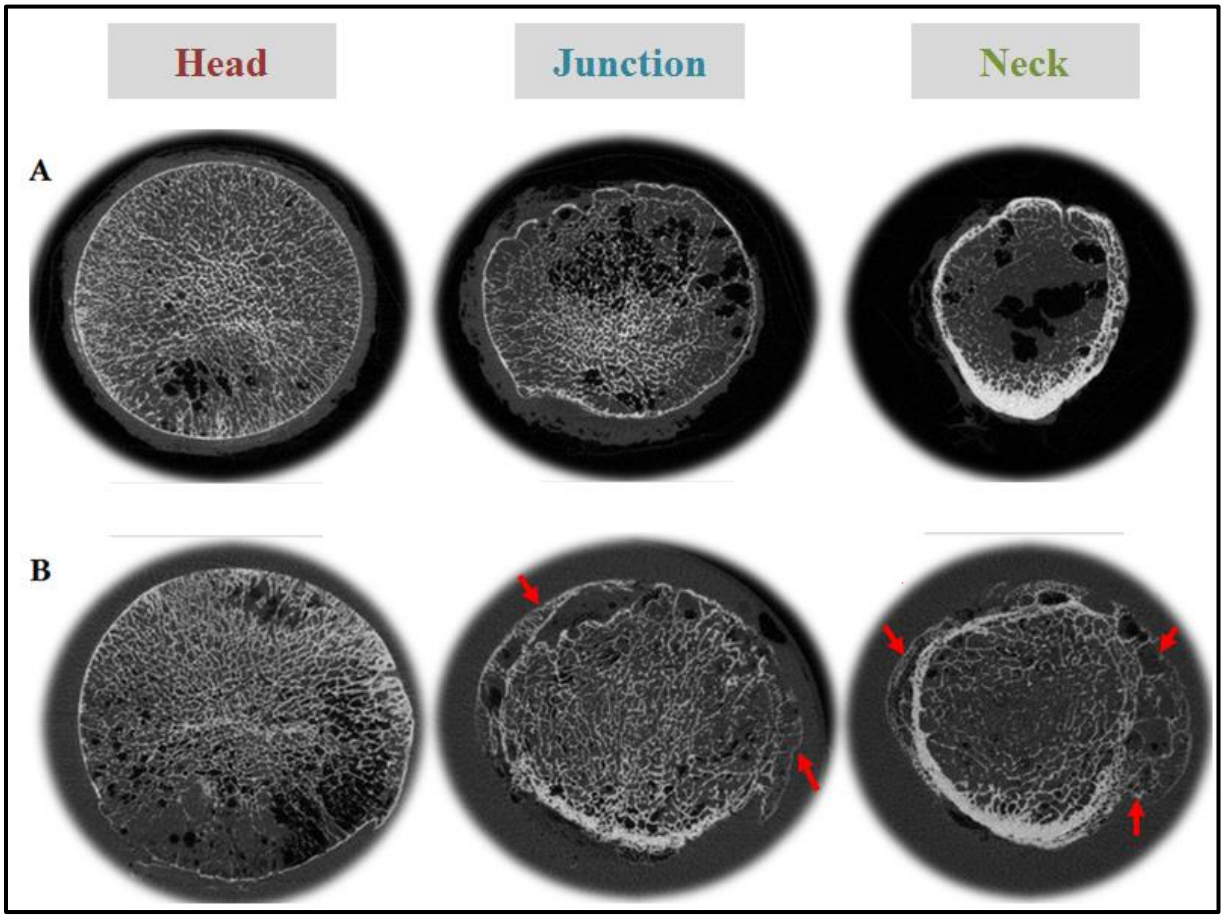

Figure 5- 3: Grayscale Morphology of Cross-sectional between OA and control along the three regions. Top row (A) indicating femoral control hip. The bottom row (B) representing hip with OA. Osteophytes were found in OA images (B) at the junction and neck regions in red arrows.

5.2 Differences in 3D Parameters between both groups

5.2.1 Bone Volume Fraction

For the quantitative comparison, bone volume fraction (BV/TV) showed an increase in hip OA than in control, but it was not significant with a 95% confidence level (Table 5-1). As shown in the bar graph (Figure 5- 4, C), the average BV/TV between the three regions was higher among the OA group (head 20%, junction 19%, neck 21%).

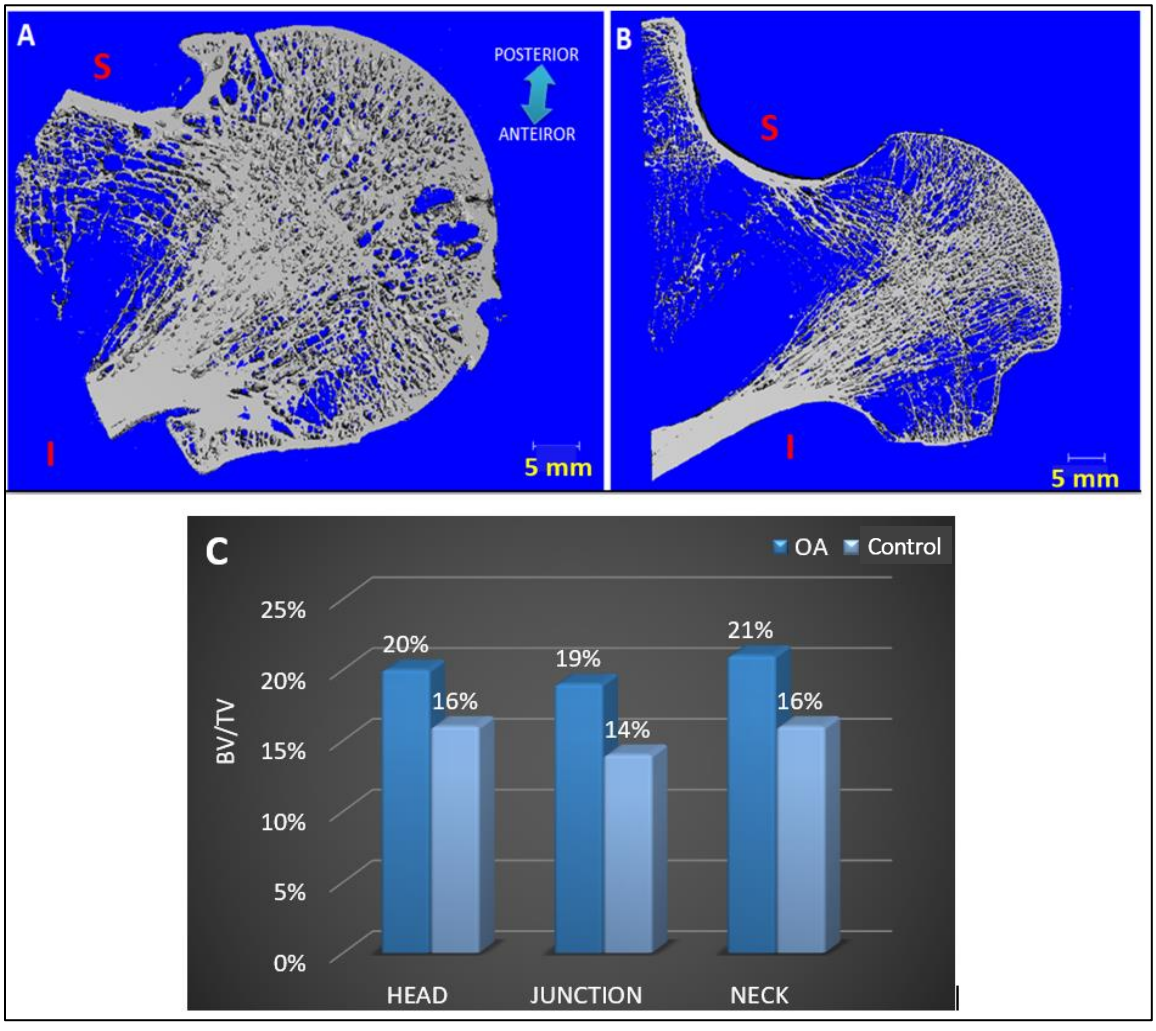

Figure 5- 4: BV/TV in all three regions between OA and control. (A-B)- 3D of hips OA (figure A) and Cadaver (figure B) were obtained using the "subdim" feature of the 3D evaluation program. (C)- mean values of BV/TV between groups in the three regions, OA samples had higher number than in control in the entire three regions.

Table 5- 1: Mean values ± SD and p-value in trabecular bone parameters between osteoarthritis and cadavers.

				OA		Control		P value (95% CI)
Head	Patients, n			9		9		
				3= male	*6=female*	*4= male*	*5=female*	
	Bone volume fraction %	BV/TV	*Ave*	20		16		*P >0.05*
			SD	3		5		
	Number of Trab. (1/mm)	Tb.N	*Ave*	0.54		1.20		*P <0.01*
			SD	0.07		0.3		
	Thickness of Trab (mm)	Tb.Th	*Ave*	0.23		0.23		*P >0.05*
			SD	0.02		0.02		
	Trab separation (mm)	Tb.Sp	*Ave*	2.30		0.97		*P <0.05*
			SD	0.28		0.36		
	Connectivity density (1/mm^3)	Conn-Dens.	*Ave*	3.12		2.09		*P <0.05*
			SD	0.89		0.56		
Junction	Bone volume fraction %	BV/TV	*Ave*	19		14		*P >0.05*
			SD	6		4		
	Number of Trab. (1/mm)	Tb.N	*Ave*	0.85		1.11		*P <0.05*
			SD	0.17		0.22		
	Thickness of Trab (mm)	Tb.Th	*Ave*	0.21		0.22		*P >0.05*
			SD	0.03		0.01		
	Trab separation (mm)	Tb.Sp	*Ave*	1.41		0.96		*P <0.01*
			SD	0.25		0.18		
	Connectivity density (1/mm^3)	Conn-Dens.	*Ave*	2.72		1.44		*P <0.05*
			SD	1.01		0.55		
Mid Neck	Bone volume fraction %	BV/TV	*Ave*	21		16		*P>0.05*
			SD	4		9		
	Number of Trab. (1/mm)	Tb.N	*Ave*	1.30		0.98		*P <0.05*
			SD	0.22		0.24		
	Thickness of Trab (mm)	Tb.Th	*Ave*	0.25		0.26		*P >0.05*
			SD	0.05		0.09		
	Trab separation (mm)	Tb.Sp	*Ave*	0.84		1.13		*P <0.05*
			SD	0.15		0.27		
	Connectivity density (1/mm^3)	Conn-Dens	*Ave*	2.54		1.41		*P <0.05*
			SD	0.66		0.89		

5.2.2 Trabecular Bone Microarchitecture

In both femoral head OA and control (Table 5-1), there was a highly significant difference in trabecular number ($P<0.0001$), trabecular separation ($P<0.0001$), and connectivity density ($P<0.01$) between OA and control group. Trabecular separation and connectivity density were significantly higher in OA (2.3mm, and 3.12 (1/mm3) respectively) than in control (0.97mm, and 2.09(1/mm3) respectively), but the trabecular number was significantly lower in OA than in control (0.54 (1/mm) and 1.2 (1/mm) respectively, $P<0.0001$). A non- significant difference was found in trabecular thickness (Tb. Th) between OA and control (0.23mm and 0.23mm, respectively). Figure (5-5) shows an example of trabecular microstructure parameters in the femoral head section with a representative 3D model of both subjects.

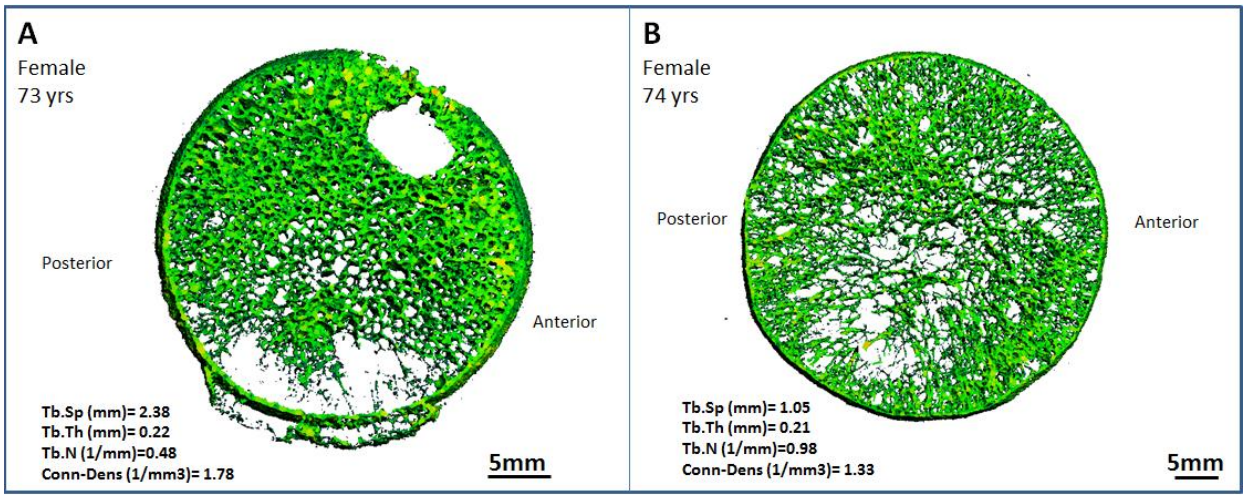

Figure 5- 5: 3D images at the femoral head region of OA and control shows the BV/TV related to different trabecular parameters. (A) OA femoral head in a woman with 73 years old indicating high amount of trabecular spacing and low number of trabeculae. (B) Femoral head of a woman with 74 years old (control sample).

In the junction region (Table 5-1), trabecular number (Tb.N), trabecular separation (Tb.Sp), and connectivity density (Conn.D) were significantly different between subjects with 95% confidence. Trabecular separation was significantly higher in OA than in control (1.41mm, and 0.96mm respectively, P<0.0001), as well as in connectivity density (2.72(1/mm3) and 1.44(1/mm3) respectively, P< 0.01). However, the trabecular number was significantly lower in OA (0.85 (1/mm)) than in control (1.10(1/mm)), (P< 0.01). In contrast, agreement between results in trabecular thickness (Tb. Th) for the same region in both subjects was found with a non- significant difference. Figure (5-6) shows an example of trabecular microstructure parameters in the junction section with representative 3D model of both subjects.

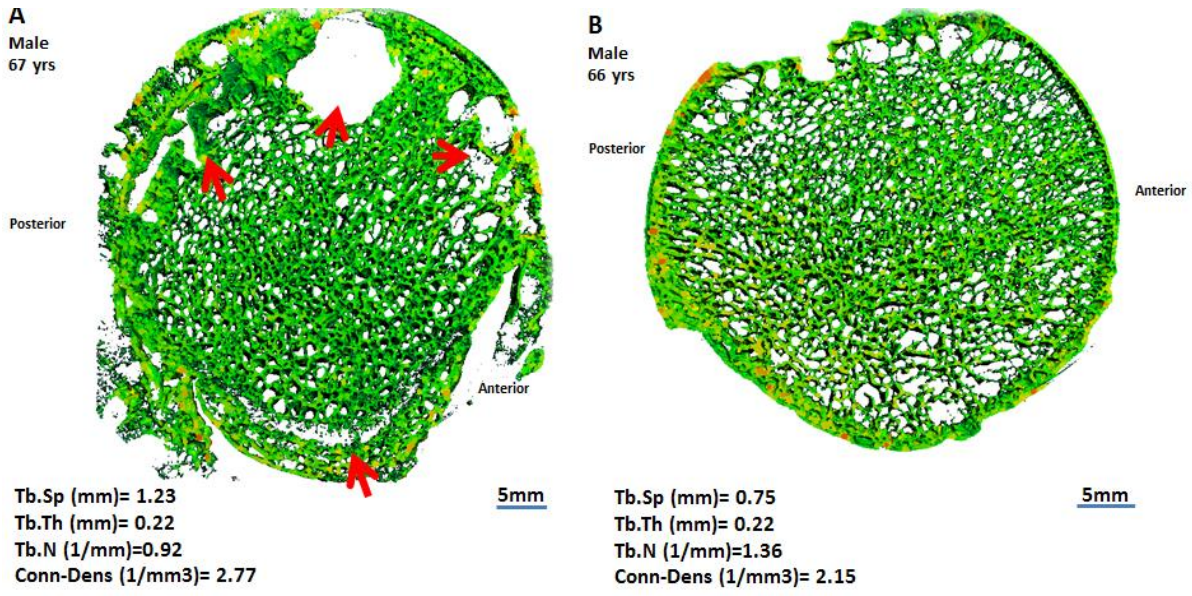

Figure 5- 6: 3D images at the femoral junction of both subjects shows the BV/TV related to different trabecular parameters. (A) Femoral junction in OA sample of a male indicating high numbers in Tb.Sp (red arrows) due to the assassination of osteophytes. High number in Conn-Dens, low number in Tb.N. (B) same location was observed in control sample.

At the mid-neck (Table 5-1), OA group was characterized by a higher trabecular number ($P<0.01$), connectivity density ($P<0.01$) and lower trabecular separation ($P<0.01$). Figure (5-7) shows an example of trabecular microstructure parameters in the mid neck section with representative 3D model of both subjects.

To sum up, the agreement between the averages in each parameter, except Tb.Sp, followed similar patterns to that of each region in both OA and control. The Bar graph in Figure (5-8), shows the mean values in trabecular bone microstructure parameters of the three regions in subjects.

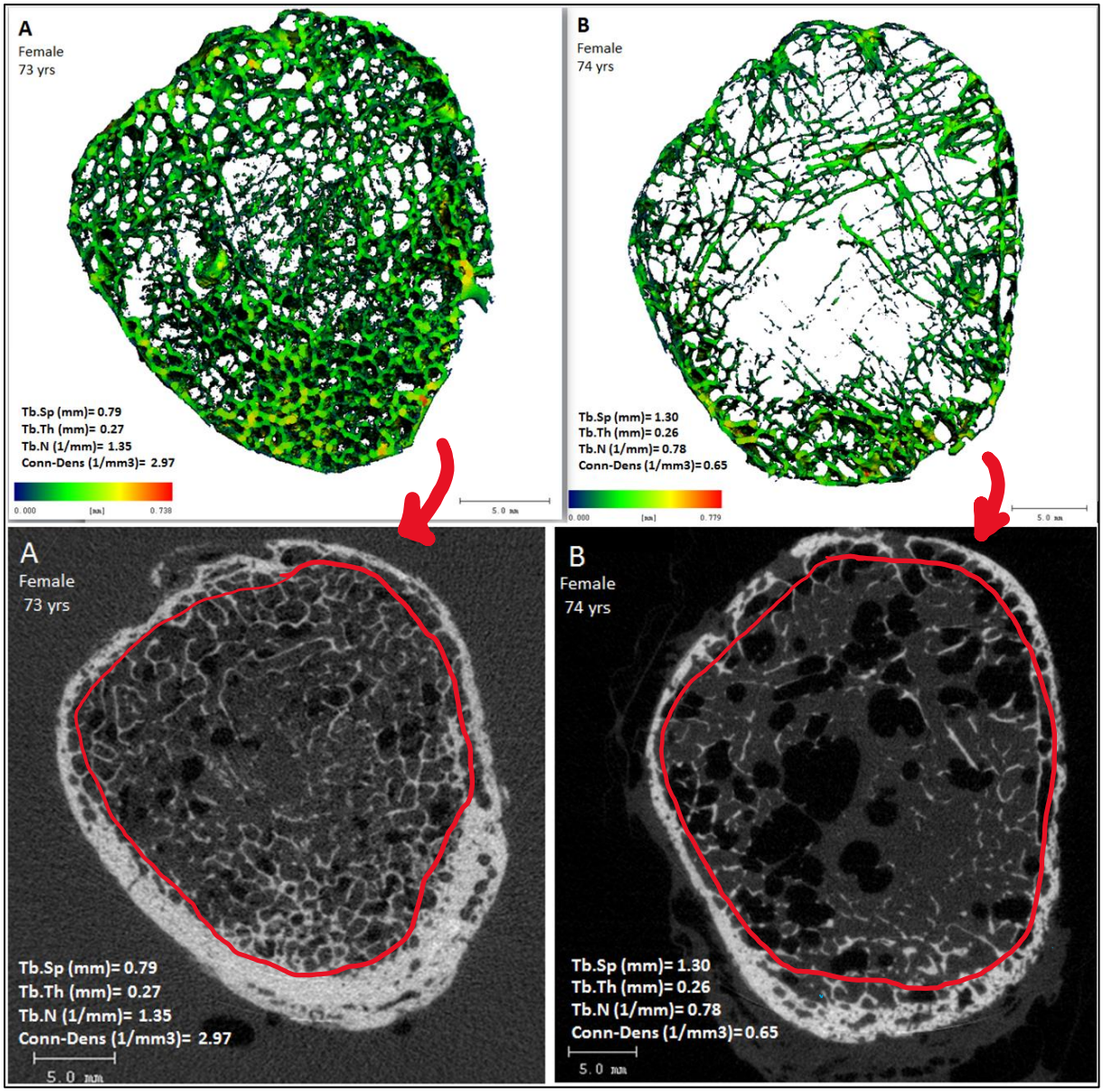

Figure 5- 7: 3D and 2D images at the femoral mid neck of subjects shows the BV/TV related to different trabecular parameters. (A) Femoral neck of a woman with OA, (B) femoral neck of control indicating the difference in trabecular parameters.

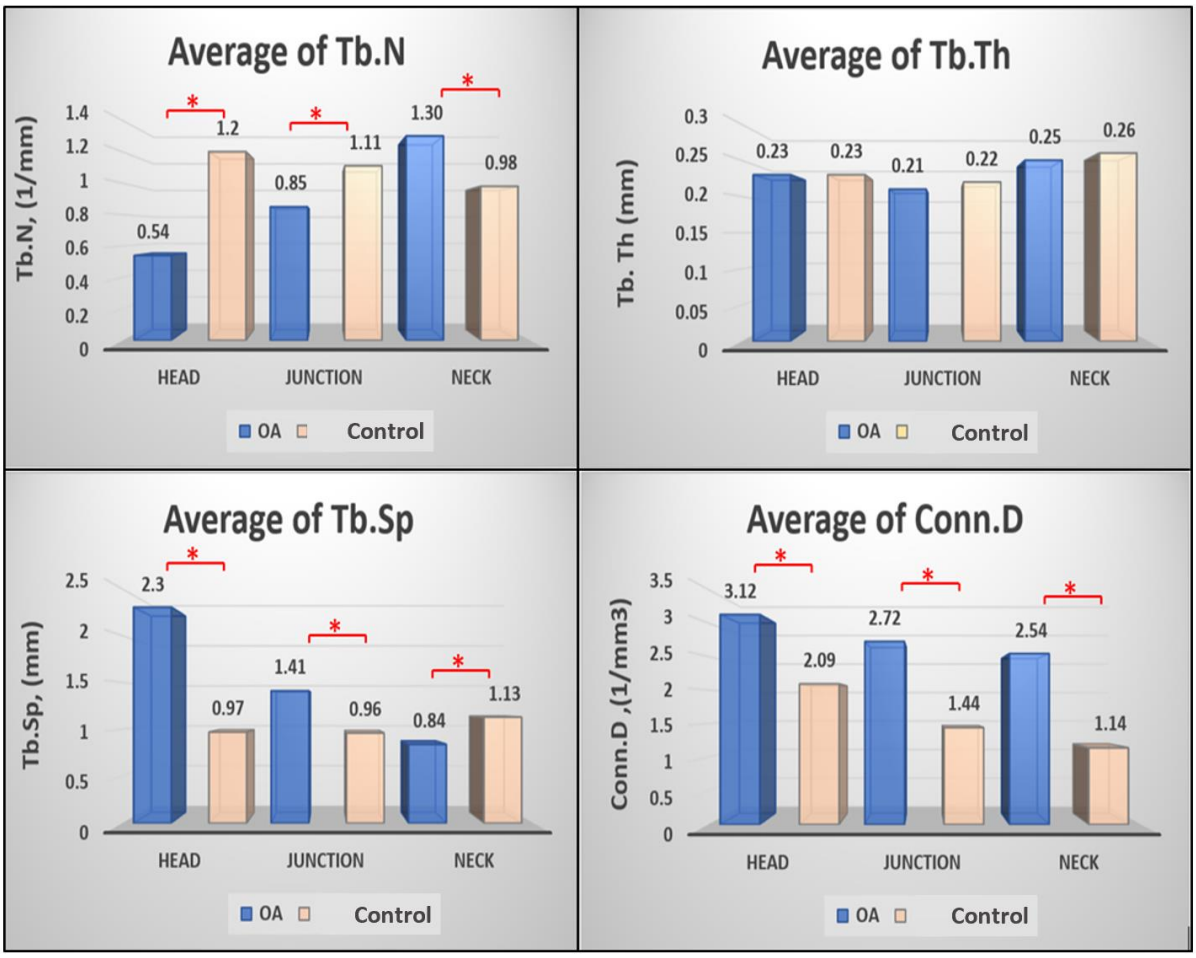

Figure 5- 8: Mean values in trabecular parameters (Tb.N, Tb.Sp. Tb.Th, and Conn.D) between subjects in the three regions. * P< 0.05.

Correlation between BV/TV and Trabecular Microstructure

Table (5-2) shows the correlation between BV/TV and trabecular microstructure parameters in each region. At the femoral head, there was a significant positive relationship between bone volume and trabecular number in both OA ($r = 0.71$, $P < 0.05$) and in control ($r = 0.70$, $P < 0.05$) shown in (Figure 5-9). In addition, BV/TV showed a strong positive relationship with Conn.D in OA ($r = 0.95$, $P < 0.001$) and in control ($r = 0.74$, $P < 0.05$) shown in (Figure 5-12), and a weak correlation between BV/TV and Tb.Th ($r = 0.38$, $P > 0.05$)

shown in (Figure 5-10) and Tb.Sp (r = - 0.29, P >0.05) in OA, shown in (Figure 5-11). In contrast, control subjects showed a strong significant positive relationship between bone volume and Tb.Th (r = 0.89, P <0.05) shown in (Figure 5-10), while there was a moderate correlation in Tb.Sp (r = 0.46, P <0.05). For both junction and mid neck regions, there was a positive relationship between BV/TV and Tb.N, Tb.Th, Conn.D in both cases. Regression analyses are shown in (Figure 5-9, 5-10, 5-11, and 5-12) for the parameters in at the three regions of the subjects.

Overall, among the OA and control groups, a positive correlation was found between BV/TV and Tb.N, Tb.Th and Conn.D and negative correlation in Th.Sp. However, positive correlation between BV/TV and Tb.Sp was found only in control head.

Table 5- 2: Correlation between BV/TV and trabecular microstructure parameters in each region.

	Tb.N	Tb.Th	Tb.Sp	Conn.D
OA Head	0.714	0.378	-0.295	0.953
p-Value	***P <0.05***	*P >0.05*	*P >0.05*	***P <0.01***
Control Head	0.699	0.894	0.463	0.741
p-Value	***P <0.05***	***P <0.01***	*P >0.05*	***P <0.05***
OA Junction	0.597	0.855	-0.417	0.878
p-Value	***P <0.01***	***P <0.01***	*P >0.05*	***P <0.01***
Control Junction	0.909	0.737	-0.794	0.892
p-Value	***P <0.01***	***P <0.05***	***P <0.01***	***P <0.01***
OA Mid Neck	0.514	0.631	-0.530	0.413
p-Value	*P >0.05*	***P <0.01***	*P >0.05*	*P >0.05*
Control Mid Neck	0.892	0.512	-0.920	0.843
p-Value	***P <0.01***	*P >0.05*	***P <0.01***	***P <0.01***

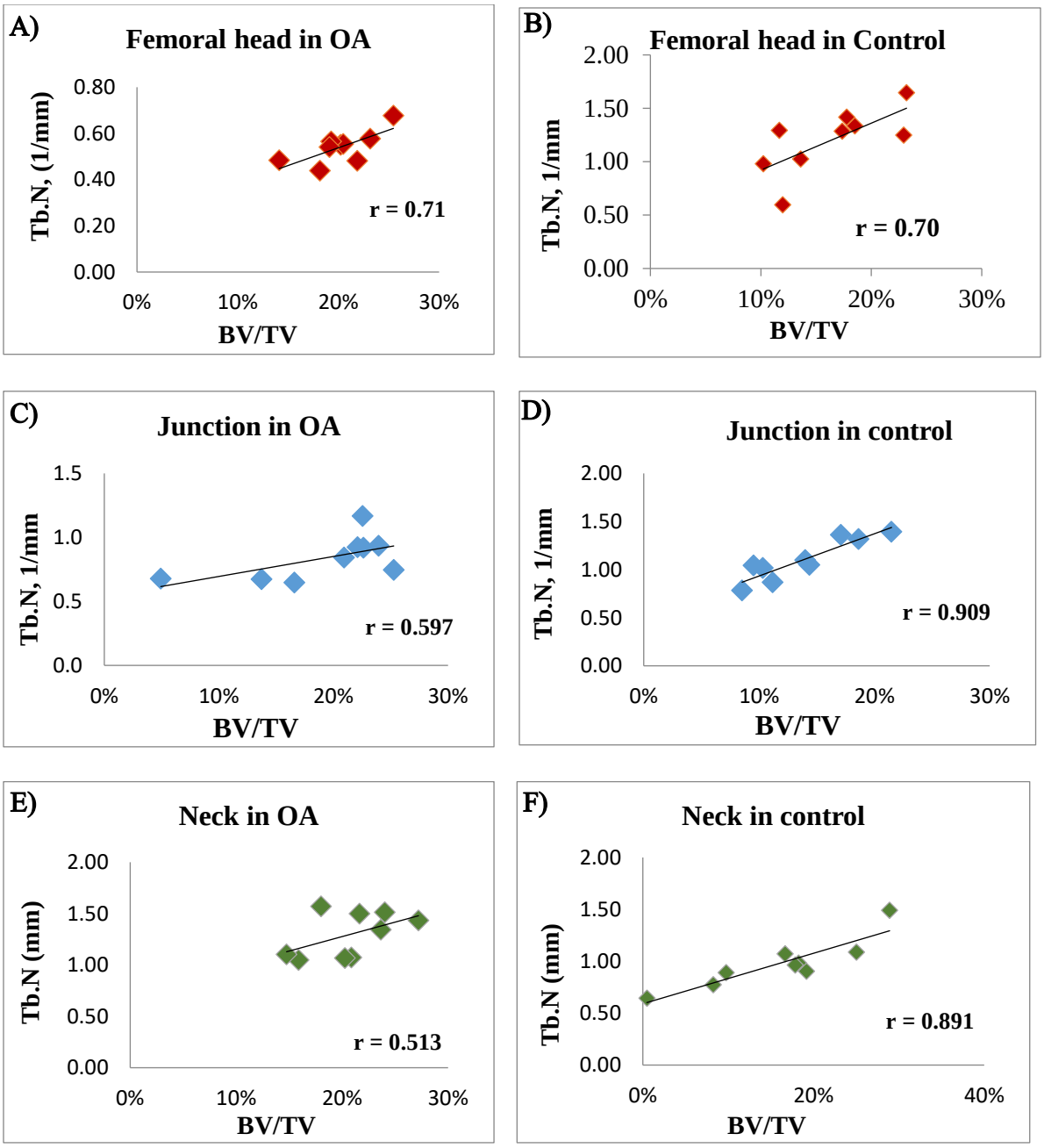

Figure 5- 9: Regression plot comparing trabecular numbers in femoral hip of both subjects at the three regions. Slopes represent the correlation between BV/TV and trabecular number. The correlation between BV/TV and Th.N in OA and control at the three regions were positive relationship. A strong correlation observed in control samples at the junction region (D) and the neck region (F).

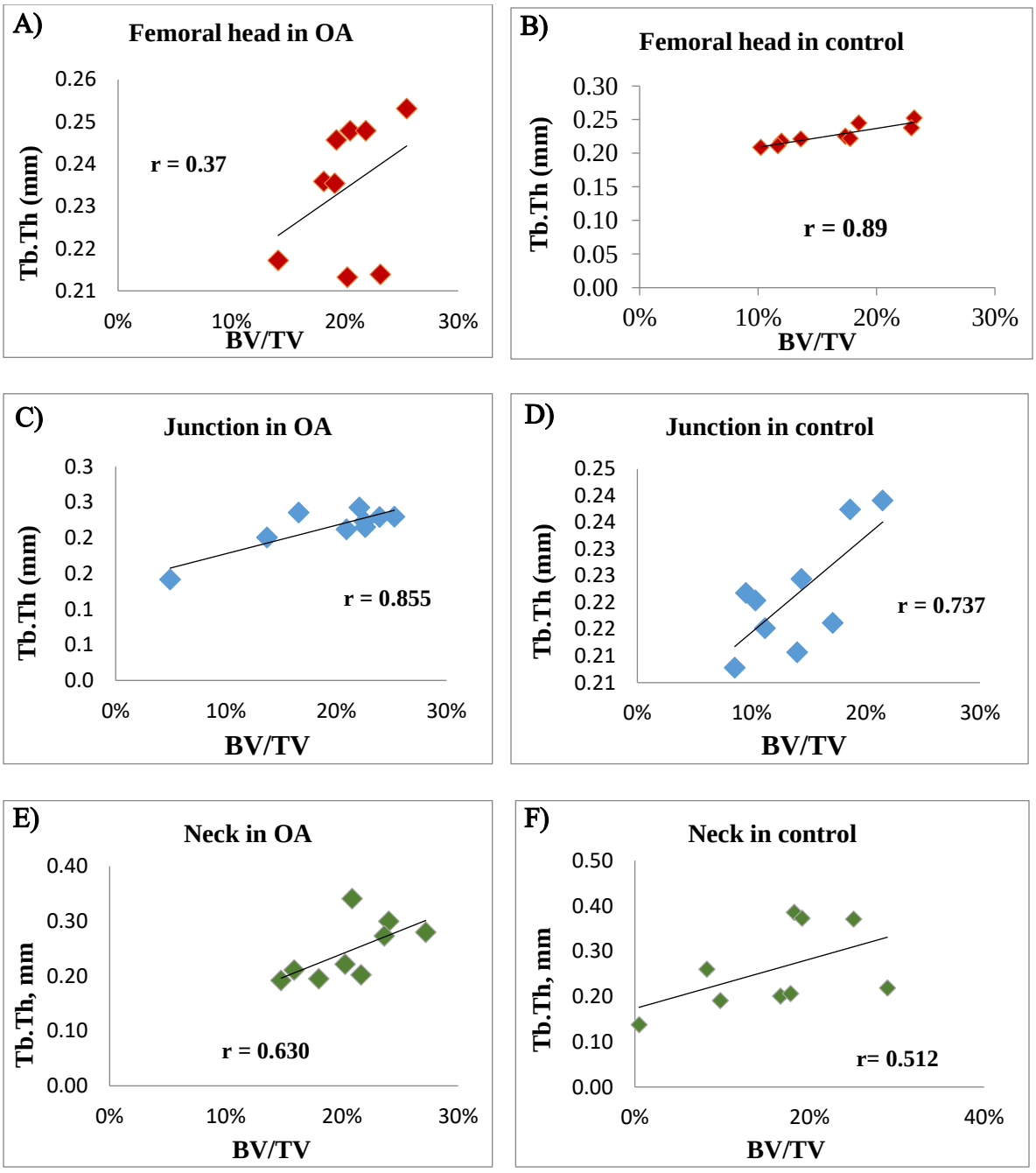

Figure 5- 10: Regression plot comparing trabecular thickness in femoral hip of both subjects at the three regions. Slopes represent the correlation between BV/TV and trabecular thickness. The correlation between BV/TV and Tb.Th in OA and control at the three regions were positive. A strong positive relationship in OA was observed in the junction region (C). In the head region of OA (A), there was no correlation observed. However, in the femoral head of control (B), the correlation was strong.

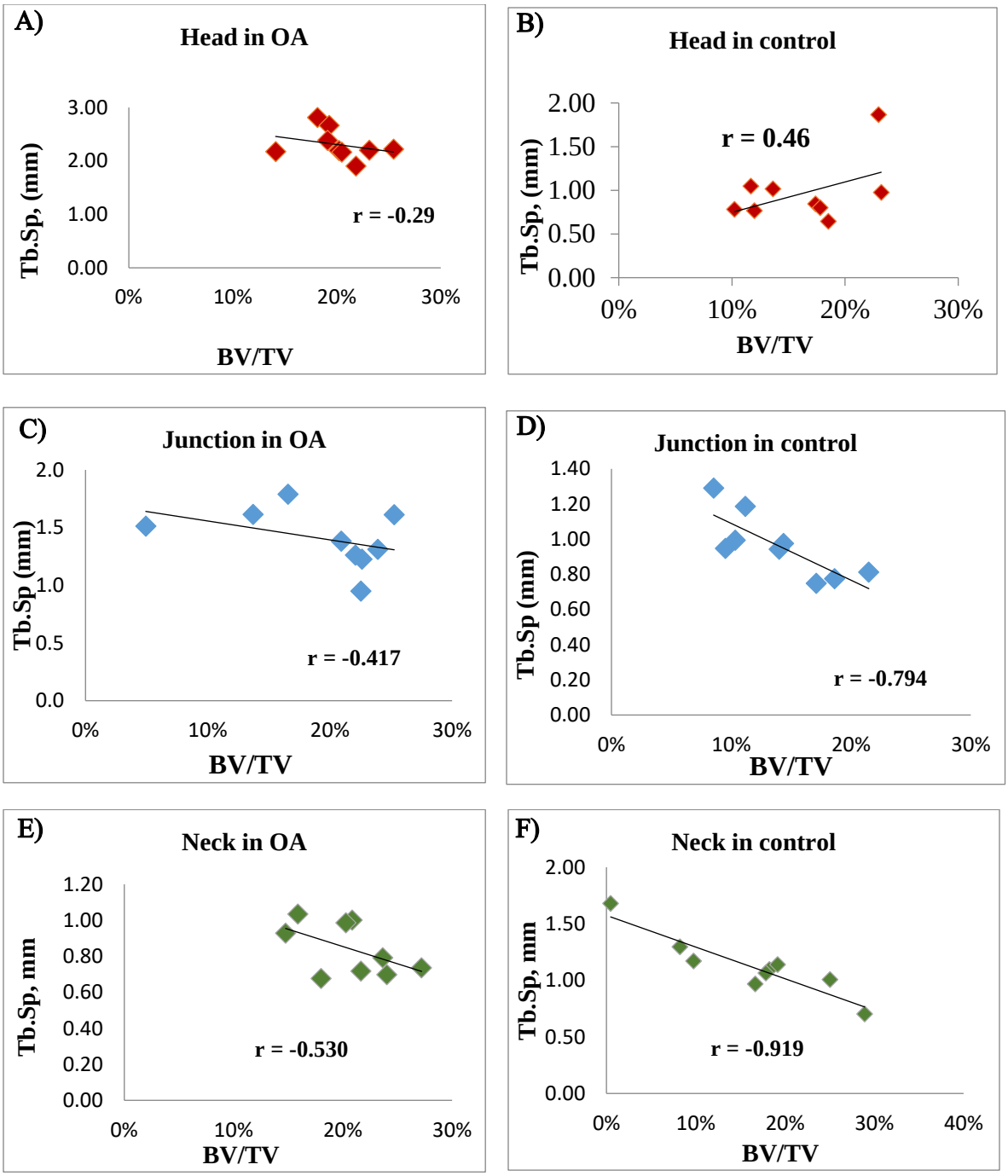

Figure 5- 11: Regression plot comparing trabecular separation in femoral hip of subjects at the three regions. Slopes represent the correlation between BV/TV and trabecular separation. The correlation between BV/TV and Tb.Th in OA and control at the three regions were negative. A strong negative relationship in control samples was observed in the neck region (F).

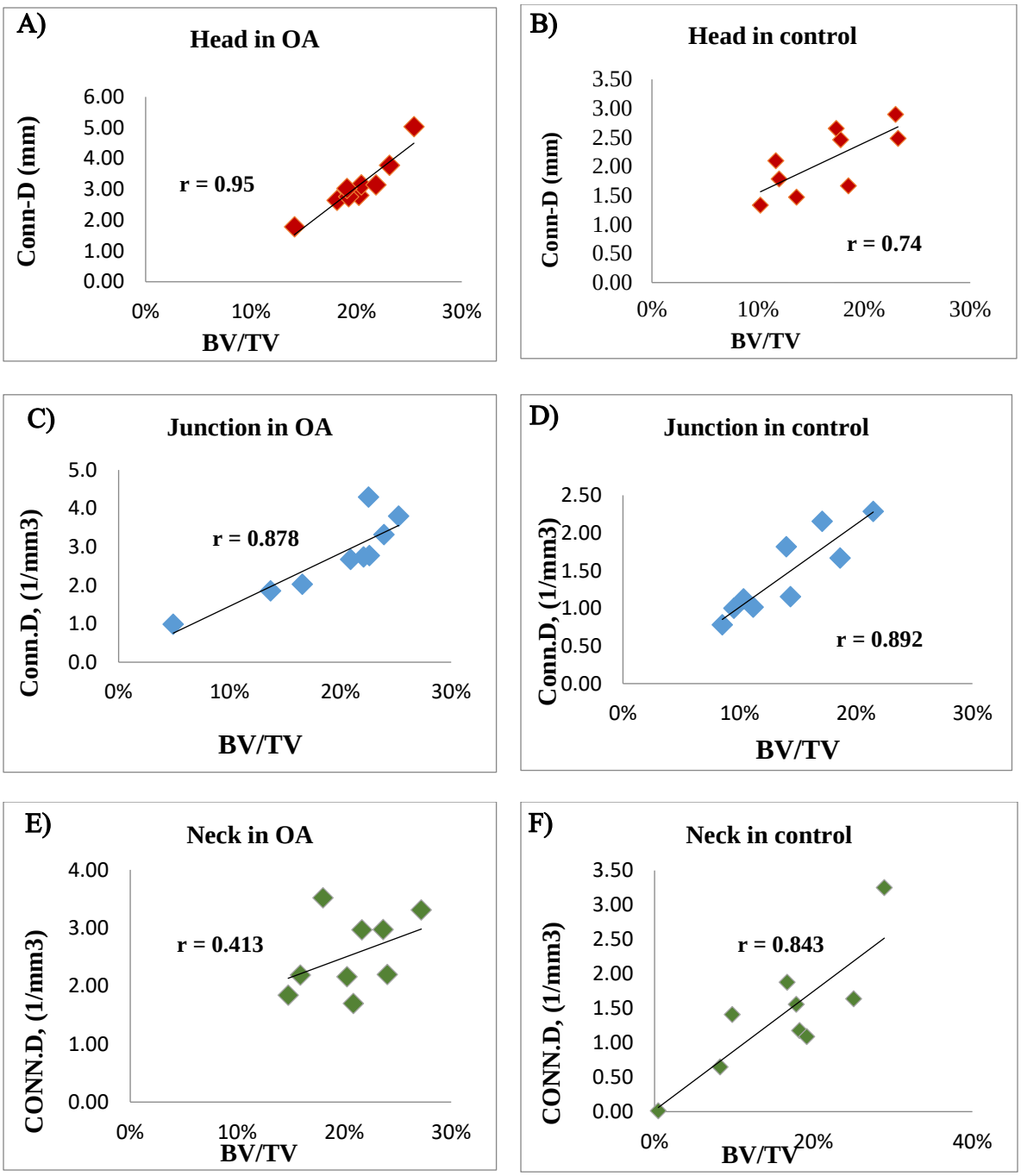

Figure 5- 12: Regression plot comparing connectivity density in femoral hip of both subjects at the three regions. Slopes represent the correlation between BV/TV and connectivity density. The correlation between BV/TV and Tb.Th in OA and control at the three regions were positive. A strong positive relationship in OA was observed in the head region (A) and the junction (C). While in control, the strong correlation was observed in the junction (D) and the region (F).

5.2.3 Cortical Bone Microarchitecture

On the entire femoral mid-neck (Table 5-3), cortical porosity was significantly higher in OA samples (27%), than in control (16%), (P< 0.05). Mean cortical thickness was not significantly different between OA and control but was slightly lower in control than in OA (1.54 mm, P > 0.05), (Figure 5-13).

Table 5- 3: Mean ± standard deviation and p-value of cortical bone parameters.

			OA	**Control**	**P value (95% CI)**
Patients, n			*9* *3= M,6= F*	*9* *4= M, 5= F*	
Porosity (%) of cortical bone	Ct. Po	*Ave*	27	16	P <0.05
		SD	4	3	
Cortical thickness (mm)	Ct. Th	*Ave*	1.78	1.54	*P >0.05*
		SD	0.15	0.38	

Correlation between BV/TV and Cortical Bone

Table 5-4 shows the correlation between BV/TV and cortical bone microstructure parameters in femoral mid neck in both subjects. Almost weak correlation was obtained between BV/TV and Ct.Po and Ct.Th. As shown in (Figure 5-14), a weak relationship between BV/TV and cortical parameters that happened to be in a negative direction.

Table 5- 4: Correlation coefficient between BV/TV and cortical parameters in subjects.

BV/TV, %	**Ct.Po, %**	**Ct.Th, mm**
OA	-0.20	0.03
P- value	*P >0.05*	*P >0.05*
Control	-0.36	-0.02
P- value	*P >0.05*	*P >0.05*

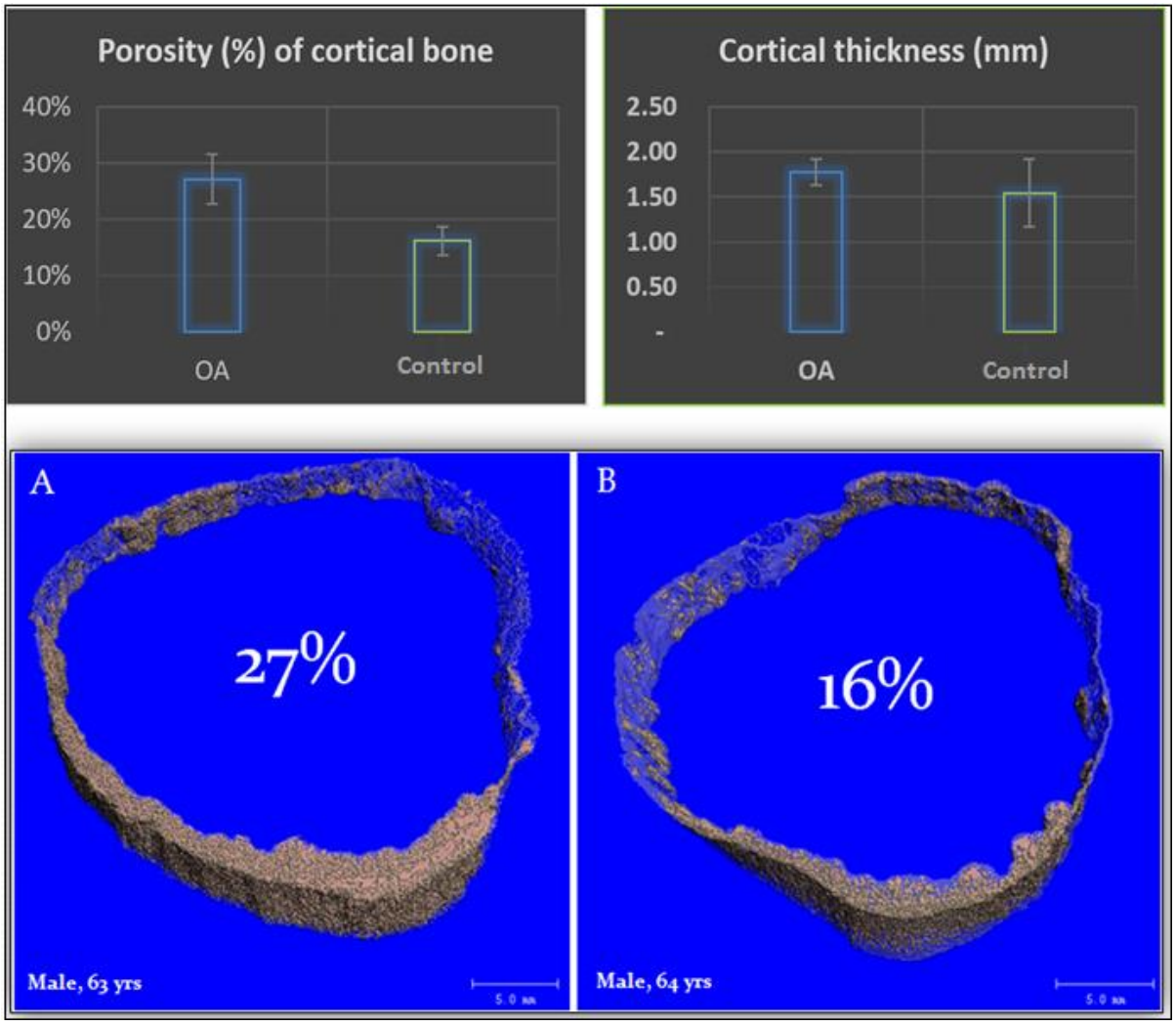

Figure 5- 13: Three- dimensional model of the segmented cortical region used for Ct.Po and Ct.Th. (A) femoral neck with OA, and (B) femoral neck of control sample. Cortical porosity was increase in OA subjects. The two plots represent the cortical parameters of cortex between subjects in the femoral neck.

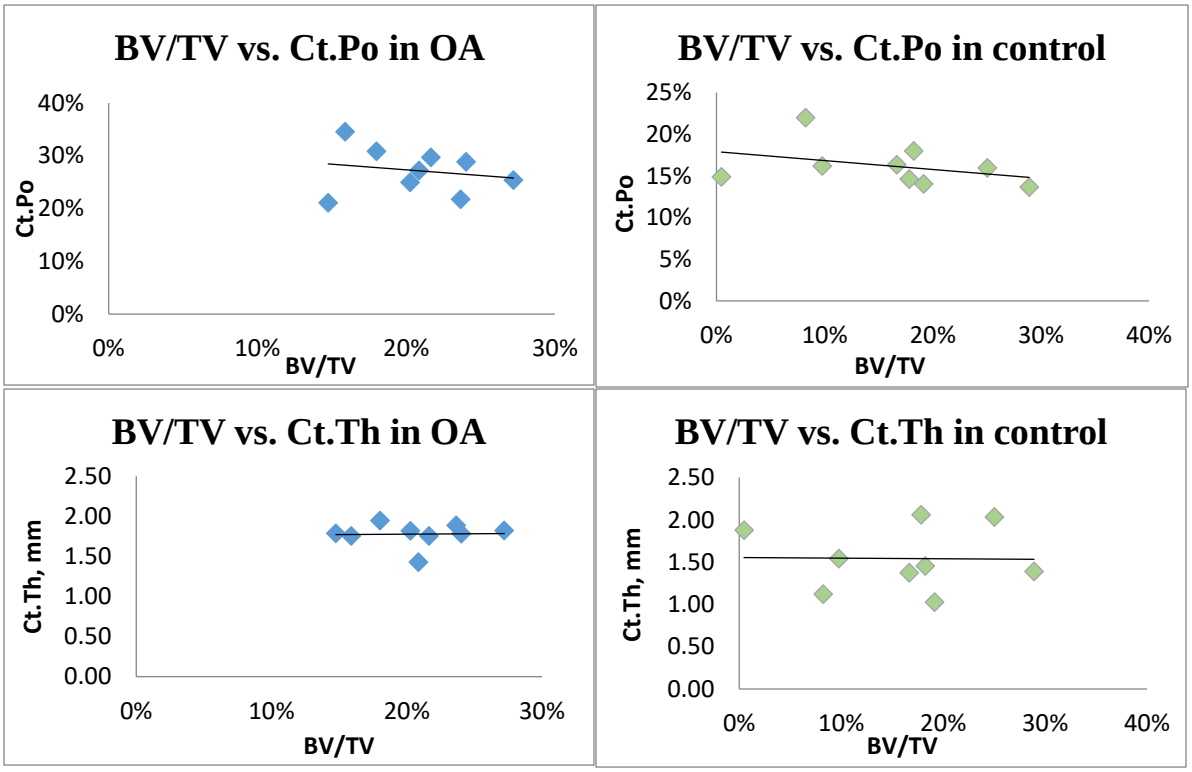

Figure 5- 14: Comparison of the correlation between BV/TV and cortical bone measurements in subjects. Regression analyses are shown for cortical porosity (Ct.Po), cortical thickness (Ct.Th). Dashed lines indicate 95% confidence level.

5.3 Hypermineralization in Cortical Bone in the Femoral Neck Region

In all OA femoral neck, the hypermineralized areas were observed at the cortical bone region under the OM and BSE imaging. Different features of hypermineralized tissue were observed with multiple cracks and missing of lamellar structure. Some cracks were found in hypermineralized tissue between periosteum and lamellar bone. Figure (5-15) is the representative BSE images of one sector, where the most common at superior to anterior, taken from cortical bone in the femoral neck comparatively to HR-pQCT images. Induvial images were taken with a magnification of 50× as it shown in (Figure 5 - 16, A-C) for better observation of the hypermineralization. For the general survey, hypermineralized tissue was also observed at the inferior region with multiple long cracks (Figure 5-17).

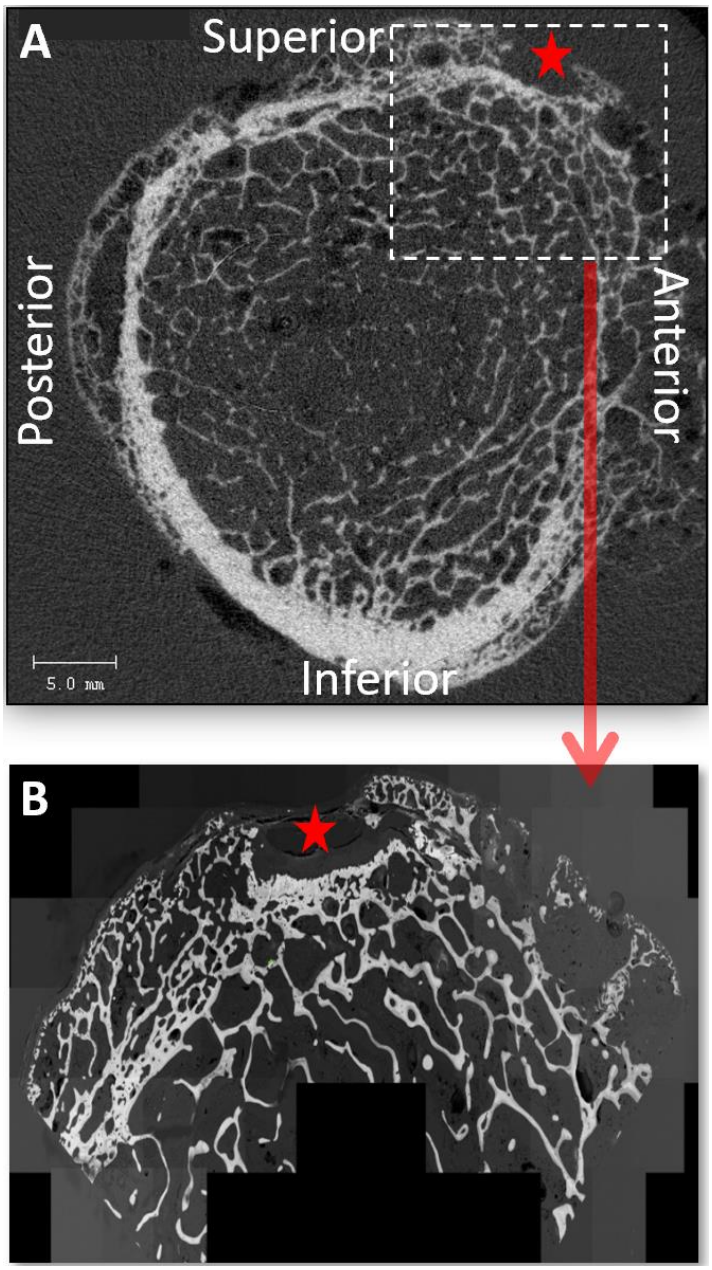

Figure 5- 15: Femoral neck in OA. BSE image of superior- anterior sector taken from cortical bone in the femoral neck comparatively to HR-pQCT images. (A) CT images of the entire femoral neck. Montage of BSE images of the mineralized tissue around cortical bone in OA. The red star indicates the region of the following figure (5-16) where the hypermineralized tissue is increased.

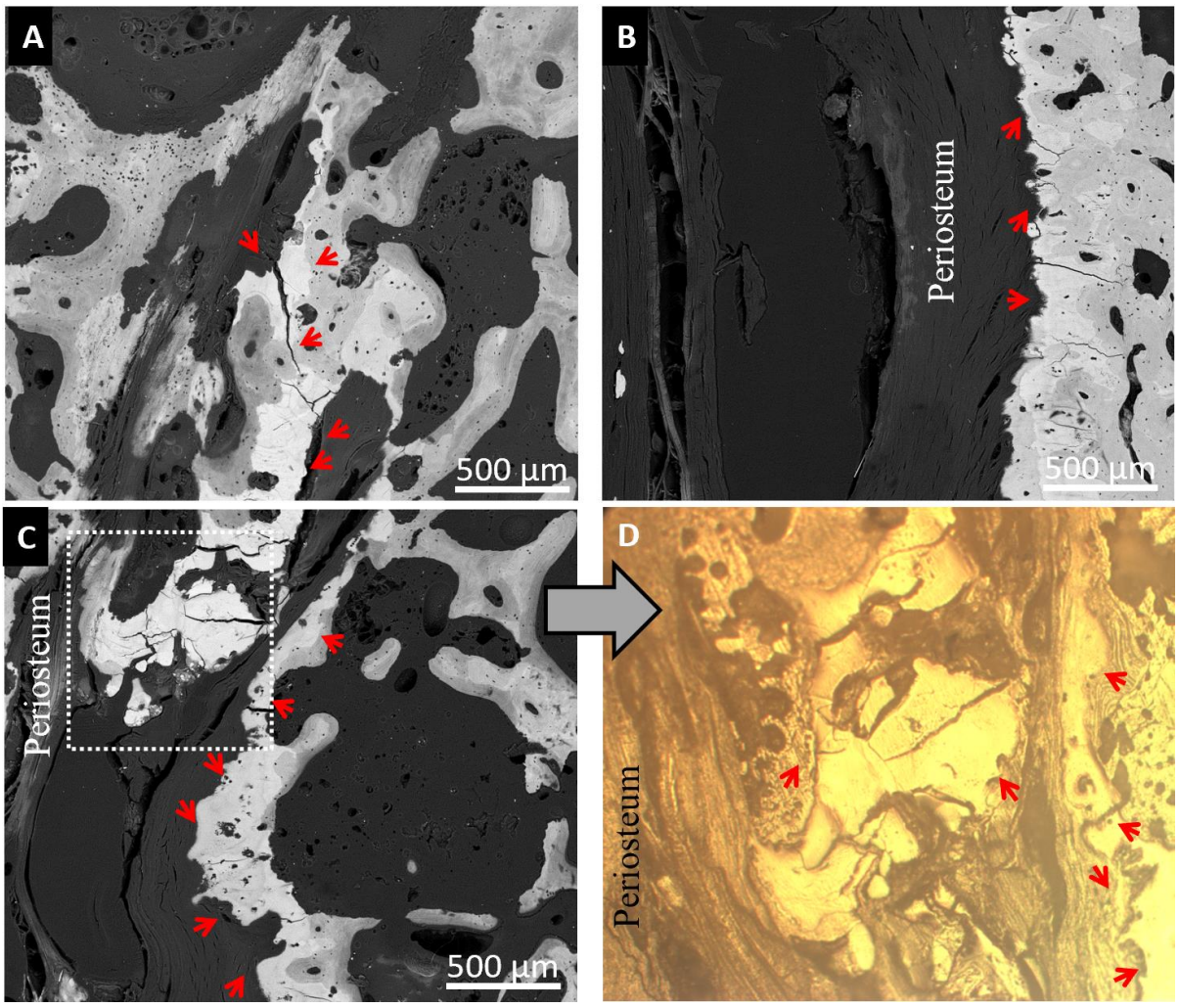

Figure 5- 16: A close-up view of the red star shown in (5-15, B). BSE and OM images taken from femoral neck of OA. (A, C) showing hypermineralized tissue in a bright region. The grey region indicates the lamellar bone. The dashed white square in (C) showing the hypermineralized tissue with multiple cracks and missing of lamellar structure. Different grey layers shown in red arrows inserts into the lamellar structure. (B) multiple cracks appeared in hypermineralized tissue between periosteum and lamellar bone. (D) A close-up OM view that including dashed White Square with a BSE image in (C) showing different features of hypermineralized tissue.

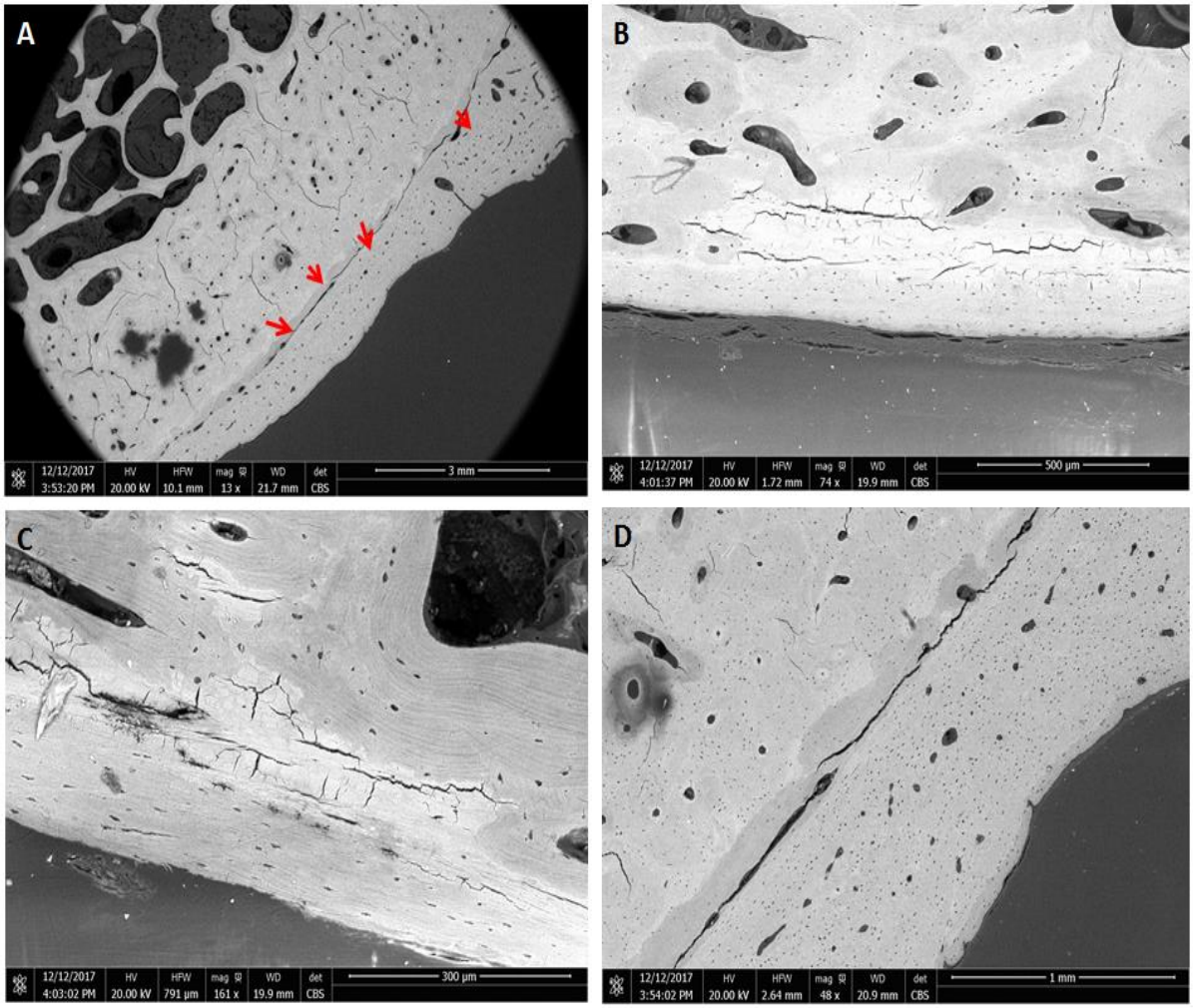

Figure 5- 17: BSE images showing features associated with hypermineralization at femoral neck of OA at the inferior region. (A) An overview of the region showing multiple and long cracks (red arrows). (D) A close-up view of the crack, this crack might result in histological processing. (B-C) Hypermineralized areas appear underneath periosteal lamellar bone with multiple cracks.

CHAPTER 6: Discussion

6.1 Discussion

6.1.1 Overview of Findings

Mainly, this study provides bone microstructure parameters for femoral hip OA and compares the result with control samples by using HR-pQCT. The purpose of this study was to investigate the whole proximal femur (head, junction, and neck) to identify bone microstructure differences between OA and non-OA (control). Additionally, morphological observations of the distribution of hypermineralization area around the femoral neck in OA was provided as a pilot study. As far as we know, this is the first *ex-vivo* study analyzing bone microstructure in the femoral head, junction and neck together in patients with osteoarthritis. Most of the previous studies have analyzed bone microstructures either in a part of femoral hip or in the knees using HR-pQCT (104, 123, 124). The results of our study confirmed the hypothesis that there is a difference between the hip OA and control when compared with trabecular and cortical bone. However, hypermineralization tissue was found in the similar features in control group which rejected our second hypothesis of being different.

By dividing the femoral hip into three regions (head, junction, neck), we were able to obtain specific areas where trabecular and cortical bone varied from OA and control. Initially, qualitative comparisons between OA and control were obtained from scout views, cross- and longitudinal-sections to provide a general observation of bone morphology. Therefore, this observation needed to be quantitatively confirmed.

The main findings of bone microstructures parameters that provided differences in their results in both subjects were : Tb.N, Tb.Sp, Conn.D, Ct.Po, and Ct.Th. We found that most microstructure parameters among OA peaked at the neck and head (Figure 6-1), whereas the same parameters remained relatively stable between the three regions of the control samples (Figure 6-2). Some research groups have indicated that BV/TV was the most significant parameter associated with bone quality [129], [130]. BV/TV on the other hand, did not show any difference in results when comparing the three regions together in the same case study. Even though we did not find differences in BV/TV between each region of hip in both cases, we did find that hip OA had a higher bone volume fraction in total than those with control samples, as shown previously in (Figure 5-4). It was reported that BV/TV decreased about 27% at aged 20- 90 years at distal radius [105], [131].

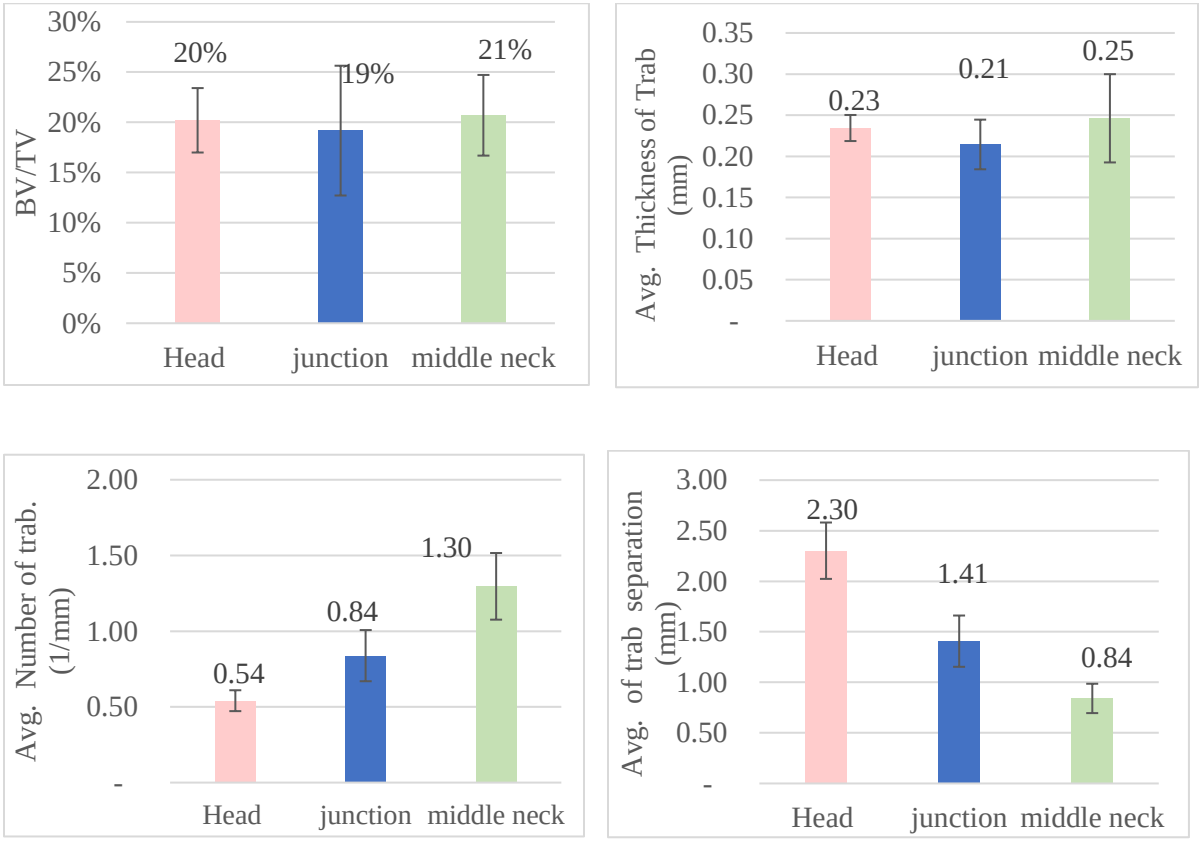

Figure 6- 1: BV/TV, Tb. N, Tb.Sp, and Tb.Th in the femoral hip at all the three regions of OA. There was not a big difference among the three regions in BV/TV and trabecular thickness. However, mean values of trabecular number and separation were different between the three regions.

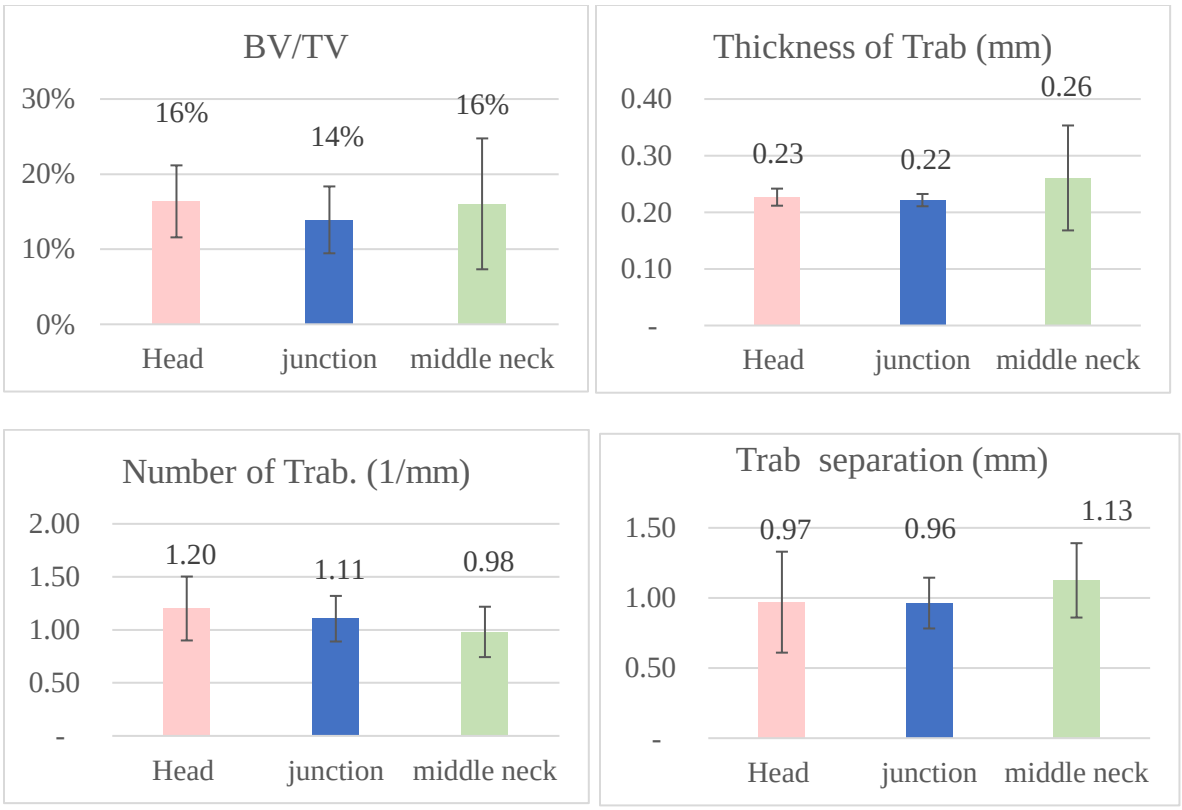

Figure 6- 2: BV/TV, Tb.N, Tb.Sp, and Tb.Th in the in the femoral hip at all the three regions of control. Almost there was no difference between the three regions in terms of the parameters.

Cadaveric hips had a larger number of trabecular and smaller amounts of spacing in the head and junction regions than patients with OA. A study found that women tend to have lower average of trabecular number and higher trabecular separation [105]. Despite the contribution of the trabecular number and spacing are higher in femoral head and junction in control than in OA, the number of the trabecular was higher in OA femoral neck than in control femoral neck. (Table 5-1). We then, evaluated whether the observed differences in theses microstructure parameters correlated with BV/TV. As expected, higher bone volume fraction was associated with large trabecular number, small bone marrow spaces, and high trabecular connectivity in almost all the regions in both cases (Table 5-2, Figure 6-3). A

study reported that even with no difference between BV/TV and trabecular thickness, trabecular separation was higher in those with previous fractures than without [130].

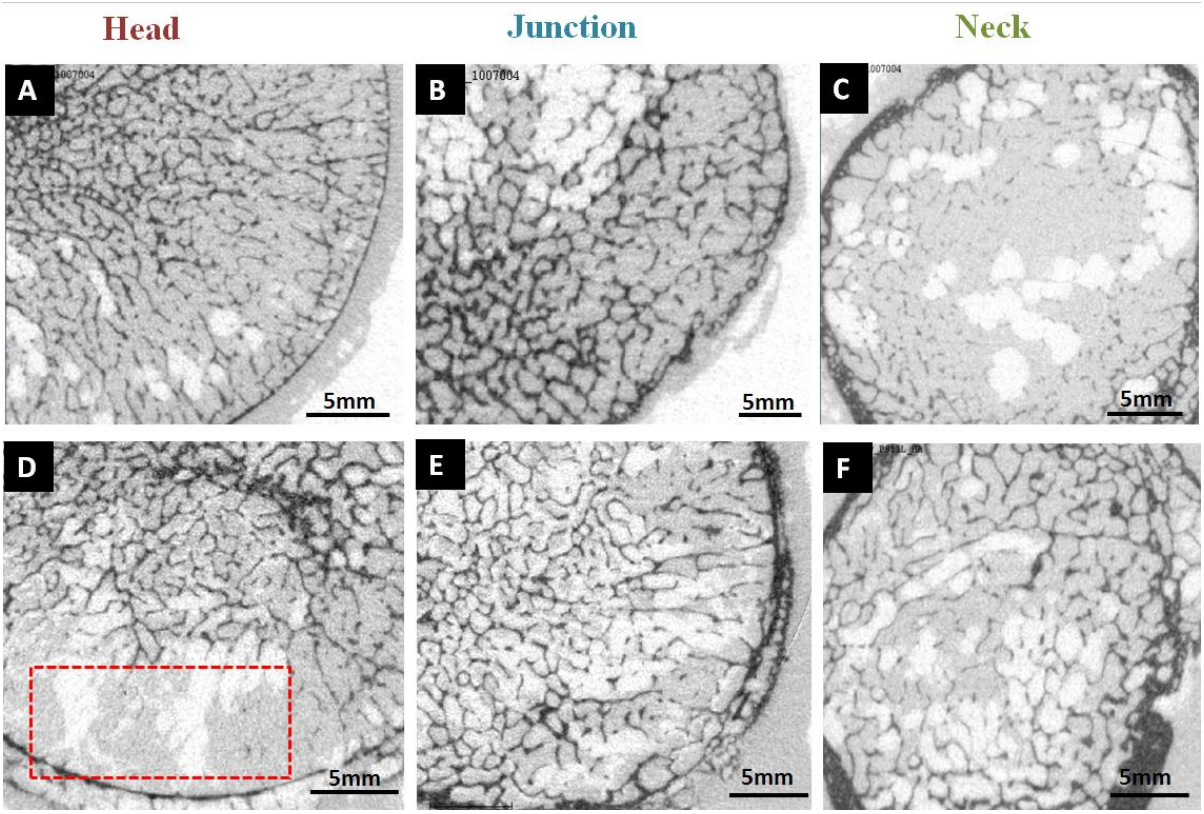

Figure 6- 3: grey-scale of human femoral hip in cadaveric hips (the top row) and OA (the bottom row). (A) Femoral head (control samples) indicating higher number of trabeculae and lower trabecular spacing than in OA (D). Dashed red rectangular in (D) shows lacking trabecular. (B) Is the junction region of control group showing the larger number of trabeculae and lesser spacing than (E) OA. However, this result in the femoral neck where the high risk of fracture was opposite, (C) femoral neck of cadaveric specimen with lesser number of trabeculae and high spacing between trabeculae. (F) is the femoral neck of OA.

Since most of human cadaver femora were over 60 years, there was a chance of being diagnosed with osteoporosis (OP). Previous studies indicated that in the case of osteoporosis, femoral hip is losing bone primarily in the principal tensile group, then run lately from the head to the greater trochanter [132]. Other studies used micro CT to study the trabecular microstructure changes in the femoral heads, necks, and trochanters and lumbar spine of human cadavers to investigate age- sex- changes [133]. They found in terms of femoral head, Tb.Sp increased while BV/TV, Tb.N, Tb.Th decreased with aging. Other group studied trabecular microstructure at 5 mm cube regions of trabecular bone from femoral OA and OP head using micro CT [134]. They reported that with OA samples, a greater BV/TV and Tb.N was observed.

Focusing on the femoral neck, we found that cortical bone with OA was 20% thicker and 70% porous than cortical bone in femoral neck with control group. It was very clear in (Figure5-7) to observe the major difference between cortical thickness and porosity at the femoral neck between OA and control. Figure (6-4) represented 3-D images of cortical bone in the femoral neck of both subjects. We noted that there was a large number of osteophytes in our OA group and that could be a contribution in their high number of porosities. Having said that, even though cortical porosity was higher in OA than in control group, femoral neck in control group is more likely to risk fracture due to the association of cortical thinning [33], [135]. In addition, femoral neck contains of both trabecular, and cortical bone and that trabecular bone contributes for cortical resistance. It was reported that the strength of cortical bone at the femoral neck in elderly associated with high BV/TV in inferior section [136]. Having said that most of control group were observed over 60 years, some group found that hip OP had higher chance to femoral neck fracture than in hip OA as they observed in a

decreased of connectivity density in OP [137]. Our result was 40% higher in connectivity in the femoral neck and junction of OA than in control group. Another group found that not only the thinner cortical bone in the femoral neck leads to the risk of fractures, but also the contribution of trabecular bone [125]. Therefore, control group bone is more likely to fracture than OA. Taking all these results from HR-pQCT together, our results confirmed the findings of recent studies on femoral OA.

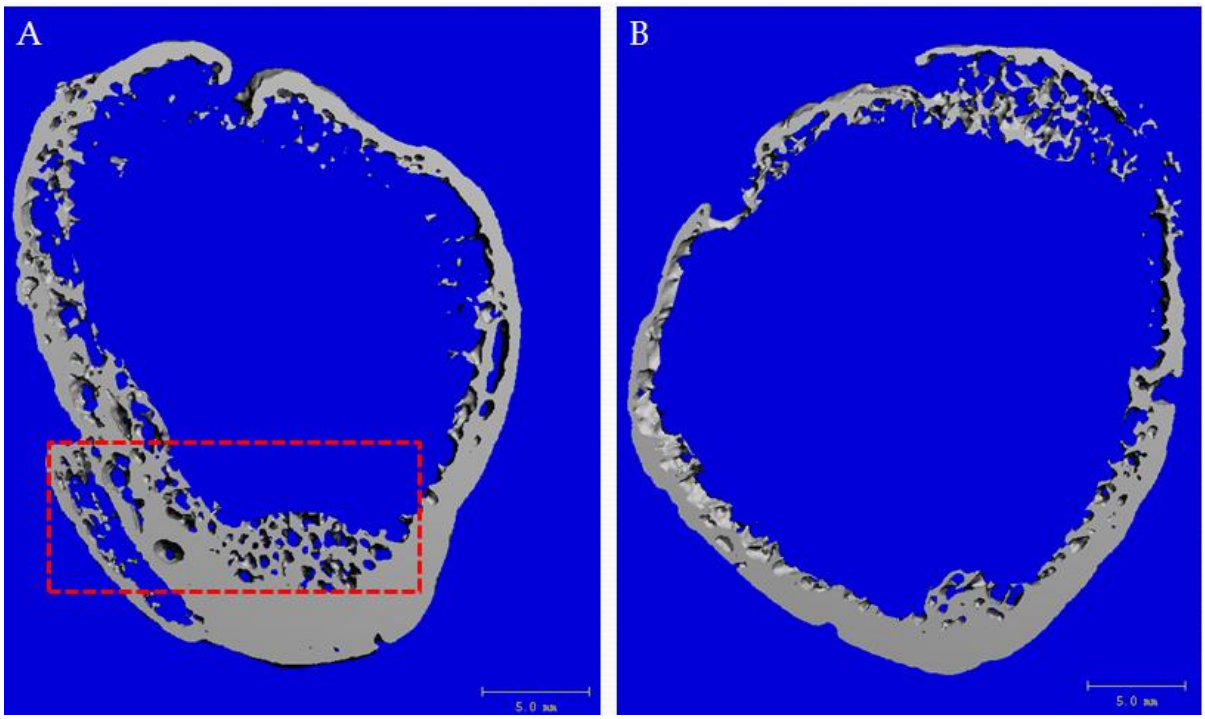

Figure 6- 4: 3D representation of the cortical thickness and porosity. (A) Femoral neck with OA showing major cortical thickness and porosity. Most of pores are large and irregularly shaped (dashed red rectangular). (B) Cortical bone of femoral neck from control sample indicating thinner cortex and less pours.

For the morphological features in the femoral neck, hypermineralized tissue was found in all OA samples at the cortical bone region around almost four sectors under OM and BES images. The highest was shown from superior to anterior going to inferior. A previous study claimed that hypermineralized tissue was more concentrated in the superior section of the femoral neck [138]. Another study reported that the anterior to inferior sector showed increased amount of hypermineralization with aging 50 [139]. In (Figure 5-16), the hypermineralized tissue can be described by the absence of lamellar bone (structure) and the appearance of different crack sizes. These features were agreeing with reviews [138]–[140]. The size of hypermineralized tissue ranged from 50 µm to 500 µm in OA samples. In the superior-anterior region as it was shown previously in (Figure 5-16), hypermineralized tissue was found in all OA samples at the cortical bone region under OM and BES images. Different levels shown in BSE images (Figure 5-16, A-C) related to different minerals density. The densest mineral provides the brightest pixels [141], [142]. Hypermineralization with fibrous insertion to the cortical was also observed in the superior- anterior region (Figure 5-16, C). The microscopic image in (Figure 5-16, D) was closely similar in the appearance of mineralized tissue that was observed in BSE image. However, some regions of hypermineralized tissue were not clearly observed under optical microscopy due to it being thinner, while it was clearly observed under BSE due to the different contrast level.

Figure (5-17) shows the appearance of hypermineralized tissue around the inferior region as well. Thin layers of hypermineralized tissue also appeared underneath the lamellar bone with multiple cracks (Figure 5-17, B-C). OM images showed the less hypermineralized tissue around the inferior to posterior region.

Compared to OA, hypermineralization at the cortical bone in femoral neck region of control group was also observed under BSE by Tengteng Tang [128]. Hypermineralized tissue in the femoral hip had similar features of hypermineralized tissue of OA that were observed in this study. Firstly, in all cadaveric samples, there was hypermineralized region found and more commonly in superior region. This hypermineralized tissue had similar structure with the absence of lamellar structure as observed in OA. Secondly, multiple cracks were appeared within the hypermineralized tissue. In addition, the size of hypermineralized tissue ranged from 50 μm to 150 μm in control samples. Moreover, hypermineralization with fibrous insertion to the cortical was also observed in the superior region of control samples.

Overall, this pilot study qualified and confirmed the existence of hypermineralized tissue at the human proximal femur with OA under BSE/SEM and OM. Form a microstructural perspective of cortical bone, different features of hypermineralization were observed the femoral neck and theses features looked similar to hypermineralized tissue in cadaveric hips. This result did not agree with the hypothesis that hypermineralization differs between OA and control at the femoral neck. Thus, the appearance of hypermineralized tissue in both subjects did not relate to the difference of bone abnormalities. It was reported that the increased amount of hypermineralization at the femoral neck was associated with aging [138], [143].

6.1.2 What Does Bone Quality Tell Us?

Bone quality is determined by structural and material properties of the bone. The structural properties of bone refer to the trabecular and cortical microstructure [56]. Bone quality is considered to be a good predictor of bone strength. The measurement of bone quality parameters has been recently receiving major attention in the field. With the development of new technology, we now have many imaging techniques with high resolution that are needed to quantify bone microstructures.

Cortical porosity plays an important parameter of bone quality. Various studies confirmed the association between age and cortical porosity. It was reported that the increase of bone porosity leads to cortical trabecularization which significantly result in bone quality [144], [145]. Although it is known that patients with osteoporosis have less bone mechanism due to the increased bone remodeling, this result showed that people with osteoarthritis had more porous cortex in the femoral neck than control group. This work also highlighted the changes in the major trabecular bone microstructures during OA and control. In this OM and BSE imaging, it was obvious to indicate that the more brittle in the hypermineralized region, the more cracking was observed (Figure 5-15). This is confirming the previous observations [138], [139]. Thus, this hypermineralized tissue has been associated with reduced resistance to fracture, which is opposing the definition of bone quality. With all these measurements, we can better understand the difference in bone quality in OA.

6.2 Limitations

A limitation in this study was the sample size of the patients. More studies with a large number in both OA and control groups are needed to be done. This would help to study bone quality in femoral hip OA to differentiate between both male and female sexes. Other

limitations can explain some moderate relationships found between BV/TV and bone microstructure. First, HOA that obtained from THR was cut randomly from the surgeons and led to exclude many femoral hip specimens due to the short length of femoral neck. Yet, differences observed in cortical porosity, especially in OA, can be partly in the presence of osteophytes as well as the difference in ROI between femoral neck of both subjects. This method was not able to extract the cortex in the head and the junction regions due to the thinner cortex. In terms of histological study, further quantitative studies are needed in the femoral neck in OA to complete the comparison of the mineral content between OA with control.

CHAPTER 7: Conclusions and Future Work

Overall, this study provided a comprehensive study in bone microstructural properties in the human proximal femur in OA and control group by using HR-pQCT. The femur was divided into three regions (head, junction, and neck) to identify trabecular and cortical bone microstructure differences between OA and control group. Mineral properties were also observed at the femoral neck of OA. Different layers and features of hypermineralization were observed. Both OM and BSE images provided that hypermineralized tissue was increased in both, superior to anterior and inferior regions.

Study 1: HR-pQCT study

The first study of my thesis highlighted that trabecular and cortical bone microstructure are different between OA and control group by using HR-pQCT scans. In this study, morphological observation and quantitative results were obtained. By dividing the hip into three regions, the primary finding from study 1 was that OA samples at the femoral head and head-neck junction have lower number of trabeculae and higher trabecular spacing than control. In addition, femoral neck with OA showed thicker cortex but higher porosity. This result confirmed the study that there is a high risk of fracture at the femoral hip in those with OA than without OA [6].

Study 2: hypermineralization study

The primary findings from study 2 was that hypermineralized tissue at the cortical bone of the femoral neck of OA was existed. This hypermineralized tissue had similar features of control samples which rejected our hypothesis. OM and BSE images proposed the same features of hypermineralized tissue in superior to anterior and inferior regions. Thus, the

appearance of hypermineralized tissue in both subjects did not relate to the difference of bone abnormalities or disease. The common factor between these subjects was age, therefore it can thus be concluded that hypermineralization was not a result of OA, but may be related to age[138], [143].

Future work is needed to provide a better understanding of bone quality in OA regarding structural and material properties. First, bone microstructure in the intertrochanter region is needed to be analyzed in both OA since this region is a high risk to hip fractures. Second, an increasing demand in investigation of material properties in both cases OA and control can affect the bone quality. Further, histological studies in the femoral junction could provide a better understanding on the distribution of hypermineralization. Specifically, in osteoarthritis, where the osteophytes appeared. In addition, there is a need to analyze the difference in mineral content of hypermineralized tissue in OA. Lastly, comparison between OA and OP is needed since both diseases occur in elderly Further research along this direction may lead to development of new diagnosis techniques and better ways of hip repairing and reconstruction.

Bibliography

[1] N. E. Lane *et al.*, "OARSI-FDA initiative: defining the disease state of osteoarthritis," *Osteoarthr. Cartil.*, vol. 19, no. 5, pp. 478–482, May 2011.

[2] K. D. Allen and Y. M. Golightly, "Epidemiology of Osteoarthritis: State of the evidence," *Curr. Opin. Rheumatol.*, vol. 27, no. 3, pp. 276–283, May 2015.

[3] C. M. Arnold and R. A. Faulkner, "The history of falls and the association of the timed up and go test to falls and near-falls in older adults with hip osteoarthritis," *BMC Geriatr.*, vol. 7, pp. 1–9, 2007.

[4] R. D. Altman, "Criteria for the Classification of Osteoarthritis of the Knee and Hip," *Scand. J. Rheumatol.*, vol. 16, no. sup65, pp. 31–39, Jan. 1987.

[5] E. S. Nahit, A. J. Silman, and G. J. Macfarlane, "The occurrence of falls among patients with a new episode of hip pain," *Ann. Rheum. Dis.*, vol. 57, no. 3, pp. 166–168, Mar. 1998.

[6] M. K. Ikutomo H, Nagai K, Tagomori K, Miura N, Nakagawa N, "Incidence and Risk Factors for Falls in Women With End-Stage Hip Osteoarthritis.," *J Geriatr Phys Ther [Internet]*, vol. 1, 2018.

[7] C. A. Gallagher *et al.*, "Osteoarthritis is associated with increased failure of proximal femoral fracture fixation," *Int. Orthop.*, pp. 1–8, Jun. 2018.

[8] M. L. Brandi, "Microarchitecture, the key to bone quality," *Rheumatology*, vol. 48, no. suppl 4, pp. iv3-iv8, Oct. 2009.

[9] A. J. Burghardt, T. M. Link, and S. Majumdar, “High-resolution Computed Tomography for Clinical Imaging of Bone Microarchitecture,” *Clin. Orthop. Relat. Res.*, vol. 469, no. 8, pp. 2179–2193, Aug. 2011.

[10] S. Weiner and H. D. Wagner, “THE MATERIAL BONE: Structure-Mechanical Function Relations,” *Annu. Rev. Mater. Sci.*, vol. 28, no. 1, pp. 271–298, Aug. 1998.

[11] S. Viguet-Carrin, P. Garnero, and P. D. Delmas, “The role of collagen in bone strength,” *Osteoporos. Int.*, vol. 17, no. 3, pp. 319–336, Mar. 2006.

[12] J. D. Currey, “The mechanical consequences of variation in the mineral content of bone,” *J. Biomech.*, vol. 2, no. 1, pp. 1–11, Mar. 1969.

[13] P. Fratzl and R. Weinkamer, “Nature’s hierarchical materials,” *Prog. Mater. Sci.*, vol. 52, no. 8, pp. 1263–1334, Nov. 2007.

[14] Yuehuei H. An and K. L. Martin., *Handbook of Histology Methods for Bone and Cartilage*. Totowa, NJ: Humana Press, 2003.

[15] D. Taylor, “Bone maintenance and remodeling: A control system based on fatigue damage,” *J. Orthop. Res.*, vol. 15, no. 4, pp. 601–606, Jul. 1997.

[16] A. M. Parfitt, “What Is Bone Mineralization?,” *J. Clin. Endocrinol. Metab.*, vol. 88, no. June, pp. 5043–5044, Oct. 2018.

[17] J.-D. P. McElderry, G. Zhao, A. Khmaladze, C. G. Wilson, R. T. Franceschi, and M. D. Morris, “Tracking circadian rhythms of bone mineral deposition in murine calvarial organ cultures,” *J. Bone Miner. Res.*, vol. 28, no. 8, pp. 1846–1854, Aug. 2013.

[18] F. Loi, L. A. Córdova, J. Pajarinen, T. Lin, Z. Yao, and S. B. Goodman, "Inflammation, fracture and bone repair," *Bone*, vol. 86, no. 86, pp. 119–130, May 2016.

[19] A. M. Parfitt, "Targeted and nontargeted bone remodeling: relationship to basic multicellular unit origination and progression," *Bone*, vol. 30, no. 1, pp. 5–7, Jan. 2002.

[20] A. L. Boskey, "Mineralization of Bones and Teeth," *Elements*, vol. 3, no. 6, pp. 385–391, Dec. 2007.

[21] P. Jayakumar and L. Di Silvio, "Osteoblasts in bone tissue engineering," *Proc. Inst. Mech. Eng. Part H J. Eng. Med.*, vol. 224, no. 12, pp. 1415–1440, Dec. 2010.

[22] T. J. Martin and N. A. Sims, "Osteoclast-derived activity in the coupling of bone formation to resorption," *Trends Mol. Med.*, vol. 11, no. 2, pp. 76–81, Feb. 2005.

[23] G. R. Mundy and T. J. Martin, *Physiology and Pharmacology of Bone*, vol. 107. Berlin, Heidelberg: Springer Berlin Heidelberg, 1993.

[24] Z. Hekimsoy, "Osteocytes-The Known and Unknown Osteositler-Bilinenler ve Bilinmeyenler," *Turkish J. Endocrinol. Metab.*, no. 2, pp. 3–7.

[25] Y. Han, S. C. Cowin, M. B. Schaffler, and S. Weinbaum, "Mechanotransduction and strain amplification in osteocyte cell processes," *Proc. Natl. Acad. Sci.*, vol. 101, no. 47, pp. 16689–16694, Nov. 2004.

[26] O. Verborgt, G. J. Gibson, and M. B. Schaffler, "Loss of Osteocyte Integrity in Association with Microdamage and Bone Remodeling After Fatigue In Vivo," *J. Bone*

Miner. Res., vol. 15, no. 1, pp. 60–67, Jan. 2000.

[27] J.-Y. Rho, L. Kuhn-Spearing, and P. Zioupos, "Mechanical properties and the hierarchical structure of bone," *Med. Eng. Phys.*, vol. 20, no. 2, pp. 92–102, Mar. 1998.

[28] S. Nawathe, H. Akhlaghpour, M. L. Bouxsein, and T. M. Keaveny, "Microstructural Failure Mechanisms in the Human Proximal Femur for Sideways Fall Loading," *J. Bone Miner. Res.*, vol. 29, no. 2, pp. 507–515, Feb. 2014.

[29] T. M. Keaveny, E. F. Morgan, G. L. Niebur, and O. C. Yeh, "Biomechanics of Trabecular Bone," *Annu. Rev. Biomed. Eng.*, vol. 3, no. 1, pp. 307–333, Aug. 2001.

[30] R. B. Martin, D. B. Burr, and N. A. Sharkey, *Skeletal Tissue Mechanics*, vol. 33. New York, NY: Springer New York, 1998.

[31] M. Shahnazari *et al.*, "Differential maintenance of cortical and cancellous bone strength following discontinuation of bone-active agents," *J. Bone Miner. Res.*, vol. 26, no. 3, pp. 569–581, Mar. 2011.

[32] P. M. Mayhew *et al.*, "Relation between age, femoral neck cortical stability, and hip fracture risk," *Lancet*, vol. 366, no. 9480, pp. 129–135, Jul. 2005.

[33] K. . Bell, N. Loveridge, J. Power, N. Garrahan, B. . Meggitt, and J. Reeve, "Regional differences in cortical porosity in the fractured femoral neck," *Bone*, vol. 24, no. 1, pp. 57–64, Jan. 1999.

[34] K. L. Bell *et al.*, "Structure of the Femoral Neck in Hip Fracture: Cortical Bone Loss in the Inferoanterior to Superoposterior Axis," *J. Bone Miner. Res.*, vol. 14, no. 1, pp.

111–119, Jan. 1999.

[35] T. Sugiyama and T. Taguchi, “Cortical stability of the femoral neck and hip fracture risk,” *Lancet*, vol. 366, no. 9496, pp. 1525–1526, Oct. 2005.

[36] M. Parker and A. Johansen, “Hip fracture,” *BMJ*, vol. 333, no. 7557, pp. 27–30, Jul. 2006.

[37] N. C. Casartelli *et al.*, “Hip muscle weakness in patients with symptomatic femoroacetabular impingement,” *Osteoarthr. Cartil.*, vol. 19, no. 7, pp. 816–821, Jul. 2011.

[38] T.-Y. Tsai, D. Dimitriou, G. Li, and Y.-M. Kwon, “Does total hip arthroplasty restore native hip anatomy? Three-dimensional reconstruction analysis,” *Int. Orthop.*, vol. 38, no. 8, pp. 1577–1583, Aug. 2014.

[39] B. K. Madeti, C. S. Rao, and B. S. K. S. S. Rao, “Biomechanics of hip joint: a review,” *Int. J. Biomed. Eng. Technol.*, vol. 15, no. 4, p. 341, 2014.

[40] J. Hewitt, F. Guilak, R. Glisson, and T. P. Vail, “Regional material properties of the human hip joint capsule ligaments,” *J. Orthop. Res.*, vol. 19, no. 3, pp. 359–364, May 2001.

[41] M. Jesse, B. Petersen, C. Strickland, and O. Mei-Dan, “Normal Anatomy and Imaging of the Hip: Emphasis on Impingement Assessment,” *Semin. Musculoskelet. Radiol.*, vol. 17, no. 03, pp. 229–247, Jun. 2013.

[42] T. M. Link, B. J. Schwaiger, and A. L. Zhang, “Regional Articular Cartilage Abnormalities of the Hip,” *Am. J. Roentgenol.*, vol. 205, no. 3, pp. 502–512, Sep.

2015.

[43] I. Gilligan, S. Chandraphak, and P. Mahakkanukrauh, “Femoral neck-shaft angle in humans: variation relating to climate, clothing, lifestyle, sex, age and side,” *J. Anat.*, vol. 223, no. 2, pp. 133–151, Aug. 2013.

[44] D. E. Lunn, A. Lampropoulos, and T. D. Stewart, “Basic biomechanics of the hip,” *Orthop. Trauma*, vol. 30, no. 3, pp. 239–246, Jun. 2016.

[45] A. W. M. M. Richard Drake, A. Wayne Vogl, *Gray’s Basic Anatomy E-Book*, 2nd Editio. Elsevier Health Sciences, 2016.

[46] R. K. Nalla, J. J. Kruzic, J. H. Kinney, and R. O. Ritchie, “Effect of aging on the toughness of human cortical bone: evaluation by R-curves,” *Bone*, vol. 35, no. 6, pp. 1240–1246, Dec. 2004.

[47] D. P. Fyhrie, “Summary--Measuring ‘bone quality’.,” *J. Musculoskelet. Neuronal Interact.*, vol. 5, no. 4, pp. 318–20, 2005.

[48] C. T. Rubin, S. Judex, Y.-X. Qin, and J. Rubin, “Prevention of Osteoporosis by Physical Signals,” in *Osteoporosis*, Elsevier, 2013, pp. 517–535.

[49] M. L. Bouxsein, *Chapter 19. Biomechanics of Age-Related Fractures*. Elsevier, 2001.

[50] H. Fonseca, D. Moreira-Gonçalves, H. J. A. Coriolano, and J. A. Duarte, “Bone quality: The determinants of bone strength and fragility,” *Sports Medicine*, vol. 44, no. 1. pp. 37–53, 03-Jan-2014.

[51] S. Vasikaran *et al.*, “Markers of bone turnover for the prediction of fracture risk and

monitoring of osteoporosis treatment: a need for international reference standards," *Osteoporos. Int.*, vol. 22, no. 2, pp. 391–420, Feb. 2011.

[52] F. R. SINGER and D. R. EYRE, "Using biochemical markers of bone turnover in clinical practice," *Cleve. Clin. J. Med.*, vol. 75, no. 10, pp. 739–750, Oct. 2008.

[53] B. Zhou, "Bone Quality Assessment Using High Resolution Peripheral Quantitative Computed Tomography (HR-pQCT)," COLUMBIA UNIVERSITY, 2015.

[54] C. H. Wilkins, "Osteoporosis screening and risk management.," *Clin. Interv. Aging*, vol. 2, no. 3, pp. 389–94, 2007.

[55] P. Garnero, E. Sornay-Rendu, B. Claustrat, and P. D. Delmas, "Biochemical Markers of Bone Turnover, Endogenous Hormones and the Risk of Fractures in Postmenopausal Women: The OFELY Study," *J. Bone Miner. Res.*, vol. 15, no. 8, pp. 1526–1536, Aug. 2000.

[56] E. Donnelly, "Methods for Assessing Bone Quality: A Review," *Clin. Orthop. Relat. Res.*, vol. 469, no. 8, pp. 2128–2138, Aug. 2011.

[57] S. Gourion-Arsiquaud *et al.*, "Use of FTIR spectroscopic imaging to identify parameters associated with fragility fracture," *J. Bone Miner. Res.*, vol. 24, no. 9, pp. 1565–1571, 2009.

[58] C. L. Gordon, T. F. Lang, P. Augat, and H. K. Genant, "Image-based assessment of spinal trabecular bone structure from high-resolution CT images," *Osteoporos. Int.*, vol. 8, no. 4, pp. 317–325, 1998.

[59] J. W. Bijlsma, F. Berenbaum, and F. P. Lafeber, "Osteoarthritis: an update with

relevance for clinical practice," *Lancet*, vol. 377, no. 9783, pp. 2115–2126, Jun. 2011.

[60] W.-N. Zeng *et al.*, "Investigation of association between hip morphology and prevalence of osteoarthritis," *Sci. Rep.*, vol. 6, no. 1, p. 23477, Sep. 2016.

[61] M. C. Castaño-Betancourt *et al.*, "Bone parameters across different types of hip osteoarthritis and their relationship to osteoporotic fracture risk," *Arthritis Rheum.*, vol. 65, no. 3, pp. 693–700, Mar. 2013.

[62] R. Kc *et al.*, "Osteoarthritis-like pathologic changes in the knee joint induced by environmental disruption of circadian rhythms is potentiated by a high-fat diet," *Sci. Rep.*, vol. 5, no. 1, p. 16896, Dec. 2015.

[63] J. C. Baker-LePain and N. E. Lane, "Role of bone architecture and anatomy in osteoarthritis," *Bone*, vol. 51, no. 2, pp. 197–203, Aug. 2012.

[64] P. Croft, D. Coggon, M. Cruddas, and C. Cooper, "Osteoarthritis of the hip: an occupational disease in farmers.," *BMJ*, vol. 304, no. 6837, pp. 1269–1272, May 1992.

[65] A. J. MacGregor, L. Antoniades, M. Matson, T. Andrew, and T. D. Spector, "The genetic contribution to radiographic hip osteoarthritis in women: Results of a classic twin study," *Arthritis Rheum.*, vol. 43, no. 11, pp. 2410–2416, Nov. 2000.

[66] G. Lenaerts *et al.*, "Subject-specific hip geometry and hip joint centre location affects calculated contact forces at the hip during gait," *J. Biomech.*, vol. 42, no. 9, pp. 1246–1251, Jun. 2009.

[67] A. Mangram *et al.*, "Geriatric trauma hip fractures: is there a difference in outcomes based on fracture patterns?," *World J. Emerg. Surg.*, vol. 9, no. 1, p. 59, 2014.

[68] M. A. Norris and A. A. De Smet, “Fractures and dislocations of the hip and femur,” *Semin. Roentgenol.*, vol. 29, no. 2, pp. 100–112, Apr. 1994.

[69] C. Cooper, G. Campion, and L. J. Melton, “Hip fractures in the elderly: A world-wide projection,” *Osteoporos. Int.*, vol. 2, no. 6, pp. 285–289, Nov. 1992.

[70] S. R. Cummings and L. J. Melton, “Osteoporosis I: Epidemiology and outcomes of osteoporotic fractures,” *Lancet*, vol. 359, no. 9319. pp. 1761–1767, May-2002.

[71] O. Johnell and J. A. Kanis, “An estimate of the worldwide prevalence and disability associated with osteoporotic fractures,” *Osteoporos. Int.*, vol. 17, no. 12, pp. 1726–1733, Oct. 2006.

[72] B. Gullberg, O. Johnell, and J. A. Kanis, “World-wide Projections for Hip Fracture,” *Osteoporos. Int.*, vol. 7, no. 5, pp. 407–413, Sep. 1997.

[73] M. L. Bouxsein, “Technology Insight: noninvasive assessment of bone strength in osteoporosis,” *Nat. Clin. Pract. Rheumatol.*, vol. 4, no. 6, pp. 310–318, Jun. 2008.

[74] J. A. Kanis, A. Odén, E. V. McCloskey, H. Johansson, D. A. Wahl, and C. Cooper, “A systematic review of hip fracture incidence and probability of fracture worldwide,” *Osteoporos. Int.*, vol. 23, no. 9, pp. 2239–2256, Sep. 2012.

[75] C. Gómez Alonso, M. Díaz Curiel, F. Hawkins Carranza, R. Pérez Cano, and A. Díez Pérez, “Femoral Bone Mineral Density, Neck-Shaft Angle and Mean Femoral Neck Width as Predictors of Hip Fracture in Men and Women,” *Osteoporos. Int.*, vol. 11, no. 8, pp. 714–720, Sep. 2000.

[76] S. R. Cummings *et al.*, “Risk Factors for Hip Fracture in White Women,” *N. Engl. J.*

Med., vol. 332, no. 12, pp. 767–774, Mar. 1995.

[77] L. J. Melton, “Who Has Osteoporosis? A Conflict Between Clinical and Public Health Perspectives,” *J. Bone Miner. Res.*, vol. 15, no. 12, pp. 2309–2314, Dec. 2000.

[78] T. E. Taha *et al.*, “Effect of cleansing the birth canal with antiseptic solution on maternal and newborn morbidity and mortality in malawi: clinical trial,” *BMJ*, vol. 315, no. 7102, pp. 216–220, Jul. 1997.

[79] M. L. Bouxsein, “Determinants of skeletal fragility,” *Best Pract. Res. Clin. Rheumatol.*, vol. 19, no. 6, pp. 897–911, Dec. 2005.

[80] P. Carpintero, “Complications of hip fractures: A review,” *World J. Orthop.*, vol. 5, no. 4, p. 402, 2014.

[81] J. S. Jensen and J. Bagger, “Long-Term Social Prognosis after Hip Fractures,” *Acta Orthop. Scand.*, vol. 53, no. 1, pp. 97–101, Jan. 1982.

[82] D. B. Burr *et al.*, “Does microdamage accumulation affect the mechanical properties of bone?,” *J. Biomech.*, vol. 31, no. 4, pp. 337–345, Apr. 1998.

[83] D. B. Burr, R. B. Martin, M. B. Schaffler, and E. L. Radin, “Bone remodeling in response to in vivo fatigue microdamage,” *J. Biomech.*, vol. 18, no. 3, pp. 189–200, Jan. 1985.

[84] D. B. Burr, M. R. Forwood, D. P. Fyhrie, R. B. Martin, M. B. Schaffler, and C. H. Turner, “Bone Microdamage and Skeletal Fragility in Osteoporotic and Stress Fractures,” *J. Bone Miner. Res.*, vol. 12, no. 1, pp. 6–15, Jan. 1997.

[85] D. B. Burr, R. B. Martin, M. B. Schaffler, and E. L. Radin, “Bone remodeling in response to in vivo fatigue microdamage,” *J. Biomech.*, vol. 18, no. 3, pp. 189–200, Jan. 1985.

[86] M. B. Schaffler, W. C. Pitchford, K. Choi, and J. M. Riddle, “Examination of compact bone microdamage using back-scattered electron microscopy,” *Bone*, vol. 15, no. 5, pp. 483–488, Sep. 1994.

[87] M. B. Schaffler, K. Choi, and C. Milgrom, “Aging and matrix microdamage accumulation in human compact bone,” *Bone*, vol. 17, no. 6, pp. 521–525, Dec. 1995.

[88] E. P. Paschalis, E. Shane, G. Lyritis, G. Skarantavos, R. Mendelsohn, and A. L. Boskey, “Bone Fragility and Collagen Cross-Links,” *J. Bone Miner. Res.*, vol. 19, no. 12, pp. 2000–2004, Aug. 2004.

[89] G. Boivin and P. J. Meunier, “Changes in Bone Remodeling Rate Influence the Degree of Mineralization of Bone,” *Connect. Tissue Res.*, vol. 43, no. 2–3, pp. 535–537, Jan. 2002.

[90] P. J. Meunier and G. Boivin, “Bone mineral density reflects bone mass but also the degree of mineralization of bone: therapeutic implications.,” *Bone*, vol. 21, no. 5, pp. 373–7, Nov. 1997.

[91] N. D. Sahar, S.-I. Hong, and D. H. Kohn, “Micro- and nano-structural analyses of damage in bone,” *Micron*, vol. 36, no. 7–8, pp. 617–629, Oct. 2005.

[92] N. . Camacho, S. Rinnerthaler, E. . Paschalis, R. Mendelsohn, A. . Boskey, and P. Fratzl, “Complementary information on bone ultrastructure from scanning small angle

X-ray scattering and Fourier-transform infrared microspectroscopy," *Bone*, vol. 25, no. 3, pp. 287–293, Sep. 1999.

[93] A. Odgaard, "Three-dimensional methods for quantification of cancellous bone architecture," *Bone*, vol. 20, no. 4, pp. 315–328, Apr. 1997.

[94] T. L. Järvinen, H. Sievänen, J. Jokihaara, and T. A. Einhorn, "Revival of Bone Strength: The Bottom Line," *J. Bone Miner. Res.*, vol. 20, no. 5, pp. 717–720, Feb. 2005.

[95] G. J. Kazakia and S. Majumdar, "New imaging technologies in the diagnosis of osteoporosis," *Rev. Endocr. Metab. Disord.*, vol. 7, no. 1–2, pp. 67–74, Jan. 2007.

[96] B. Zhou *et al.*, "High-resolution peripheral quantitative computed tomography (HR-pQCT) can assess microstructural and biomechanical properties of both human distal radius and tibia: Ex vivo computational and experimental validations," *Bone*, vol. 86, pp. 58–67, May 2016.

[97] W. Tjong, G. J. Kazakia, A. J. Burghardt, and S. Majumdar, "The effect of voxel size on high-resolution peripheral computed tomography measurements of trabecular and cortical bone microstructure," *Med. Phys.*, vol. 39, no. 4, pp. 1893–1903, Mar. 2012.

[98] A. J. Burghardt *et al.*, "Multicenter precision of cortical and trabecular bone quality measures assessed by high-resolution peripheral quantitative computed tomography," *J. Bone Miner. Res.*, vol. 28, no. 3, pp. 524–536, Mar. 2013.

[99] H. Fuller, R. Fuller, and R. M. R. Pereira, "High resolution peripheral quantitative computed tomography for the assessment of morphological and mechanical bone

parameters," *Rev. Bras. Reumatol. (English Ed.*, vol. 55, no. 4, pp. 352–362, Jul. 2015.

[100] S. Nagaraja, T. L. Couse, and R. E. Guldberg, "Trabecular bone microdamage and microstructural stresses under uniaxial compression," *J. Biomech.*, vol. 38, no. 4, pp. 707–716, Apr. 2005.

[101] R. M. Zebaze *et al.*, "Intracortical remodelling and porosity in the distal radius and post-mortem femurs of women: a cross-sectional study," *Lancet*, vol. 375, no. 9727, pp. 1729–1736, May 2010.

[102] A. Laib, H. J. Häuselmann, and P. Rüegsegger, "In vivo high resolution 3D-QCT of the human forearm.," *Technol. Health Care*, vol. 6, no. 5–6, pp. 329–37, Dec. 1998.

[103] T. Hildebrand and P. Ruegsegger, "A new method for the model-independent assessment of thickness in three-dimensional images," *J. Microsc.*, vol. 185, no. 1, pp. 67–75, Jan. 1997.

[104] S. Boutroy, M. L. Bouxsein, F. Munoz, and P. D. Delmas, "In Vivo Assessment of Trabecular Bone Microarchitecture by High-Resolution Peripheral Quantitative Computed Tomography," *J. Clin. Endocrinol. Metab.*, vol. 90, no. 12, pp. 6508–6515, Dec. 2005.

[105] S. Khosla *et al.*, "Effects of Sex and Age on Bone Microstructure at the Ultradistal Radius: A Population-Based Noninvasive In Vivo Assessment," *J. Bone Miner. Res.*, vol. 21, no. 1, pp. 124–131, Oct. 2005.

[106] N. Dalzell *et al.*, "Bone micro-architecture and determinants of strength in the radius and tibia: age-related changes in a population-based study of normal adults measured

with high-resolution pQCT," *Osteoporos. Int.*, vol. 20, no. 10, pp. 1683–1694, Oct. 2009.

[107] H. M. Macdonald, K. K. Nishiyama, J. Kang, D. A. Hanley, and S. K. Boyd, "Age-related patterns of trabecular and cortical bone loss differ between sexes and skeletal sites: A population-based HR-pQCT study," *J. Bone Miner. Res.*, vol. 26, no. 1, pp. 50–62, Jan. 2011.

[108] L. A. Binkovitz and M. J. Henwood, "Pediatric DXA: technique and interpretation," *Pediatr. Radiol.*, vol. 37, no. 1, pp. 21–31, Jan. 2007.

[109] T. Chevalley, J. P. Bonjour, B. van Rietbergen, S. Ferrari, and R. Rizzoli, "Fractures during Childhood and Adolescence in Healthy Boys: Relation with Bone Mass, Microstructure, and Strength," *J. Clin. Endocrinol. Metab.*, vol. 96, no. 10, pp. 3134–3142, Oct. 2011.

[110] L. A. Burt, H. M. Macdonald, D. A. Hanley, and S. K. Boyd, "Bone microarchitecture and strength of the radius and tibia in a reference population of young adults: an HR-pQCT study," *Arch. Osteoporos.*, vol. 9, no. 1, p. 183, Dec. 2014.

[111] L. A. Burt, D. A. Hanley, and S. K. Boyd, "Cross-sectional Versus Longitudinal Change in a Prospective HR-pQCT Study.," *J. Bone Miner. Res.*, vol. 32, no. 7, pp. 1505–1513, Jul. 2017.

[112] X. Wang, Q. Wang, A. Ghasem-zadeh, A. Evans, and C. Mcleod, "Differences in Macro- and Microarchitecture of the AppendicularSkeleton in Young Chinese and White Women," *J. BONE Miner. RESEARC*, vol. 24, no. 12, pp. 1946–1952, Dec.

2009.

[113] M. L. Bouxsein, “Bone structure and fracture risk: Do they go arm in arm?,” *J. Bone Miner. Res.*, vol. 26, no. 7, pp. 1389–1391, Jul. 2011.

[114] E. Sornay-Rendu, J.-L. Cabrera-Bravo, S. Boutroy, F. Munoz, and P. D. Delmas, “Severity of Vertebral Fractures Is Associated With Alterations of Cortical Architecture in Postmenopausal Women,” *J. Bone Miner. Res.*, vol. 24, no. 4, pp. 737–743, Apr. 2009.

[115] X. S. Liu *et al.*, “Individual trabeculae segmentation (ITS)-based morphological analysis of high-resolution peripheral quantitative computed tomography images detects abnormal trabecular plate and rod microarchitecture in premenopausal women with idiopathic osteoporosis,” *J. Bone Miner. Res.*, vol. 25, no. 7, pp. 1496–1505, Feb. 2010.

[116] E. M. Stein *et al.*, “Microarchitectural Abnormalities Are More Severe in Postmenopausal Women with Vertebral Compared to Nonvertebral Fractures,” *J. Clin. Endocrinol. Metab.*, vol. 97, no. 10, pp. E1918–E1926, Oct. 2012.

[117] E. Sornay-Rendu, S. Boutroy, F. Munoz, and P. D. Delmas, “Alterations of Cortical and Trabecular Architecture Are Associated With Fractures in Postmenopausal Women, Partially Independent of Decreased BMD Measured by DXA: The OFELY Study,” *J. Bone Miner. Res.*, vol. 22, no. 3, pp. 425–433, Mar. 2007.

[118] L. J. Melton *et al.*, “Contribution of In Vivo Structural Measurements and Load/Strength Ratios to the Determination of Forearm Fracture Risk in

Postmenopausal Women," *J. Bone Miner. Res.*, vol. 22, no. 9, pp. 1442–1448, May 2007.

[119] L. Vico *et al.*, "High-Resolution pQCT Analysis at the Distal Radius and Tibia Discriminates Patients With Recent Wrist and Femoral Neck Fractures," *J. Bone Miner. Res.*, vol. 23, no. 11, pp. 1741–1750, Nov. 2008.

[120] E. M. Stein *et al.*, "Abnormal microarchitecture and reduced stiffness at the radius and tibia in postmenopausal women with fractures," *J. Bone Miner. Res.*, vol. 25, no. 12, pp. 2572–2581, Dec. 2010.

[121] P. Szulc, S. Boutroy, N. Vilayphiou, A. Chaitou, P. D. Delmas, and R. Chapurlat, "Cross-sectional analysis of the association between fragility fractures and bone microarchitecture in older men: The STRAMBO study," *J. Bone Miner. Res.*, vol. 26, no. 6, pp. 1358–1367, Jun. 2011.

[122] K. K. Nishiyama, H. M. Macdonald, D. A. Hanley, and S. K. Boyd, "Women with previous fragility fractures can be classified based on bone microarchitecture and finite element analysis measured with HR-pQCT," *Osteoporos. Int.*, vol. 24, no. 5, pp. 1733–1740, May 2013.

[123] N. Vilayphiou *et al.*, "Finite element analysis performed on radius and tibia HR-pQCT images and fragility fractures at all sites in men," *J. Bone Miner. Res.*, vol. 26, no. 5, pp. 965–973, May 2011.

[124] C. Graeff *et al.*, "High resolution quantitative computed tomography-based assessment of trabecular microstructure and strength estimates by finite-element analysis of the

spine, but not DXA, reflects vertebral fracture status in men with glucocorticoid-induced osteoporosis," *Bone*, vol. 52, no. 2, pp. 568–577, Feb. 2013.

[125] S. Boutroy *et al.*, "Comparison of 2D and 3D bone microarchitecture evaluation at the femoral neck, among postmenopausal women with hip fracture or hip osteoarthritis," *Bone*, vol. 49, no. 5, pp. 1055–1061, Nov. 2011.

[126] K. Chiba, A. J. Burghardt, M. Osaki, and S. Majumdar, "Heterogeneity of bone microstructure in the femoral head in patients with osteoporosis: An ex vivo HR-pQCT study," *Bone*, vol. 56, no. 1, pp. 139–146, Sep. 2013.

[127] National Center for Health Statistics, "Dual Energy X-ray Absorptiometry (DXA) Procedures Manual," no. January, p. 115, 2007.

[128] T. Tang, "FRACTURE MECHANISMS AND STRUCTURAL FRAGILITY OF HUMAN FEMORAL CORTICAL BONE," University of British Columbia, 2018.

[129] M. Jindal, L. Op, K. Omkar, S. Agarwal, and G. Keerty, "Bone Density versus Bone Quality as a Predictor of Bone Strength," *Orthop. Rheumatol.*, vol. 12, no. 1, 2018.

[130] E. Legrand *et al.*, "Trabecular Bone Microarchitecture, Bone Mineral Density, and Vertebral Fractures in Male Osteoporosis," *J. Bone Miner. Res.*, vol. 15, no. 1, pp. 13–19, Jan. 2000.

[131] E.-M. Lochmüller *et al.*, "Site-Specific Deterioration of Trabecular Bone Architecture in Men and Women With Advancing Age," *J. Bone Miner. Res.*, vol. 23, no. 12, pp. 1964–1973, Dec. 2008.

[132] E. M. Alhava and J. Puittinen, "Fractures of the upper end of the femur as an index of

senile osteoporosis in Finland.," *Ann. Clin. Res.*, vol. 5, no. 6, pp. 398–403, Dec. 1973.

[133] M. Stauber and R. Müller, "Age-related changes in trabecular bone microstructures: global and local morphometry," *Osteoporos. Int.*, vol. 17, no. 4, pp. 616–626, Apr. 2006.

[134] W.-Q. Cui *et al.*, "Age-and region-dependent changes in three-dimensional microstructural properties of proximal femoral trabeculae," *Osteoporos. Int.*, vol. 19, no. 11, pp. 1579–1587, Nov. 2008.

[135] K. . Bell, N. Loveridge, G. . Jordan, J. Power, C. . Constant, and J. Reeve, "A novel mechanism for induction of increased cortical porosity in cases of intracapsular hip fracture," *Bone*, vol. 27, no. 2, pp. 297–304, Aug. 2000.

[136] G. Holzer, G. von Skrbensky, L. A. Holzer, and W. Pichl, "Hip Fractures and the Contribution of Cortical Versus Trabecular Bone to Femoral Neck Strength," *J. Bone Miner. Res.*, vol. 24, no. 3, pp. 468–474, Mar. 2009.

[137] G. . Jordan *et al.*, "Increased femoral neck cancellous bone and connectivity in coxarthrosis (hip osteoarthritis)," *Bone*, vol. 32, no. 1, pp. 86–95, Jan. 2003.

[138] E. G. Vajda and R. D. Bloebaum, "Age-related hypermineralization in the female proximal human femur," *Anat. Rec.*, vol. 255, no. 2, pp. 202–211, Jun. 1999.

[139] T. M. Boyce and R. D. Bloebaum, "Cortical aging differences and fracture implications for the human femoral neck," *Bone*, vol. 14, no. 5, pp. 769–778, Sep. 1993.

[140] J. E. Shea, E. G. Vajda, and R. D. Bloebaum, "Evidence of a hypermineralised

calcified fibrocartilage on the human femoral neck and lesser trochanter.," *J. Anat.*, vol. 198, no. Pt 2, pp. 153–62, Feb. 2001.

[141] P. Roschger, E. P. Paschalis, P. Fratzl, and K. Klaushofer, "Bone mineralization density distribution in health and disease," *Bone*, vol. 42, no. 3, pp. 456–466, Mar. 2008.

[142] P. Roschger, P. Fratzl, J. Eschberger, and K. Klaushofer, "Validation of quantitative backscattered electron imaging for the measurement of mineral density distribution in human bone biopsies," *Bone*, vol. 23, no. 4, pp. 319–326, Oct. 1998.

[143] M. R. Allen and D. B. Burr, "Human femoral neck has less cellular periosteum, and more mineralized periosteum, than femoral diaphyseal bone," *Bone*, vol. 36, no. 2, pp. 311–316, Feb. 2005.

[144] W. K. Sietsema, "Animal models of cortical porosity," *Bone*, vol. 17, no. 4, pp. S297–S305, Oct. 1995.

[145] D. M. L. Cooper, C. D. L. Thomas, J. G. Clement, A. L. Turinsky, C. W. Sensen, and B. Hallgrímsson, "Age-dependent change in the 3D structure of cortical porosity at the human femoral midshaft," *Bone*, vol. 40, no. 4, pp. 957–965, Apr. 2007.

Appendices

Appendix A Chapter 4- Row Data

Table S4- 1: Microstructural parameters by HR-pQCT of OA at the femoral Head region

number	SampNo	BV/TV	Conn-Dens.	Tb.N	Tb.Th	Tb.Sp
1	545	20%	2.80	0.55	0.21	2.19
2	561	18%	2.64	0.44	0.24	2.81
3	596	23%	3.78	0.58	0.21	2.20
4	540	14%	1.78	0.48	0.22	2.38
5	543	20%	3.14	0.55	0.25	2.17
6	544	19%	2.75	0.57	0.25	2.16
7	582	22%	3.14	0.48	0.25	2.67
8	594	25%	5.03	0.68	0.25	1.90
9	597	19%	3.03	0.54	0.24	2.22
mean		***20%***	***3.1***	***0.54***	***0.2***	***2.3***
STD		***3%***	***0.89***	***0.07***	***0.02***	***0.28***
cv		***16%***	***28%***	***13%***	***7%***	***12%***

Table S4- 2: Microstructural parameters by HR-pQCT of control at the femoral Head region

number	SampNo	BV/TV	Conn-Dens.	Tb.N	Tb.Th	Tb.Sp
1	461	17%	2.65	1.28	0.23	0.84
2	456	18%	2.46	1.42	0.22	0.80
3	457	14%	1.47	1.02	0.22	1.01
4	452	10%	1.33	0.98	0.21	1.05
5	459	19%	1.67	1.33	0.24	0.78
6	460	23%	2.48	1.64	0.25	0.64
7	463	23%	2.90	1.25	0.24	0.97
8	464	12%	1.78	0.59	0.22	1.86
9	467	12%	2.10	1.29	0.21	0.77
average		***16%***	***2.09***	***1.20***	***0.23***	***0.97***
STD		***5%***	***0.56***	***0.30***	***0.02***	***0.36***
cv		***29%***	***27%***	***25%***	***7%***	***37%***

Table S4- 3: Microstructural parameters by HR-pQCT of OA at the femoral head-neck region

number	SampNo	BV/TV	Conn-Dens.	Tb.N	Tb.Th	Tb.Sp
1	545	21%	2.7	0.8	0.2	1.4
2	561	24%	3.3	0.9	0.2	1.3
3	596	23%	2.8	0.9	0.2	1.2
4	540	14%	1.9	0.7	0.2	1.6
5	543	23%	4.3	1.2	0.2	0.9
6	544	17%	2.0	0.6	0.2	1.8
7	582	22%	2.7	0.9	0.2	1.3
8	594	25%	3.8	0.7	0.2	1.6
9	597	5%	1.0	0.7	0.1	1.5
mean		***19%***	***2.72***	***0.84***	***0.21***	***1.41***
STD		***6%***	***1.01***	***0.17***	***0.03***	***0.25***
cv		***34%***	***37%***	***20%***	***14%***	***18%***

Table S4- 4: Microstructural parameters by HR-pQCT of control at the femoral head- neck region

number	SampNo	BV/TV	Conn-Dens.	Tb.N	Tb.Th	Tb.Sp
1	461	14%	1.82	1.10	0.21	0.94
2	456	17%	2.15	1.36	0.22	0.75
3	457	11%	1.01	0.87	0.22	1.19
4	452	9%	0.78	0.79	0.21	1.29
5	459	14%	1.15	1.05	0.22	0.98
6	460	19%	1.67	1.32	0.24	0.77
7	463	21%	2.29	1.40	0.24	0.81
8	464	10%	1.13	1.02	0.22	0.99
9	467	10%	1.00	1.04	0.22	0.95
mean		***14%***	***1.44***	***1.11***	***0.22***	***0.96***
STD		***4%***	***0.55***	***0.22***	***0.01***	***0.18***
cv		***32%***	***38%***	***19%***	***5%***	***19%***

Table S4- 5: Microstructural parameters by HR-pQCT of OA at the femoral neck region

number	SampNo	BV/TV	Conn-Dens.	Tb.N	Tb.Th	Tb.Sp
1	545	21%	1.70	1.07	0.34	1.00
2	561	24%	2.19	1.52	0.30	0.70
3	596	27%	3.31	1.44	0.28	0.74
4	540	24%	2.97	1.35	0.27	0.79
5	544	16%	2.19	1.05	0.21	1.03
6	597	20%	2.16	1.07	0.22	0.99
7	582	22%	2.96	1.50	0.20	0.72
8	594	15%	1.84	1.10	0.19	0.93
9	543	18%	3.52	1.57	0.20	0.68
mean		**21%**	**2.54**	**1.30**	**0.25**	**0.84**
STD		***4.0%***	***0.66***	***0.22***	***0.05***	***0.15***
cv		**19%**	**26%**	**17%**	**22%**	**17%**

Table S4- 6: Microstructural parameters by HR-pQCT of control at the femoral neck region

sample #	SampNo	BV/TV	Conn-Dens.	Tb.N	Tb.Th	Tb.Sp
1	461	18%	1.18	0.98	0.39	1.10
2	456	25%	1.63	1.09	0.37	1.01
3	457	19%	1.09	0.91	0.37	1.14
4	452	8%	0.65	0.78	0.26	1.30
5	467	17%	1.88	1.07	0.20	0.97
6	463	29%	3.25	1.49	0.22	0.70
7	459	18%	1.56	0.97	0.21	1.06
8	460	0%	0.01	0.64	0.14	1.68
9	464	10%	1.41	0.89	0.19	1.17
mean		**16%**	**1.41**	**0.98**	**0.26**	**1.13**
STD		**9%**	**0.89**	**0.24**	**0.09**	**0.27**
cv		**54%**	**64%**	**24%**	**36%**	**24%**